

ON THE DUNFIELD–GUKOV–RASMUSSEN CONJECTURE

ANNA BELIAKOVA, KRZYSZTOF K. PUTYRA, LOUIS-HADRIEN ROBERT, AND EMMANUEL WAGNER

ABSTRACT. In 2005 Dunfield, Gukov and Rasmussen conjectured an existence of a differential from the reduced triply graded Khovanov–Rozansky homology of a knot to its knot Floer homology defined by Ozsváth and Szabó. The main result of this paper is a proof of a suitably updated version of their conjecture: we show that the reduced triply graded homology is related to knot Floer homology by two spectral sequences, going through the intermediate \mathfrak{gl}_0 homology constructed by the last two authors. The \mathfrak{gl}_0 homology comes equipped with a spectral sequence from the reduced triply graded homology, and here we construct the other spectral sequence, from the \mathfrak{gl}_0 homology to knot Floer homology. The new spectral sequence is of Bockstein type and arises from a subtle manipulation of coefficients. The main tools are quantum traces of foams and of singular Soergel bimodules and a \mathbb{Z} -valued cube of resolutions model for knot Floer homology, originally constructed by Ozsváth–Szabó over the field of two elements. As an application we deduce that both the \mathfrak{gl}_0 homology and the reduced triply graded Khovanov–Rozansky homology detect the unknot, the two trefoils, the figure eight knot and the cinquefoil.

CONTENTS

1. Introduction	2
1.1. Main results	4
1.2. Applications	6
1.3. Outline	7
1.4. Acknowledgements	7
2. Preliminaries	8
2.1. Conventions	8
2.2. Symmetric polynomials and Soergel bimodules	8
2.3. Hochschild homology	10
2.4. Webs and foams	12
2.5. Foams and webs as Soergel bimodules	16
2.6. A quantum trace deformation of annular foams	20
3. Combinatorial link homologies	22
3.1. The general cube construction	22
3.2. Triply graded Khovanov–Rozansky homology	24
3.3. \mathfrak{gl}_1 homology	26
3.4. \mathfrak{gl}_0 homology	28
3.5. The spectral sequence from the reduced triply graded homology to \mathfrak{gl}_0 homology	29
4. Heegaard Floer homology	31
4.1. Heegaard diagrams and holomorphic disks	31
4.2. The Heegaard Floer complex	35
4.3. Skein exact triangles	37
4.4. Computation for planar singular links	41
5. Main results	43
5.1. The normalized Gilmore complex	44
5.2. The identification with \widehat{HFK}	48

Date: January 20, 2025.

5.3.	An identification with the original Gilmore complex	52
5.4.	A pseudo completion	53
5.5.	The spectral sequence	54
Appendix A.	On Bockstein spectral sequences	55
A.1.	Limits of spectral sequences	55
A.2.	The mod- p Bockstein spectral sequence.	56
A.3.	The $(q \mapsto 1)$ Bockstein sequence	57
Appendix B.	Cyclicity of the quantum Hochschild homology	58
Appendix C.	Computations of \mathfrak{gl}_0 homology	60
C.1.	Trefoils	60
C.2.	Figure-eight knot	61
C.3.	$(5,2)$ -torus knot	62
References		63

1. INTRODUCTION

The discovery of the Alexander polynomial $\Delta_K(q)$ in 1929 marked the birth of knot theory, manifested in the transition from conjectures to proofs. In the 1970s Conway found a first diagrammatic algorithm to compute $\Delta_K(q)$ using the so-called skein relation:

$$(1) \quad \begin{array}{c} \diagup \diagdown \\ \diagdown \diagup \end{array} - \begin{array}{c} \diagdown \diagup \\ \diagup \diagdown \end{array} = (q - q^{-1}) \begin{array}{c} \curvearrowright \\ \curvearrowleft \end{array},$$

where the three pictures represent link diagrams that coincide outside of the small regions depicted above.

In the 1980s the second big player in knot theory was introduced by Jones and later extended to the two variable HOMFLY-PT polynomial $P_K(a, q)$ with the skein relation

$$(2) \quad a \begin{array}{c} \diagup \diagdown \\ \diagdown \diagup \end{array} - a^{-1} \begin{array}{c} \diagdown \diagup \\ \diagup \diagdown \end{array} = (q - q^{-1}) \begin{array}{c} \curvearrowright \\ \curvearrowleft \end{array}.$$

It specializes to the Alexander polynomial for $a = 1$ and to the Jones polynomial for $a = q^2$. Setting $a = q^N$ recovers the \mathfrak{sl}_N polynomial of the knot K . Introducing *webs*, oriented planar trivalent graphs, we can rewrite (2) as

$$(3) \quad a \begin{array}{c} \diagup \diagdown \\ \diagdown \diagup \end{array} = \begin{array}{c} \diagup \diagdown \\ \diagdown \diagup \end{array} - q^{-1} \begin{array}{c} \curvearrowright \\ \curvearrowleft \end{array} \quad \text{and} \quad a^{-1} \begin{array}{c} \diagdown \diagup \\ \diagup \diagdown \end{array} = \begin{array}{c} \diagdown \diagup \\ \diagup \diagdown \end{array} - q \begin{array}{c} \curvearrowright \\ \curvearrowleft \end{array},$$

where the second diagram in both equations represents a *singular* crossing.

At the beginning of this century Jones and HOMFLY-PT polynomials were moved one categorical level higher by Khovanov and Khovanov–Rozansky [Kho00, KR08a, KR08b]. These new theories associate with a link diagram graded chain complexes, the homologies of which yield new powerful link invariants. The polynomials can be reconstructed by taking the graded Euler characteristics of these chain complexes. One important feature of the categorified invariants is their functoriality with respect to link cobordisms, i.e. surfaces bounded by links induce maps on homology. This does not hold for the Euler characteristics.

After presenting a knot K as a closure of a braid β with n crossings, the Khovanov–Rozansky chain complex is defined by resolving each crossing of β in two ways as suggested by (3) and then by assigning to each such resolution, which is a web, a Soergel bimodule. Webs are then organized as vertices of an n -dimensional cube. With the edges of the cube we associate differentials given

by bimodule maps induced by singular 2-dimensional cobordisms called *foams*. This construction is based on a functor of bicategories

$$(4) \quad B: \mathbf{Foam} \rightarrow \mathbf{sSBim}$$

discussed in Section 2. Closing up the braid is achieved by taking the horizontal trace of B , which assigns to a closed web the Hochschild homology of the associated Soergel bimodule. The homology HHH of the resulting cube complex is a triply graded link invariant that categorifies $P_K(\mathbf{a}, \mathbf{q})$. By putting a basepoint on the diagram and killing the corresponding variable in the Soergel bimodule, we obtain the so-called *reduced* homology HHH^{red} , which in case of knots does not depend on the position of the basepoint. The *quantum* horizontal trace of (4), the *quantum* Hochschild homology as well as the *quantum* annular link homology were constructed in [BPW19]. Note that the quantum horizontal trace of \mathbf{Foam} is the category of *quantum annular foams* constituted by annular foams together with a membrane, subject to additional relations involving the membrane and a quantum parameter q . All mentioned constructions admit algorithmic computations.

Parallel to these developments, the Alexander polynomial was categorified by Ozsváth and Szabó using completely different, geometric techniques. Here chain complexes are generated by Lagrangian intersections in a symmetric product of (pointed) Heegaard diagrams and the differential counts holomorphic discs. The resulting homology, known as *Heegaard Floer knot* homology or simply knot Floer homology, is denoted by \widehat{HFK} . This homology has important topological applications: it detects the genus and fiberedness of a knot [Ni07]. The list of knots detected by \widehat{HFK} is constantly growing. However, this theory is essentially non-local and hard to compute in general.

During many years the relationship between the algebraic Khovanov–Rozansky and the geometric Heegaard Floer knot homologies remained mysterious. In 2005 Dunfield, Gukov and Rasmussen made a series of influential conjectures [DGR06]. They predicted an existence of the differentials ∂_N and ∂_0 on HHH , such that $H_\bullet(HHH, \partial_N)$ is the \mathfrak{sl}_N homology and $H_\bullet(HHH, \partial_0)$ is \widehat{HFK} , lifting the specializations of $P_K(\mathbf{a}, \mathbf{q})$ at $\mathbf{a} = q^N$ and $\mathbf{a} = 1$, respectively. A version of this conjecture was established by Rasmussen in [Ras15] for $N \geq 1$, who constructed a differential d_N on HHH that leads to a spectral sequence to \mathfrak{sl}_N homology. It is an open problem whether this spectral sequence collapses immediately.

In this paper we prove a suitable version of the second part of Dunfield–Gukov–Rasmussen conjecture by connecting algebraic HHH^{red} and geometric \widehat{HFK} knot homologies with two spectral sequences. We will refer to this result as DGR Conjecture. An important ingredient of our proof is a new knot homology theory $H^{\mathfrak{gl}_0}$, that was constructed by the last two authors of the present paper in [RW22]. The \mathfrak{gl}_0 homology categorifies the Alexander polynomial and comes equipped with a spectral sequence from HHH^{red} over \mathbb{Q} . In this paper we construct the second spectral sequence starting with $H^{\mathfrak{gl}_0}$ and converging to \widehat{HFK} . Let us stress that even if $H^{\mathfrak{gl}_0}$ and \widehat{HFK} categorify the same polynomial invariant, there is a priori no reason to assume that these homologies are isomorphic. In fact, we will prove here that $H^{\mathfrak{gl}_0}$ and \widehat{HFK} are different.

Our construction of a spectral sequence from $H^{\mathfrak{gl}_0}$ to \widehat{HFK} uses the cube of resolutions model for \widehat{HFK} developed by Ozsváth and Szabó in [OS09] and reformulated in algebraic terms by Gilmore [Gil16]. This model requires twisted coefficients $\mathbb{F}[q^{-1}, q]$, which is a ring of power series in q over the field of two elements \mathbb{F} . This ring of coefficients is needed to kill higher differentials in the cube. The problem is however that $q - 1$ is invertible in $\mathbb{F}[q^{-1}, q]$, and hence, this coefficient ring does not admit a specialization at $q = 1$ that is needed to connect with Soergel bimodules and $H^{\mathfrak{gl}_0}$. This motivated Manolescu in [Man14] to untwist the cube of resolutions model for \widehat{HFK} . As a result, he was able to reduce DGR conjecture to a computation of certain Tor-groups.

In this paper we choose a different approach and work with twisted coefficients. In [Gil16] the state spaces associated with vertices of the cube were identified with quotients of a twisted version

of Soergel bimodules. This motivated us to search for a more conceptual understanding of these spaces in terms of the *quantum* Hochschild homology of Soergel bimodules.

Let us finally mention that the cube of resolutions model was extensively studied by Dowlin in two unpublished papers [Dow17, Dow18], where the cube construction was assumed to work with integral coefficients.

1.1. Main results. We start by promoting the coefficients from \mathbb{F} to \mathbb{Z} , meaning that we provide an algebraic model that computes \widehat{HFK} over $\mathbb{Z}[q^{-1}, q]$ via the cube of resolutions. For this we represent a knot K as a braid closure $\widehat{\beta}$ and associate with it a complex $C^{AG}(\widehat{\beta})$ of $\mathbb{Z}[q, q^{-1}]$ -modules, such that

$$(5) \quad H_{\bullet}(C^{AG}(\widehat{\beta}) \otimes \mathbb{Z}[q^{-1}, q]) \cong \widehat{HFK}(K) \otimes \mathbb{Z}[q^{-1}, q].$$

The first complex satisfying (5) with \mathbb{F} instead of \mathbb{Z} was constructed by Alison Gilmore in [Gil16]. With vertices of the cube she associated quotients of polynomial rings by local and non-local relations.

On the geometric side, the proof of (5) requires a choice of a coherent system of orientations for moduli spaces of holomorphic disks associated with a multipointed Heegaard diagram and to track signs in all proofs of [OS09]. Let us mention that even though the results of [OSS09] and [OS09] were stated over \mathbb{F} , these papers contain the expected signs. This makes the comparison easier. The main ingredients of our proof are the result of [AE15] about the existence and properties of coherent systems of orientations, Theorem 4.19 establishing the skein exact triangle over \mathbb{Z} , as well as Proposition 4.21 and Theorem 5.10 that allow to identify the algebras assigned to vertices of the cube. In addition, we improve and streamline many arguments in [OS09]. For example, we consistently work with admissible diagrams, however link diagrams used in [OS09] are not admissible, and we conceptualize the construction of twisted complexes.

On the algebraic side, we extend Gilmore's construction to all annular webs and interpret it in terms of Soergel bimodules. Here we work over an arbitrary commutative ring \mathbb{k} with a fixed invertible element q . The space $\mathcal{A}(\omega)$ that we assign to an annular web ω is a quotient of the quantum Hochschild homology [BPW19] of the Soergel bimodule associated with the web by (renormalized) non-local relations. In the case of a resolution of a braid this quotient is identified with Gilmore's algebra after renormalizing her variables: we check that Gilmore's local relations coincide with the Soergel relations, whereas non-local relations with those defined for webs.

Combining previous results with the general theory of quantum traces [BPW19] we obtain a new conceptual interpretation of Gilmore's construction, opening the floor for its further generalizations. Recall that similarly to the non-quantized setting, the quantum horizontal trace induces a functor from quantum annular foams to the quantum Hochschild homology of Soergel bimodules. In Proposition 5.5 we prove that the non-local relations are preserved by this functor. Hence, we obtain a new functorial evaluation of quantum annular foams by using the *quotient* of the quantum Hochschild homology by the non-local relations. This quotient can be used to generalize Gilmore's construction and to define new homology theories.

In particular, we modify $\mathcal{A}(\omega)$ by killing q -torsion. Namely, given a web ω we consider the map

$$(6) \quad Q_{\omega}: \mathcal{A}(\omega, \mathbb{Z}[q^{-1}, q]) \longrightarrow \mathcal{A}(\omega; \mathbb{Z}[q^{-1}, q])$$

induced by the inclusion of coefficient rings. In general the map Q_{ω} is not injective. Dividing the previous construction by the kernel of Q_{ω} and tensoring it with \mathbb{k} over $\mathbb{Z}[q^{-1}, q]$ produces a new functorial assignment of a \mathbb{k} -algebra $qAG(w)$ to a quantum annular web ω . By inserting these algebras into a cube of resolutions for a knot $K = \widehat{\beta}$ we obtain our main player—a new chain complex¹ $qAG(\widehat{\beta})$, the homology of which we denote by $qAGH(\widehat{\beta})$. Since qAG is defined over

¹The name of the new complex is motivated by the fact that it interpolates the **A**lgebraic categorification of the last two authors and the **G**eometric categorification of Ozsváth and Szabó.

$\mathbb{Z}[q^{-1}, q]$, it can be specialized at $q = 1$, resolving our main problem. We denote these specializations at $q = 1$ by $AG(\widehat{\beta})$ and $AGH(\widehat{\beta})$ respectively. As we shall see, this new chain complex interpolates between the algebraic and geometric settings previously discussed in the following way.

Proposition A. *The homology theories AGH and $H^{\mathfrak{gl}_0}$ coincide. Hence, AGH is a knot invariant if \mathbb{K} is a field.*

We expect the following to be true.

Conjecture 1. *If \mathbb{K} is a field of characteristic 0, then $qAGH$ is a knot invariant for any q .*

In the next step we analyse the Bockstein spectral sequence associated with the specialization of $qAGH$ at $q = 1$. Note that this spectral sequence preserves the Alexander grading. To be more precise, we fix an arbitrary field \mathbb{K} and work over the principal ideal domain $\mathbb{K}[q, q^{-1}]$. Thanks to Proposition A we can identify the first page of our spectral sequence with $H^{\mathfrak{gl}_0}$ and by (5) the last page, which is the quotient of $qAGH \otimes \mathbb{K}$ by its torsion submodule, is isomorphic to \widehat{HFK} (compare this with Proposition A.7).

Theorem B. *Assume that \mathbb{K} is a field and K is a knot represented by a braid closure $\widehat{\beta}$. Then the $(q \mapsto 1)$ Bockstein spectral sequence applied to $qAG(\widehat{\beta}; \mathbb{K}[q, q^{-1}])$ has $H^{\mathfrak{gl}_0}(K; \mathbb{K})$ as its first page and converges after finitely many steps. The last page is (non-canonically) isomorphic to $\widehat{HFK}(K; \mathbb{K})$.*

Recall that in [RW22] a spectral sequence from HHH^{red} to $H^{\mathfrak{gl}_0}$ was constructed over \mathbb{Q} .

Theorem ([RW22]). *There exists a differential d_0 of $(\mathfrak{a}, \mathfrak{q}, \mathfrak{t})$ -degree $(-2, 0, 1)$ on the Hochschild homology of reduced Soergel bimodules over any field of characteristic 0 that induces a spectral sequence from HHH^{red} to $H^{\mathfrak{gl}_0}$.*

The above theorem uses the following convention for gradings: the Koszul differential d_K is of $(\mathfrak{a}, \mathfrak{q}, \mathfrak{t})$ -degree $(-2, 2, 1)$, whereas the degree of the hypercube differential d_{top} is $(0, 0, 1)$.

Combining this spectral sequence with the one from Theorem B we get the main result of this paper.

Theorem C (DGR Conjecture). *For any knot K and any field of characteristic zero, the bigraded dimension of HHH^{red} (after forgetting the \mathfrak{a} -grading) is greater or equal to the bigraded dimension of \widehat{HFK} .*

The conjectural degree of the differential ∂_0 of Dunfield–Gukov–Rasmussen was expected to be $(\mathfrak{a}, \mathfrak{q}, \mathfrak{t}) = (2, 0, 1)$ and $(2k, 0, 1)$ for $k > 1$ in general if one expects a full spectral sequence. This degree is precisely $2\deg(d_{\text{top}}) - \deg(d_0)$, which is the degree of the differential on the complex of the filtered spectral sequence formed by computing d_0 and then d_{top} (after homology with respect to d_K and ascending filtration associated to the \mathfrak{a} -grading are taken). Notice that the combination of the two spectral sequences guarantees that higher differentials are always of degree 1 with respect to the \mathfrak{t} -grading, hence are compatible with the conjectural degrees and establish the bigraded rank inequality.

To investigate the question whether our spectral sequence collapses at the first step we compute the homology $H^{\mathfrak{gl}_0}$. Over \mathbb{Q} this question can be handled using the known computations for HHH^{red} and the spectral sequence between HHH^{red} and $H^{\mathfrak{gl}_0}$.

Consider the first case of interest, namely the $T(3, 4)$ -torus knot. The Poincaré polynomial of the reduced triply graded link homology of this knot is

$$\begin{aligned} P(\mathfrak{t}, \mathfrak{a}, \mathfrak{q}) = & \mathfrak{a}^{-6}\mathfrak{q}^{-6}\mathfrak{t}^6 + \mathfrak{a}^{-8}\mathfrak{q}^{-4}\mathfrak{t}^5 + \mathfrak{a}^{-6}\mathfrak{q}^{-2}\mathfrak{t}^4 + (\mathfrak{a}^{-8}\mathfrak{q}^{-2} + \mathfrak{a}^{-8}\mathfrak{q}^0)\mathfrak{t}^3 \\ & + (\mathfrak{a}^{-6}\mathfrak{q}^0 + \mathfrak{a}^{-6}\mathfrak{q}^2 + \mathfrak{a}^{-10}\mathfrak{q}^0)\mathfrak{t}^2 + (\mathfrak{a}^{-8}\mathfrak{q}^2 + \mathfrak{a}^{-8}\mathfrak{q}^4)\mathfrak{t}^1 + \mathfrak{a}^{-6}\mathfrak{q}^6\mathfrak{t}^0. \end{aligned}$$

On one hand, a direct investigation using the degree of the differential d_0 shows that the total dimension of the $H^{\mathfrak{gl}_0}$ [RW22] is at least 9: the only terms that can cancel out are $a^{-8}q^0t^3$ and $a^{-6}q^0t^2$. On the other hand, the total dimension of \widehat{HFK} for the same knot is 5, with three pairs that should cancel out:

$$a^{-10}q^0t^2 \leftrightarrow a^{-8}q^0t^3, \quad a^{-8}q^2t^1 \leftrightarrow a^{-6}q^2t^2, \quad \text{and} \quad a^{-8}q^{-2}t^3 \leftrightarrow a^{-6}q^{-2}t^4.$$

A direct consequence is that $H^{\mathfrak{gl}_0}$ and \widehat{HFK} do not coincide over \mathbb{Q} . Hence, the combination of our two spectral sequences does not always degenerate.

In the example of $T(3, 4)$, the term $a^{-8}q^0t^3$ cancels out with either $a^{-10}q^0t^2$ or $a^{-6}q^0t^2$. It is a priori unclear, though, with which one and in which of the two spectral sequences this cancellation happens. However recent computations by Laura Marino (adapting her program [Mar23]) show that $HHH^{\text{red}}(T(3, 4))$ and $H^{\mathfrak{gl}_0}(T(3, 4))$ have the same rank, hence the cancellation occurs in the Bockstein type spectral sequence.

1.2. Applications. As it was already noticed by Manolescu [Man15], the existence of a spectral sequence from the reduced triply graded homology HHH^{red} to knot Floer homology \widehat{HFK} yields a couple of detection results for HHH^{red} . In this section we establish these detection results for both HHH^{red} and $H^{\mathfrak{gl}_0}$ with \mathbb{Q} -coefficients.

Recall that in [OS04a] it was proven that \widehat{HFK} detects the Seifert genus of the knot and hence the unknot, which is the only knot of genus 0. The statement was originally formulated for $\mathbb{k} = \mathbb{Z}$. However, as noticed by many authors (see for instance [BVV18, BM20]), it remains true over any field. Theorems C and B allow us to extend this result to HHH^{red} and $H^{\mathfrak{gl}_0}$.

Corollary D. *The \mathfrak{gl}_0 homology and the reduced triply graded homology (both with \mathbb{Q} -coefficients) detect the unknot.*

If Conjecture 1 holds, then the same is true for $qAGH$ at any q .

Proof. Suppose K has the same \mathfrak{gl}_0 homology as the unknot, that is $H^{\mathfrak{gl}_0}(K) = \mathbb{Q}$ concentrated in bidegree $(0, 0)$. Nothing can happen in the spectral sequence from $H^{\mathfrak{gl}_0}$ to \widehat{HFK} , so that $\widehat{HFK}(K, \mathbb{Q}) = \mathbb{Q}$ in bidegree $(0, 0)$ and K is therefore the unknot. The argument for HHH^{red} is the same. \square

By the results of Ghiggini [Ghi08] and Ni [Ni07], \widehat{HFK} detects fiberedness of the knot and the only fibered knots of genus 1 are the two trefoils and the figure-eight knot. The knot Floer homologies of these knots appear to be different. Hence, \widehat{HFK} detects these knots too. In addition, it was proven more recently that knot Floer homology detects the cinquefoil [FRW22]. Applying Theorems C and B we deduce that all these knots are also detected by HHH^{red} and $H^{\mathfrak{gl}_0}$. Note that \mathfrak{gl}_0 and reduced triply graded homology groups for these knots are given in Appendix C.

Corollary E. *The \mathfrak{gl}_0 homology and the reduced triply graded homology (both with \mathbb{Q} -coefficients) detect the two trefoils, the figure-eight knot and the cinquefoil.*

Besides of telling knots apart, Corollary E demonstrates strength of algebraic knot homology theories.

Proof. The argument is exactly the same for both homology theories and all knots: by degree reasons there are no cancellations in the spectral sequences. Let us provide a detailed proof for \mathfrak{gl}_0 homology. Suppose that the Poincaré polynomial of the \mathfrak{gl}_0 homology of a knot is equal to the one of the cinquefoil, $q^4 + q^2t^1 + t^2 + q^{-2}t^3 + q^{-4}t^4$. Because the $(q \mapsto 1)$ Bockstein spectral sequence preserves the q -degree, this knot has the same knot Floer homology as the cinquefoil. Hence, by [FRW22], it is the cinquefoil. Exactly the same argument works for both trefoils. In case of the figure-eight knot, the homology in the (q, t) -degree $(0, 0)$ has rank 3. However, since

the differential in the $(q \mapsto 1)$ Bockstein spectral sequence has (\mathbf{q}, \mathbf{t}) -degree $(0, 1)$, there is again no cancellation. To conclude the result for HHH^{red} we check that the Poincaré polynomials listed in Appendix C have no cancelling pairs with respect to differentials of $(\mathbf{a}, \mathbf{q}, \mathbf{t})$ -degree $(2k, 0, 1)$. \square

Let us mention that similar detection results are also valid for Khovanov homology [KM11, BS22, BHS21, BDL⁺21], where the last two papers are based on the Dowlin spectral sequence [Dow18] that uses an integral version of [OS09]. Combined with our \mathbb{Z} -valued cube of resolutions model for \widehat{HFK} , these results are fully justified.

The above mentioned detection results for HHH^{red} can also be obtained by combining Dowlin’s and Rasmussen’s [Ras15] spectral sequences. Notice that in this case, one should work with the single δ -graded (rather than bigraded) versions of Khovanov and knot Floer homologies. Recently, in [BS22] Baldwin and Sivek again used the Dowlin spectral sequence to prove that HHH^{red} detects an infinite family of pretzel knots $P(-3, 3, 2n+1)$, $n \in \mathbb{Z}$, that are all not fibered. We would expect that our methods also allow to reprove these results.

1.3. Outline. Besides Introduction, this paper is divided in four sections. The first section is devoted to algebraic preliminaries: we recall classical facts and introduce notations concerning symmetric polynomials, Soergel bimodules and quantum Hochschild homology. Then we discuss webs and foams and finally we apply the technology of quantum traces [BPW19] to webs and foams. We define the functor B from (4) and discuss its quantum horizontal trace. Furthermore, we show that the higher quantum Hochschild homology of a singular Soergel bimodule for generic quantum parameters vanishes (Theorem 2.36). In Section 3 we review the general cube of resolutions construction and three different combinatorial link homologies based on it:

- (1) the triply graded Khovanov–Rozansky link homology,
- (2) the symmetric \mathfrak{gl}_1 link homology based on the Robert–Wagner foam evaluation formula,
- (3) the \mathfrak{gl}_0 homology introduced by the two last authors in [RW22].

In Section 4 we review the construction of the twisted Heegaard Floer homology for singular links and systematically upgrade coefficients to \mathbb{Z} . Then we construct skein exact triangles and compute homology over \mathbb{Z} for planar singular knots. Section 5 is the heart of the paper: here we finish the construction of the cube of resolutions over \mathbb{Z} , define the algebra $\mathcal{A}(\omega)$ for any annular web, prove (5) and finally introduce the complex $qAGH$, the homology of which interpolates between \mathfrak{gl}_0 homology and knot Floer homology. By applying the Bockstein spectral sequence we prove main results of this paper — Theorems B and C. Finally, Appendix A provides a self-contained account on spectral sequences, Appendix B contains a technical lemma about quantum Hochschild homology and Appendix C includes computation of $H^{\mathfrak{gl}_0}$ needed for the detection results.

1.4. Acknowledgements. The authors would like to thank John Baldwin, Paolo Ghiggini and Ciprian Manolescu for helpful conversations, as well as Peter Ozsváth and Zoltan Szabó for the clarification of details in their cube construction. They are also indebted to the anonymous referees who helped us to improve the exposition with their careful readings and valuable comments. AB and EW are grateful to the organizers of the Budapest and Annular meetings of the Simons Collaboration “New Structures in Low-Dimensional Topology” in 2023/24 for creating a stimulating working environments. AB is also supported by the above mentioned Simons Collaboration and the Swiss National Science Foundation grant 200020_207374. AB and KP are supported by NCCR SwissMAP of the Swiss National Science Foundation. LHR was supported by the Luxembourg National Research Fund PRIDE17/1224660/GPS. EW is partially supported by the ANR projects AlMaRe (ANR-19-CE40-0001-01), AHA (JCJC ANR-18-CE40-0001) and CHARMES (ANR-19-CE40-0017).

2. PRELIMINARIES

2.1. Conventions. In this paper we work over a fixed commutative unital ring \mathbb{k} with no further restrictions and we pick an invertible $q \in \mathbb{k}$. An unadorned tensor product means a tensor product over \mathbb{k} .

The bold letter \mathbf{q} is used for a shift functor in a graded category. In particular, $\mathbf{q}^d M$ is a graded module M shifted upwards by d , so that $(\mathbf{q}^d M)_i = M_{i-d}$. More generally, if $p(q) = \sum_{i \in \mathbb{Z}} a_i q^i$ is a Laurent polynomial in q with positive integral coefficients, then

$$p(\mathbf{q})M := \bigoplus_i \mathbf{q}^i M^{\oplus a_i}$$

We often use *quantum integers*, *quantum factorials*, and *quantum binomials*, defines respectively as

$$[k] = \frac{q^k - q^{-k}}{q - q^{-1}}, \quad [k]! = \prod_{i=1}^k [i] \quad \text{and} \quad \begin{bmatrix} n \\ k \end{bmatrix} = \frac{[n]!}{[k]![n-k]!}$$

for any integers $0 \leq k \leq n$.

Complexes have differentials of degree $+1$, with the only exception of the Hochschild homology (Section 2.3). We use \mathbf{t} for the standard homological shift, so that $(\mathbf{t}^a C)_i = C_{i+a}$ and the *mapping cone complex* $C(f)$ of a chain map $f: C \rightarrow D$ is modeled on $\mathbf{t}C \oplus D$.

Finally, braids and webs are drawn and read from left to right, whereas foams are drawn and read from bottom to top. Other notation used through the paper:

- β is a braid (diagram) and $\widehat{\beta}$ is its braid closure;
- \mathfrak{X} denotes the set of crossings in the diagram;
- n_+, n_-, n_\times are the numbers of positive, negative and singular crossings, respectively.

2.2. Symmetric polynomials and Soergel bimodules. In this section we summarize some useful facts about symmetric polynomials and Soergel bimodules. We refer to [Mac15] and [EMTW20] for a detailed account.

Notation 2.1. The number of boxes of a given Young diagram λ is denoted by $|\lambda|$. Given two non-negative integers a and b , we write $T(a, b)$ for the set of Young diagrams with at most a columns and at most b rows. The maximal diagram, a rectangle of width a and height b , is hereafter denoted by $\text{box}(a, b)$. Given a Young diagram $\lambda \in T(a, b)$ we construct its

- *complement* $\lambda^c \in T(a, b)$ by rotating by 180 degrees the set of boxes from $\text{box}(a, b)$ that are not in λ ,
- *transpose* $\lambda^t \in T(b, a)$ by exchanging rows with columns in λ ,
- *dual* $\widehat{\lambda} \in T(b, a)$ as the diagram $(\lambda^t)^c = (\lambda^c)^t$.

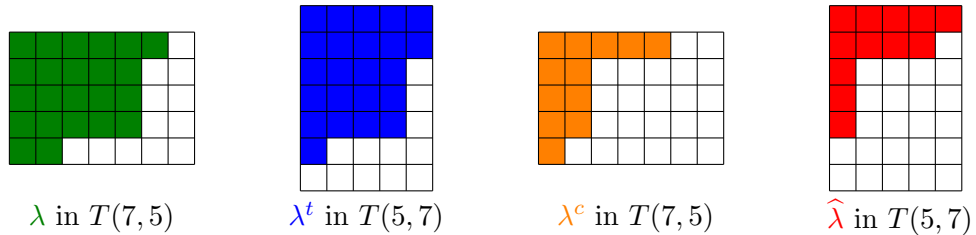


FIGURE 1. Pictorial definition of λ^c , λ^t and $\widehat{\lambda}$.

Fix a positive number $N > 0$ and recall that \mathbb{k} is a fixed commutative unital ring. Consider the polynomial ring $R := \mathbb{k}[x_1, \dots, x_N]$ with an action of the symmetric group \mathfrak{S}_N that permutes

the variables. Endow R with a grading by declaring that all x_i are homogeneous of degree 2. It is a standard fact that the ring of invariant polynomials

$$\text{Sym}_N := R^{\mathfrak{S}_N}$$

is freely generated by elementary symmetric functions

$$e_k(x_1, \dots, x_N) = \sum_{i_1 < \dots < i_k} x_{i_1} \cdots x_{i_k}$$

for $k = 1, \dots, N$. A linear basis of Sym_N is given by *Schur polynomials* s_λ parametrized by Young diagrams λ with at most N rows. They satisfy

$$s_\lambda s_\mu = \sum_{\nu} c_{\lambda\mu}^{\nu} s_\nu$$

where $c_{\lambda,\mu}^{\nu} \in \mathbb{N}$, the Littlewood–Richardson coefficients, are independent of N . Because $c_{\lambda\mu}^{\nu} = 0$ unless $|\lambda| + |\mu| = |\nu|$, the above sum is finite.

Proposition 2.2. *Let X, Y and Z be pairwise disjoint finite sets of variables. Then the following equations hold for any Young diagram λ :*

$$(7) \quad s_\lambda(X \sqcup Z) = \sum_{\alpha, \beta} c_{\alpha\beta}^{\lambda} s_\alpha(X) s_\beta(Z),$$

$$(8) \quad s_\lambda(X) = \sum_{\alpha, \beta} c_{\alpha\beta}^{\lambda} (-1)^{|\beta|} s_\alpha(X \sqcup Z) s_{\beta^t}(Z), \text{ and}$$

$$(9) \quad \sum_{\alpha, \beta} (-1)^{|\beta|} c_{\alpha\beta}^{\lambda} s_\alpha(X) s_{\beta^t}(Y) = \sum_{\alpha, \beta} (-1)^{|\beta|} c_{\alpha\beta}^{\lambda} s_\alpha(X \sqcup Z) s_{\beta^t}(Y \sqcup Z).$$

Proof. The derivation of (7) can be found in [Mac15, eq.(5.9)] and the formula (8) is the special case of (9) for $Y = \emptyset$. The last equality is proven in [RW20a, Lemma A.7]. \square

Corollary 2.3. *Let a, b be two non-negative integers and X, Y, Z pairwise disjoint finite sets of variables. Then*

$$\sum_{\alpha \in T(a,b)} (-1)^{|\hat{\alpha}|} s_\alpha(X) s_{\hat{\alpha}}(Y) = \sum_{\alpha \in T(a,b)} (-1)^{|\hat{\alpha}|} s_\alpha(X \sqcup Z) s_{\hat{\alpha}}(Y \sqcup Z).$$

Proof. Set $\lambda = \text{box}(a, b)$ in (9). \square

A sequence of positive numbers $\underline{k} = (k_1, \dots, k_r)$ with $k_1 + \dots + k_r = N$ is called a *composition* of N . It determines a parabolic subgroup $\mathfrak{S}_{\underline{k}} := \mathfrak{S}_{k_1} \times \dots \times \mathfrak{S}_{k_r}$ of \mathfrak{S}_N and a ring $R^{\underline{k}} := R^{\mathfrak{S}_{\underline{k}}}$ of polynomials invariant under the action of the subgroup. In particular, $R^{(1, \dots, 1)} = R$ and $R^{(N)} = \text{Sym}_N$. Clearly, $R^{\underline{k}} \cong \text{Sym}_{k_1} \otimes \dots \otimes \text{Sym}_{k_r}$.

We say that a composition $\underline{\ell}$ is a *refinement* of \underline{k} if it is obtained by replacing each k_i with a composition of k_i , possibly of length 1. In such case $\mathfrak{S}_{\underline{\ell}} \subseteq \mathfrak{S}_{\underline{k}}$ and $R^{\underline{k}}$ is a subring of $R^{\underline{\ell}}$. The following is a standard fact from representation theory.

Theorem 2.4 ([EMTW20, Theorem 24.40]). *Let \underline{k} be a composition of N and $\underline{\ell}$ a refinement of \underline{k} . Then $R^{\underline{k}} \subseteq R^{\underline{\ell}}$ is a graded Frobenius extension.² In particular, $R^{\underline{\ell}}$ is a free module over $R^{\underline{k}}$.*

²An extension $A \subseteq B$ is *Frobenius* if there is a nondegenerate A -linear trace $\epsilon: B \rightarrow A$. It is a *graded extension of degree d* if A and B are graded and ϵ is homogeneous of degree $-2d$.

Example 2.5 (cf. [KLMS12, Theorem 2.12]). Assume that $\underline{\ell} = (\ell_1, \dots, \ell_{r+1})$ is an *elementary* refinement of \underline{k} , i.e. there exists an index i , such that

$$k_j = \begin{cases} \ell_j, & j < i, \\ \ell_i + \ell_{i+1}, & j = i, \\ \ell_{j+1}, & j > i. \end{cases}$$

Then the extension $R^{\underline{k}} \subset R^{\underline{\ell}}$ has degree $\ell_i \ell_{i+1}$ and the basis of $R^{\underline{\ell}}$ is given by elements

$$b_\lambda := 1^{\otimes i} \otimes s_\lambda \otimes 1^{\otimes r-i}$$

with $\lambda \in T(\ell_{i+1}, \ell_i)$. The trace map $\epsilon: R^{\underline{\ell}} \rightarrow R^{\underline{k}}$ takes b_λ to 1 if $\lambda = \text{box}(\ell_{i+1}, \ell_i)$ and to 0 otherwise.

Example 2.6. The ring $R^{\underline{k}}$ is a free module over $R^{(N)} \cong \text{Sym}_N$. It has a basis given by pure tensors of Schur polynomials

$$1 \otimes s_{\lambda_2} \otimes \dots \otimes s_{\lambda_r},$$

where λ_i is a Young diagram with at most $k_1 + \dots + k_{i-1}$ columns and k_i rows.

Let **Bim** be the bicategory of rings, bimodules, and bimodule maps, with the horizontal composition given by the tensor product of bimodules. Consider the induction and restriction bimodules

$$\text{Ind}_{\underline{k}}^{\underline{\ell}} \cong_{R^{\underline{\ell}}(R^{\underline{k}})_{R^{\underline{k}}}} \quad \text{Res}_{\underline{k}}^{\underline{\ell}} \cong_{R^{\underline{k}}(\mathbf{q}^d R^{\underline{\ell}})_{R^{\underline{\ell}}}}$$

for all Frobenius extensions $R^{\underline{k}} \subset R^{\underline{\ell}}$, where d is the degree of the extension. Their finite compositions, i.e. tensor products over the polynomial rings, are called *singular Bott–Samelson bimodules*.

Definition 2.7. The *bicategory of singular Soergel bimodules* **sSBim** is the full graded additive and idempotent complete subcategory of **Bim** with rings $R^{\underline{k}}$ as objects and 1-morphisms generated by singular Bott–Samelson bimodules. In other words, every 1-morphism in **sSBim**($R^{\underline{k}}, R^{\underline{\ell}}$) is a direct summand of a bimodule of the form $\bigoplus_{i=1}^r \mathbf{q}^{d_i} B_i$, where each $B_i \in \mathbf{Bim}(R^{\underline{k}}, R^{\underline{\ell}})$ is a singular Bott–Samelson bimodule.

Remark 2.8. It follows directly from the definition that a singular Soergel bimodule is projective when seen as a left or as a right module. Moreover, it is free when it is a direct sum of singular Bott–Samelson bimodules.

Remark 2.9. The morphism category **sSBim**(R, R) is the category of classical (i.e. non-singular) Soergel bimodules.

2.3. Hochschild homology. Let A be a \mathbb{k} -algebra and M an (A, A) -bimodule. The *Hochschild homology* of M is the homology of the chain complex $CH_\bullet(A, M)$ with chain groups $CH_n(A, M) := M \otimes A^{\otimes n}$ and the differential given by the alternating sum

$$\begin{aligned} \partial(m \otimes a_1 \otimes \dots \otimes a_n) &= m a_1 \otimes a_2 \otimes \dots \otimes a_n \\ &+ \sum_{i=1}^{n-1} (-1)^i m \otimes a_1 \otimes \dots \otimes a_i a_{i+1} \otimes \dots \otimes a_n \\ &+ (-1)^n a_n m \otimes a_1 \otimes \dots \otimes a_{n-1}. \end{aligned} \tag{10}$$

The quotient $HH_0(A, M) \cong M/[A, M]$ is known as the *space of coinvariants* of M , where $[A, M] := \{am - ma \mid a \in A, m \in M\}$ is the *commutator* of A and M .

Given an algebra automorphism $\varphi \in \text{Aut}(A)$, we can replace the last term of the differential with

$$(-1)^n \varphi(a_n) m \otimes a_1 \otimes \dots \otimes a_{n-1}. \tag{11}$$

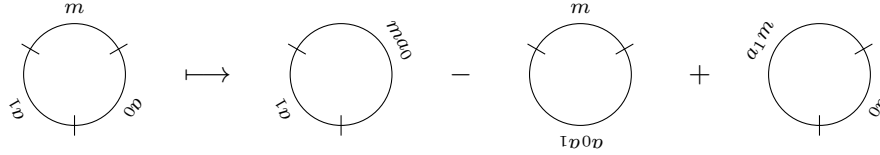
The resulting complex $CH_\bullet^\varphi(A, M)$ is the φ -*twisted Hochschild complex*. When both A and M are graded, then the complex admits a natural automorphism, which leads to *quantum Hochschild*

homology introduced in [BPW19]. Fix an invertible element $q \in \mathbb{k}$ and define $\varphi(a) = q^{-|a|}$, where $|a|$ is the degree of a homogeneous element $a \in A$. Then the last term of the twisted Hochschild differential (11) takes the form

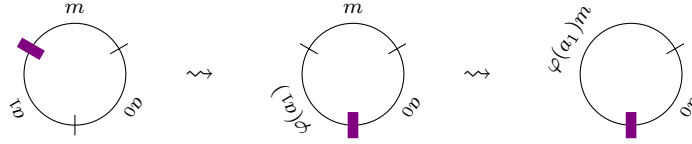
$$(12) \quad (-1)^n q^{-|a_n|} a_n m \otimes a_1 \otimes \cdots \otimes a_{n-1}.$$

The *quantum Hochschild homology* of M , denoted by $qHH_\bullet(A, M)$, is the homology of this complex. This construction was also reviewed in [Lip20]. Following the usual conventions we write $qCH(A)$ and $qHH(A)$ when $M = A$. Additionally, when A is clear from the context, we write $qHH(M)$.

Remark 2.10. Hochschild chains can be visualized by circles divided into segments, one labeled with $m \in M$ and the others with a_0, \dots, a_n . Each of the terms of the differential merges two segments multiplying their labels.



In the twisted case add a mark on the circle between segments labeled m and a_n . To merge these two segments, one has to move a_n over the mark, acting upon it with φ as depicted below.



The quantum Hochschild homology can be seen as arising from twisting bimodules by algebra automorphisms. Namely, given $\varphi \in \text{Aut}(A)$ and a left A -module M , denote by ${}_\varphi M$ its φ -twist, defined as the module M with the action twisted by φ , i.e. $a \cdot m := \varphi(a)m$. If M is an (A, A) -bimodule, then it follows directly from the definition that

$$(13) \quad CH^\varphi_\bullet(A, M) \cong CH_\bullet(A, {}_\varphi M).$$

The following property is proven in [BPW19].

Proposition 2.11. *Choose graded \mathbb{k} -algebras A, B, C and graded (A, B) - and (B, C) -bimodules M and N . Then for any invertible scalars $q_1, q_2 \in \mathbb{k}$ there is a bimodule isomorphism*

$$q_1 M \otimes_B q_2 N \xrightarrow{\cong} q_1 q_2 (M \otimes_B N)$$

defined as $m \otimes n \mapsto q_2^{|m|} m \otimes n$ for homogeneous $m \in M$ and $n \in N$.

This implies together with (13) that the quantum Hochschild homology is invariant under cyclic permutation of tensor factors.

Proposition 2.12. *Pick graded \mathbb{k} -algebras A and B and graded (A, B) - and (B, A) -bimodules M and N that are projective as left modules. Then there is an isomorphism*

$$qHH_\bullet(A, M \otimes_B N) \cong qHH_\bullet(B, N \otimes_A M)$$

for any invertible parameter $q \in \mathbb{k}$.

We end this section with a statement about the quantum Hochschild homology for the algebra R^k . The proof, which is rather technical, is postponed to Appendix B.

Proposition 2.13. *Suppose that $1 - q^d$ is invertible for $d \neq 0$. Then the inclusion $\mathbb{k} \subset R^k$ induces a homotopy equivalence of chain complexes*

$$qCH_\bullet(R^k) \simeq qCH_\bullet(\mathbb{k}) \simeq \mathbb{k},$$

where \mathbb{k} lives in homological degree 0. In particular, higher quantum Hochschild homology vanishes.

2.4. Webs and foams. This section provides the basics of webs and foams and results that are fundamental for this paper. More details can be found in [RW20a, RW22] and [QR16, QRS18]. We consider only webs and foams embedded in smooth manifolds and for a technical reason we assume that they have *collared boundary*. This means that for a smooth manifold M we fix a smooth embedding $\partial M \times [0, 1] \rightarrow M$ that takes $(x, 0)$ to x . This technical condition implies a canonical smooth structure on the gluing of two such manifolds along a boundary component.

Definition 2.14. Let Σ be an oriented smooth surface with a collared boundary. A *web* $\omega \subset \Sigma$ is an oriented trivalent graph, possibly with endpoints, smoothly embedded³ in Σ in a way, such that it coincides with $\partial\omega \times [0, 1)$ on the collar of $\partial\Sigma$. The edges of the web are labeled with positive integers such that at each trivalent vertex the *flow condition* holds: the sum of labels of incoming edges is equal to the sum of labels of outgoing edges. We write $E(\omega)$ and $V(\omega)$ respectively for the sets of edges and vertices of a web ω and $\ell(e)$ for the label of an edge e . We call $\ell(e)$ the *thickness* of e .

The flow condition implies that each vertex of a web is either a *split* or a *merge*, illustrated respectively on the left and the right hand side of Figure 2.



FIGURE 2. A split and a merge vertex in a web.

In this paper we are mostly interested in webs in a strip $[0, 1] \times \mathbb{R}$ (*planar webs*) or an annulus $\mathbb{S}^1 \times \mathbb{R}$ (*annular webs*). We say that such a web ω is *directed* if the projection on $[0, 1]$ or \mathbb{S}^1 respectively has no critical points when restricted to ω and that projection of orientations agree with that of $[0, 1]$ or \mathbb{S}^1 respectively. Such a web can be visualized as a result of a tangential gluing of parallel intervals oriented from left to right (or circles oriented anticlockwise in the annular case), see Figure 3. The reverse operation is called a *lamination* [QW21]. In particular, a directed web ω



FIGURE 3. A directed planar web of index 4 (on the left) and its lamination (on the right).

can be decomposed into a sequence of merges and splits. Hence, the sum of thicknesses at a generic section $\omega_t := \omega \cap (\{t\} \times \mathbb{R})$ is constant. We call it the *index* of ω . In case of webs in a strip, the section ω_0 and ω_1 are called respectively the *input* and the *output* of ω .

Remark 2.15. Directed annular webs are called *vinyl graphs* in [RW20b].

Definition 2.16. Let M be an oriented smooth 3-manifold with a collared boundary. A *foam* $W \subset M$ is a collection of *facets*, that are compact oriented surfaces labeled with positive integers and glued together along their boundary points in a way, such that every point p of W has a closed neighborhood homeomorphic to one of the following:

³Meaning that each edge is smoothly embedded when seen as a 1-dimensional manifold with boundary.

- a disk, when p belongs to a unique facet,
- $Y \times [0, 1]$, where Y is a merge or a split web, when p belongs to three facets, or
- the cone over the 1-skeleton of a tetrahedron with p as the vertex of the cone (so that it belongs to six facets).

See Figure 4 for a pictorial representation of these three cases. The set of points of the second type is a collection of curves called *bindings* and the points of the third type are called *singular vertices*. The *boundary* ∂W of W is the closure of the set of boundary points of facets that do not belong to a binding. It is understood that W coincides with $\partial W \times [0, 1]$ on the collar of ∂M . We write $F(W)$ for the collection of facets of W and $\ell(f)$ for the thickness of a facet f . A foam W is *decorated* if each facet $f \in F(W)$ is assigned a symmetric polynomial $P_f \in \text{Sym}_{\ell(f)}$.

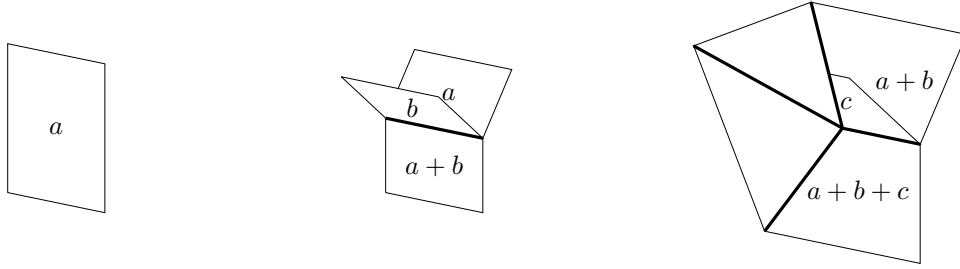


FIGURE 4. The three local models for a foam.

Remark 2.17. A foam satisfies a 2-dimensional version of the flow condition: three facets meet at each binding in a way, such that the thickness of one of them is equal to the sum of thicknesses of the other two. The binding induces orientation from the two thinner facets; it is opposite to the one induced from the thickest facet.

The boundary of a foam $W \subset M$ is a web in ∂M . In case $M = \Sigma \times [0, 1]$ is a thickened surface, we require that $\partial W \cap (\partial \Sigma \times [0, 1])$ is a collection of vertical lines, that are lines of the form $\{x\} \times [0, 1]$ for $x \in W$. A generic section $W_t := W \cap (\Sigma \times \{t\})$ is a web, each with the same boundary. The bottom and top webs W_0 and W_1 are called respectively the *input* and *output* of W .

Let $\text{Foam}(M)$ be the \mathbb{k} -module generated by decorated foams in M modulo *local relations*, defined as follows. Consider the collection of Robert–Wagner evaluations

$$\langle -, - \rangle_N : \text{Foam}(\mathbb{D}^3) \otimes \text{Foam}(\mathbb{D}^3) \rightarrow \text{Sym}_N$$

from [RW20a]. We impose the relation $a_1 W_1 + \dots + a_r W_r = 0$ whenever there is a 3-ball $B \subset M$, such that all sets $W_i \setminus B$ coincide and the linear combination $\sum_i a_i (W_i \cap B)$ is in the radical of $\langle -, - \rangle_N$ for all $N > 0$. The set $\text{Foam}(M)$ is graded by $\mathbb{Z} \oplus \mathbb{Z}$, see [ETW18] for details.⁴

2.4.1. The bicategory of directed foams. Let us now consider foams between planar directed webs (so that $\Sigma = [0, 1] \times \mathbb{R}$). In this situations we impose the additional condition that a foam W is “directed” itself, i.e. that the projection onto the side square $[0, 1] \times [0, 1]$ has no critical points when restricted to W . This immediately implies that a generic section of W is a directed web as defined above. A foam of this type can be decomposed into seven basic homogeneous pieces: traces of isotopies and six singular blocks shown in Figure 5. For all of them the second component of the $(\mathbb{Z} \oplus \mathbb{Z})$ -grading vanishes, so that the space of directed foams is \mathbb{Z} -graded.

Definition 2.18. Let **Foam** be the bicategory of ∞ -foams, in which

- objects are finite sequences of points on a line, labeled with positive integers,

⁴This $\mathbb{Z} \oplus \mathbb{Z}$ -grading is related to the \mathbb{Z} -grading of \mathfrak{gl}_n foams by collapsing (a, b) into $a + Nb$.

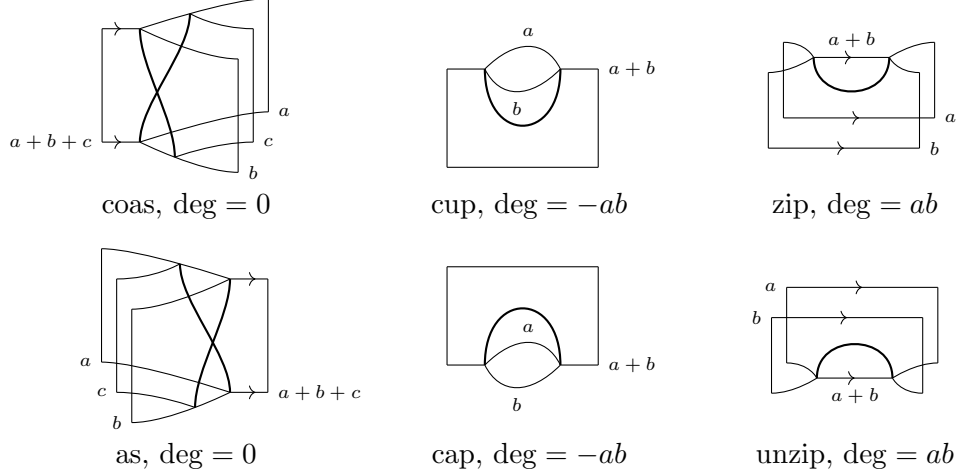


FIGURE 5. Local models for all singularities of directed foams, together with their degrees.

- 1-morphisms from \underline{a} to \underline{b} are formal finite direct sums $\bigoplus_i \mathbf{q}^{d_i} \omega_i$, where each ω_i is a directed web $\omega \subset [0, 1] \times \mathbb{R}$ with input \underline{a} and output \underline{b} , and $d_i \in \mathbb{Z}$.
- 2-morphisms from $\bigoplus_i \mathbf{q}^{d_i} \omega_i$ to $\bigoplus_j \mathbf{q}^{d'_j} \omega'_j$ are matrices (m_{ij}) , where m_{ij} is a linear combination of decorated directed foams in a thickened strip with input ω_i , output ω'_j , and degree $d'_j - d_i$.

Remark 2.19. The approach to **Foam** is slightly different in [QR16]. There one first constructs a bicategory $n\mathbf{Foam}$ of (directed) \mathfrak{gl}_n foams using techniques from higher representation theory and writes down its presentation in terms of generators and relations. Then it is shown that these categories admit a limit when N goes to infinity. It can be shown that the limit category coincides with **Foam** as defined above.

Proposition 2.20 ([RW20b, Proposition 5.10], [QR16]). *There are graded isomorphisms of webs in **Foam***

$$\begin{aligned}
 & \begin{array}{c} a \\ b \\ c \end{array} \begin{array}{c} \nearrow \\ \nearrow \\ \nearrow \end{array} \begin{array}{c} a+b \\ \nearrow \\ \nearrow \end{array} \rightarrow a+b+c \cong \begin{array}{c} a \\ b \\ c \end{array} \begin{array}{c} \nearrow \\ \nearrow \\ \nearrow \end{array} \begin{array}{c} a+b \\ \nearrow \\ \nearrow \end{array} \rightarrow a+b+c \\
 & \begin{array}{c} a+b+c \end{array} \begin{array}{c} \nearrow \\ \nearrow \\ \nearrow \end{array} \begin{array}{c} a+b \\ \nearrow \\ \nearrow \end{array} \rightarrow \begin{array}{c} a \\ b \\ c \end{array} \cong \begin{array}{c} a+b+c \end{array} \begin{array}{c} \nearrow \\ \nearrow \\ \nearrow \end{array} \begin{array}{c} a+b \\ \nearrow \\ \nearrow \end{array} \rightarrow \begin{array}{c} a \\ b \\ c \end{array} \\
 & \begin{array}{c} a+b \end{array} \begin{array}{c} \nearrow \\ \nearrow \end{array} \begin{array}{c} a \\ b \end{array} \rightarrow a+b \cong \begin{bmatrix} a+b \\ a \end{bmatrix} \xrightarrow{a+b} \text{---} \\
 & \begin{array}{c} a \\ b+c \end{array} \begin{array}{c} \nearrow \\ \nearrow \end{array} \begin{array}{c} a+d \\ \nearrow \\ \nearrow \end{array} \begin{array}{c} b \\ a+d-c \end{array} \rightarrow a+c \cong \bigoplus_{j=\max(0, b-a)}^b \begin{bmatrix} c \\ d-j \end{bmatrix} \begin{array}{c} a \\ a+j-b \end{array} \begin{array}{c} \nearrow \\ \nearrow \end{array} \begin{array}{c} b-j \\ \nearrow \\ \nearrow \end{array} \begin{array}{c} b \\ a+c+j \end{array} \rightarrow a+c
 \end{aligned}$$

Of particular interest to us are webs and foams with labels at most 2, the former having all endpoints labeled one. They arise naturally as resolutions of uncolored link diagrams. Following [RW22] we call them *elementary*. In what follows we write $\mathbf{Foam}^{\leq 2}$ for the linear subcategory

of **Foam** generated by elementary foams and webs. More precisely, this is the smallest subcategory containing elementary foams and webs that is closed under direct sums of webs and linear combinations of foams.

Proposition 2.21. *There are isomorphisms of elementary webs in $\mathbf{Foam}^{\leq 2}$:*

$$(14) \quad \begin{array}{c} 1 \\ \swarrow \quad \searrow \\ 2 \quad \rightarrow \quad 2 \\ \nwarrow \quad \nearrow \\ 1 \end{array} \cong [2] \xrightarrow{2}$$

$$(15) \quad \begin{array}{c} 1 \quad 2 \quad 1 \quad 2 \\ \swarrow \quad \searrow \quad \swarrow \quad \searrow \\ 1 \quad 1 \quad 1 \quad 1 \\ \nwarrow \quad \nearrow \quad \nwarrow \quad \nearrow \\ 1 \quad 2 \quad 1 \quad 2 \end{array} \oplus \begin{array}{c} 1 \quad 1 \\ \rightarrow \quad \rightarrow \\ 1 \quad 1 \end{array} \cong \begin{array}{c} 1 \quad 2 \quad 1 \quad 2 \\ \swarrow \quad \searrow \quad \swarrow \quad \searrow \\ 1 \quad 1 \quad 1 \quad 1 \\ \nwarrow \quad \nearrow \quad \nwarrow \quad \nearrow \\ 1 \quad 2 \quad 1 \quad 2 \end{array} \oplus \begin{array}{c} 1 \quad 2 \\ \rightarrow \quad \rightarrow \\ 1 \quad 1 \end{array}$$

2.4.2. Directed annular webs and foams. Consider now directed annular webs, so that $\Sigma = \mathbb{S}^1 \times \mathbb{R}$. Again, we consider only *directed foams* between them, on which the projection onto $\mathbb{S}^1 \times [0, 1]$ has no critical points. These foams have the same six types of singularities from Figure 5 as directed foams in a thickened strip.

Annular webs and foams constitute a category \mathcal{AFoam} constructed in the same fashion as **Foam**, keeping in mind that annular webs have no endpoints. The objects of \mathcal{AFoam} are formal finite direct sums $\bigoplus_i \mathbf{q}^{d_i} \omega_i$, where each ω_i is a directed annular web, and morphisms from $\bigoplus_i \mathbf{q}^{d_i} \omega_i$ to $\bigoplus_j \mathbf{q}^{d'_j} \omega_j$ are matrices (m_{ij}) , where each m_{ij} is a linear combination of decorated directed annular foams with input ω_i , output ω_j , and degree $d'_j - d_i$. We impose the same local relations as discussed above. It contains a subcategory $\mathcal{AFoam}^{\leq 2}$ of *elementary annular webs and foams*, where we consider only webs and foams with edges and facets of thickness at most 2.

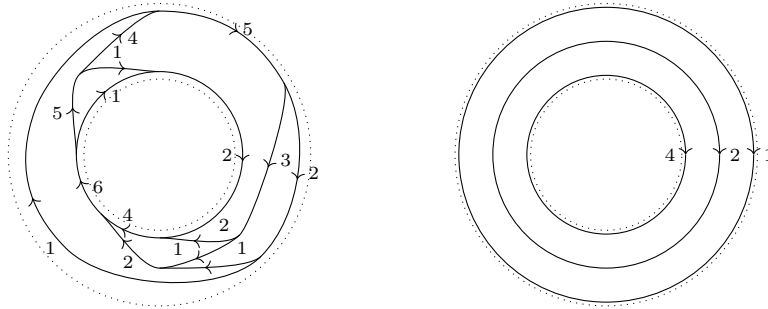


FIGURE 6. Examples of directed annular webs of index 7. The one to the right is $\mathbb{S}_{(4,2,1)}$.

Example 2.22. Given a finite sequence $\underline{k} = (k_1, \dots, k_r)$ one can consider a disjoint union of r concentric clockwise oriented circles with thicknesses k_1, \dots, k_r , read from the most nested circle towards the unnested one. We called it a *circular web* and denote by $\mathbb{S}_{\underline{k}}$.

The next proposition follows from the Queffelec–Rose–Sartori reduction algorithm for annular webs.

Proposition 2.23 (cp. [QRS18, Theorem 3.2]). *Given an annular directed web ω , there are graded direct sums of circular webs S_L and S_R , such that $\omega \oplus S_L \cong S_R$ in \mathcal{AFoam} .*

There is a similar result for elementary annular webs, with circular webs replaced by another class of webs.

Definition 2.24. A *chain of dumbbells of index k* is an annular web D_k obtained from k concentric circles by glueing each pair of neighboring circles along an arc, such that i -th circle is glued with $(i+1)$ -th immediately after it is glued with $(i-1)$ -th, see Figure 7.

Note that a chain of dumbbells of index $k \geq 3$ consists of $k - 1$ thick edges and $2k - 1$ thin edges. We say that an elementary web is *basic* if it is a concentric collections of circles and chains

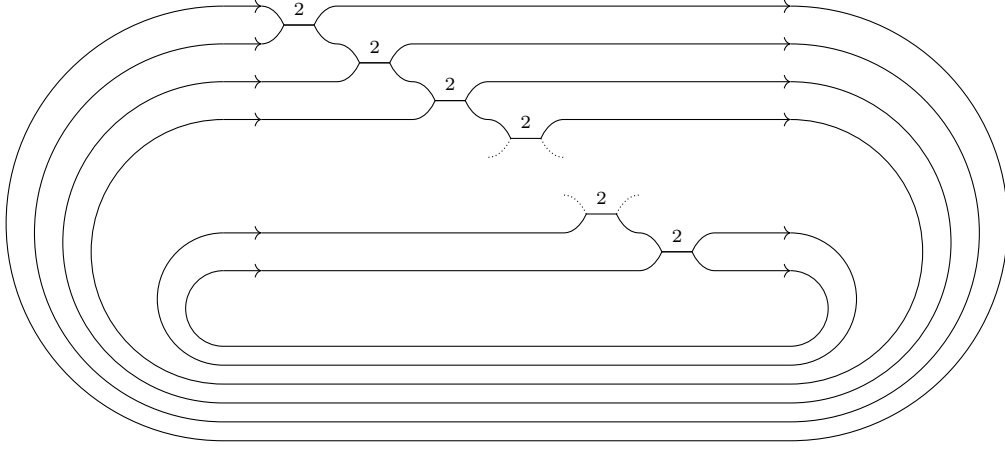


FIGURE 7. A chain of dumbbells.

of dumbbells. They play the role of circular webs in $\mathcal{AFoam}^{\leq 2}$.

Proposition 2.25 ([RW22, Corollary 2.5]). *Given an elementary annular directed web ω , there are graded direct sums of basic elementary webs X_L and X_R , such that $\omega \oplus X_L \cong X_R$ in $\mathcal{AFoam}^{\leq 2}$.*

2.4.3. Pointed annular webs. The last category of webs we consider is the category \mathcal{AFoam}^* of *pointed annular webs*, the objects of which are directed annular webs, each with a *marking* \star placed on an edge of thickness 1 on the outer side of the web i.e. it can be connected to the infinity by a curve disjoint from the web. Moreover the markings of all webs are located at a fixed point of the ambient annulus. In particular, not all webs appear in this category. Morphisms between two such webs are generated by annular foams with the property that the markings of the top and bottom boundary webs lie at the boundary of the same facet and are connected by a vertical interval embedded in this facet. This interval splits the facet into two parts that are treated as separate facets.⁵ In particular, they can be decorated with different polynomials. Forgetting the markings of webs and lines connecting them in foams gives a forgetful functor $\mathcal{AFoam}^* \rightarrow \mathcal{AFoam}$.

Note that there is no direct analogue of Proposition 2.23. However, a version of Proposition 2.25 still holds in the pointed setting:

Proposition 2.26 ([RW22, Proof of Lemma 4.29]). *Given an elementary annular directed web ω with a marking on an outer thin edge, there are graded direct sums of basic elementary webs X_L and X_R with markings on the outer thin edge, such that $\omega \oplus X_L \cong X_R$ in $\mathcal{AFoam}^{\leq 2*}$.*

2.5. Foams and webs as Soergel bimodules. Directed webs and foams can be seen as a graphical representation of Soergel bimodules and bimodule maps. Indeed, there is a fully faithful functor from foams to Soergel bimodules, the construction of which we recall in what follows. We refer to [Wed19, RW20b] for more details.

Pick a web ω and associate with each edge $u \in E(\omega)$ of thickness r the graded \mathbb{k} -algebra of symmetric polynomials $R_u := \mathbb{k}[x_{u,1}, \dots, x_{u,r}]^{\mathfrak{S}_r}$, where $\deg x_{u,i} = 2$. For simplicity we will often write X_u for the set of variables corresponding to the edge u . The tensor product over \mathbb{k}

$$D(\omega) := \bigotimes_{u \in E(\omega)} R_u,$$

⁵Essentially, one can consider the marking as a bivalent vertex.

is called the *space of decorations* of ω . It is the algebra of polynomials in edge variables that are symmetric with respect to permutations that preserve each set X_u . A pure tensor from $D(\omega)$ corresponds to assigning a symmetric polynomial $P_u \in R_u$ to each edge $u \in E(\omega)$. Therefore, we represent such elements with collections of dots on edges of ω , each labeled with the corresponding polynomial, see Figure 8. As special cases we consider

- a dot labeled by a Young diagram λ representing the Schur polynomial s_λ , and
- a dot labeled by an integer $i > 0$ on an edge u of thickness 1 to represent the monomial x_u^i .

Dots on the same edge follow the multiplicative convention: two dots labeled P_1 and P_2 on the same edge are equal to a dot labeled $P_1 P_2$ and an edge with no dot is decorated by 1.

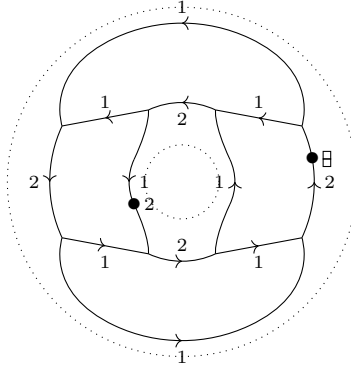


FIGURE 8. An annular web with a decoration.

Consider now the ideal of *local relations* $I(\omega) \subset D(\omega)$ generated by all differences

$$(16) \quad P(X_u) - P(X_{u'} \sqcup X_{u''}),$$

where u is an edge of thickness $a + b$ that splits into or is a merge of u' of thickness a and u'' of thickness b , and P is a symmetric polynomial in $a + b$ variables. Diagrammatically,

$$(17) \quad \begin{aligned} & \begin{array}{c} a+b \text{ edge} \xrightarrow{P} \begin{array}{l} \nearrow a \\ \searrow b \end{array} \end{array} = \sum_i \begin{array}{c} a+b \text{ edge} \xrightarrow{\quad} \begin{array}{l} \nearrow \begin{array}{c} Q_{(i)} \\ \bullet \end{array} a \\ \searrow \begin{array}{c} R_{(i)} \\ \bullet \end{array} b \end{array} \end{array} \quad \text{and} \\ & \begin{array}{c} \begin{array}{l} a \\ b \end{array} \text{ edges} \xrightarrow{\quad} \begin{array}{c} \bullet \\ P \end{array} \rightarrow a+b \end{array} = \sum_i \begin{array}{c} \begin{array}{l} a \\ b \end{array} \text{ edges} \xrightarrow{\quad} \begin{array}{c} \begin{array}{c} Q_{(i)} \\ \bullet \end{array} \\ \begin{array}{c} R_{(i)} \\ \bullet \end{array} \end{array} \rightarrow a+b \end{array} \end{aligned}$$

where the symmetric polynomials $Q_{(i)}$ and $R_{(i)}$ satisfy

$$P(X_{u'} \sqcup X_{u''}) = \sum_i Q_{(i)}(X_{u'}) R_{(i)}(X_{u''}).$$

Note that the generators of $I(\omega)$ are homogeneous, so that the ideal is graded. Finally, given a vertex $v \in V(\omega)$ denote by $\text{gr}(v)$ the product of thicknesses of the thin edges adjacent to v . The *Soergel space* associated with ω is the graded \mathbb{k} -module

$$B(\omega) := \mathbf{q}^{-\frac{1}{2} \sum_{v \in V(\omega)} \text{gr}(v)} D(\omega) / I(\omega).$$

In particular, the space is shifted downwards by the number of thick edges when ω is an annular elementary web. The grading shift is not necessarily integral unless the web is closed. Indeed,

for closed webs $\sum_{v \in V(\omega)} \text{gr}(v) = 2 \sum_{v \in V_s(\omega)} \text{gr}(v) = 2 \sum_{v \in V_m(\omega)} \text{gr}(v)$ where $V_s(\omega)$ (resp. $V_m(\omega)$) stands for the set of split (resp. merge) vertices.

Suppose now that $\omega \subset [0, 1] \times \mathbb{R}$ is a planar directed web of index k . Its input and output determine compositions \underline{a} and \underline{b} of k and $B(\omega)$ admits a left and a right action by the algebras $R^{\underline{a}}$ and $R^{\underline{b}}$ respectively. Furthermore, when ω consists of a single vertex that is a merge (resp. a split), then $B(\omega)$ coincides up to a grading shift with the induction $\text{Ind}_{\underline{b}}^{\underline{a}}$ (resp. restriction $\text{Res}_{\underline{b}}^{\underline{a}}$) bimodule. The results below follow immediately from the above and the definition of the Soergel space for a web.

Proposition 2.27. *Let ω_1 and ω_2 be planar directed webs with $\text{out}(\omega_1) = \underline{a} = \text{in}(\omega_2)$. Then*

$$B(\omega_1 \circ \omega_2) \cong B(\omega_1) \otimes_{R^{\underline{a}}} B(\omega_2).$$

In particular, $B(\omega)$ is a singular Soergel bimodule for any planar directed web ω .

Proposition 2.28. *Let $\widehat{\omega}$ be the annular closure of a directed web ω . Then $B(\widehat{\omega}) \cong HH_0(B(\omega))$.*

Example 2.29. The Soergel bimodule associated with the directed web ω in Figure 3 is a quotient of the tensor product

$$R(\omega) = R^{(3,1)} \otimes R^{(4)} \otimes R^{(2,2)}$$

by relations that identify any generator of $R^{(4)}$ with its image in either of the two other factors. Hence, taking into account the overall shift,

$$B(\omega) = \mathbf{q}^{-\frac{7}{2}} R^{(3,1)} \otimes_{R^{(4)}} R^{(2,2)}.$$

Let us now introduce maps between Soergel spaces that correspond to the basic building blocks of foams depicted in Figure 5 (compare [Wed19, RW20b]). The first four arise as the units and traces of associated graded Frobenius extensions [EMTW20].

The cup foam is assigned the inclusion

$$\begin{aligned} \text{cup: } B\left(\overrightarrow{\text{---} \xrightarrow{a+b} \text{---}}\right) &\longrightarrow \mathbf{q}^{ab} B\left(a+b \text{---} \begin{array}{c} \nearrow^a \\ \searrow_b \end{array} \text{---} a+b\right) \\ \overrightarrow{\text{---} \xrightarrow{a+b} \text{---}} &\longmapsto a+b \text{---} \begin{array}{c} \nearrow^a \\ \searrow_b \end{array} \text{---} a+b, \end{aligned}$$

whereas with the cap foam we associate the projection

$$\begin{aligned} \text{cap: } B\left(a+b \text{---} \begin{array}{c} \nearrow^a \\ \searrow_b \end{array} \text{---} a+b\right) &\longrightarrow \mathbf{q}^{ab} B\left(\overrightarrow{\text{---} \xrightarrow{a+b} \text{---}}\right) \\ a+b \text{---} \begin{array}{c} \nearrow^a \\ \searrow_b \end{array} \text{---} a+b &\longmapsto a+b \xrightarrow{\bullet} \text{---} \bullet \text{---} a+b, \end{aligned}$$

where $P \star Q = \sum_{\substack{I \sqcup J = \{1, \dots, a+b\} \\ \#I=a, \#J=b}} \frac{P(x_I)Q(x_J)}{\nabla(x_I, x_J)}$ and $\nabla(x_I, x_J) = \prod_{\substack{i \in I \\ j \in J}} (x_j - x_i)$.

This map is surjective since the target bimodule is generated by 1 and 1 is reached since $e_a^b \star 1 = 1$.

An *unzip* is associated with the projection

$$\text{unzip: } B \left(\begin{array}{c} a \\ b \end{array} \begin{array}{c} \nearrow \\ \searrow \end{array} \begin{array}{c} a+b \\ \xrightarrow{\quad} \end{array} \begin{array}{c} \searrow \\ \nearrow \end{array} \begin{array}{c} a \\ b \end{array} \right) \longrightarrow \mathbf{q}^{-ab} B \left(\begin{array}{c} a \\ b \end{array} \begin{array}{c} \xrightarrow{\quad} \\ \xrightarrow{\quad} \end{array} \right)$$

$$\begin{array}{c} a \\ b \end{array} \begin{array}{c} \nearrow \\ \searrow \end{array} \begin{array}{c} a+b \\ \xrightarrow{\quad} \end{array} \begin{array}{c} \searrow \\ \nearrow \end{array} \begin{array}{c} a \\ b \end{array} \longmapsto \begin{array}{c} a \\ b \end{array} \begin{array}{c} \xrightarrow{\quad} \\ \xrightarrow{\quad} \end{array}.$$

The *unzip* is surjective since the target bimodule is generated by 1 and 1 is reached.

A *zip* is associated with the inclusion

$$\text{zip: } B \left(\begin{array}{c} a \\ b \end{array} \begin{array}{c} \xrightarrow{\quad} \\ \xrightarrow{\quad} \end{array} \right) \longrightarrow \mathbf{q}^{-ab} B \left(\begin{array}{c} a \\ b \end{array} \begin{array}{c} \nearrow \\ \searrow \end{array} \begin{array}{c} a+b \\ \xrightarrow{\quad} \end{array} \begin{array}{c} \searrow \\ \nearrow \end{array} \begin{array}{c} a \\ b \end{array} \right)$$

$$\begin{array}{c} a \\ b \end{array} \begin{array}{c} \xrightarrow{\quad} \\ \xrightarrow{\quad} \end{array} \longmapsto \sum_{\alpha \in T(a,b)} (-1)^{|\widehat{\alpha}|} \begin{array}{c} a \\ b \end{array} \begin{array}{c} \nearrow \\ \searrow \end{array} \begin{array}{c} a+b \\ \xrightarrow{\quad} \end{array} \begin{array}{c} \searrow \\ \nearrow \end{array} \begin{array}{c} a \\ b \end{array},$$

Since the composition of zip followed by the unzip is a multiplication with a given polynomial, the zip map is injective.

The *multiplication* by a homogeneous symmetric polynomial P is the map

$$m_P: B \left(\begin{array}{c} a \\ \xrightarrow{\quad} \end{array} \right) \longrightarrow \mathbf{q}^{-\deg P} B \left(\begin{array}{c} a \\ \xrightarrow{\quad} \end{array} \right)$$

$$a \xrightarrow{\quad} \longmapsto a \xrightarrow{\quad \bullet \quad}.$$

Finally, the *associativity* and *coassociativity* foams are assigned the maps

$$\text{as: } B \left(\begin{array}{c} a \\ b \\ c \end{array} \begin{array}{c} \nearrow \\ \nearrow \\ \searrow \end{array} \begin{array}{c} a+b \\ \xrightarrow{\quad} \end{array} \begin{array}{c} \searrow \\ \searrow \\ \nearrow \end{array} \begin{array}{c} a+b+c \end{array} \right) \longrightarrow B \left(\begin{array}{c} a \\ b \\ c \end{array} \begin{array}{c} \nearrow \\ \nearrow \\ \searrow \end{array} \begin{array}{c} a+b+c \end{array} \right)$$

$$\begin{array}{c} a \\ b \\ c \end{array} \begin{array}{c} \nearrow \\ \nearrow \\ \searrow \end{array} \begin{array}{c} a+b \\ \xrightarrow{\quad} \end{array} \begin{array}{c} \searrow \\ \searrow \\ \nearrow \end{array} \begin{array}{c} a+b+c \end{array} \longmapsto \begin{array}{c} a \\ b \\ c \end{array} \begin{array}{c} \nearrow \\ \nearrow \\ \searrow \end{array} \begin{array}{c} a+b+c \end{array}$$

$$\text{coas: } B \left(\begin{array}{c} a+b+c \\ \nearrow \\ \nearrow \\ \searrow \end{array} \begin{array}{c} a+b \\ \xrightarrow{\quad} \end{array} \begin{array}{c} \searrow \\ \searrow \\ \nearrow \end{array} \begin{array}{c} a \\ b \\ c \end{array} \right) \longrightarrow B \left(\begin{array}{c} a+b+c \\ \nearrow \\ \nearrow \\ \searrow \end{array} \begin{array}{c} a+b \\ \xrightarrow{\quad} \end{array} \begin{array}{c} \searrow \\ \searrow \\ \nearrow \end{array} \begin{array}{c} a \\ b \\ c \end{array} \right)$$

$$\begin{array}{c} a+b+c \\ \nearrow \\ \nearrow \\ \searrow \end{array} \begin{array}{c} a+b \\ \xrightarrow{\quad} \end{array} \begin{array}{c} \searrow \\ \searrow \\ \nearrow \end{array} \begin{array}{c} a \\ b \\ c \end{array} \longmapsto \begin{array}{c} a+b+c \\ \nearrow \\ \nearrow \\ \searrow \end{array} \begin{array}{c} a+b \\ \xrightarrow{\quad} \end{array} \begin{array}{c} \searrow \\ \searrow \\ \nearrow \end{array} \begin{array}{c} a \\ b \\ c \end{array}.$$

Because of the local nature of the above definitions, they can be interpreted as maps assigned to foams between either planar or annular directed webs. It is known that this assignment preserves local relations.

Proposition 2.30. *When applied to planar directed webs, the above describe a functor of bicategories*

$$B: \mathbf{Foam} \rightarrow \mathbf{sSBim}$$

and in case of annular directed webs, a functor

$$B: \mathcal{AFoam} \rightarrow \mathbf{grMod}.$$

Finally, there is a functor

$$\overline{B}: \mathcal{AFoam}^* \rightarrow \text{grMod}$$

that assigns the quotient $\overline{B}(\omega) := B(\omega)/(x_\star)$ to a pointed web ω , where the variable x_\star is associated with the marked edge.

2.6. A quantum trace deformation of annular foams. Following [BPW19] one can show that \mathcal{AFoam} is equivalent to the so-called *horizontal trace* $\text{hTr}(\mathbf{Foam})$ of the bicategory \mathbf{Foam} . What it roughly means is that

- every annular web is isomorphic to a web with vertices away from a fixed *section* $\mu := \{*\} \times \mathbb{R}$ of the annulus $\mathbb{S}^1 \times \mathbb{R}$, to which we refer as the *trace section*,
- morphisms are generated by foams that intersect the *membrane* $M := \mu \times [0, 1]$ in a directed web modulo local relations away from the membrane and the *horizontal trace relation* that allows to isotope a piece of a foam through M .

The horizontal trace can be defined on any bicategory and is functorial [BPW19]. Having such a description of \mathcal{AFoam} we can now deform it by replacing the horizontal trace relation with its quantum version, which we will now state more precisely. Notice first that an orientation of the circle $\mathbb{S}^1 \times \{0\} \times \{0\}$ induces a coorientation of the trace section μ and membrane M . Let W be an annular foam W that intersects M in a web ω and consider a generic admissible ambient isotopy ϕ that pushes M according to its coorientation, so that

- $\phi(W)$ intersects M in a web ω' , and
- $M' := \phi(M)$ intersects M only at the collar, where both M and M' coincide.

Then M and M' bound a 3-ball B with a foam $W \cap B$ from ω' to ω inside. The *quantum horizontal trace relation* states that in this setting

$$W = q^{-\deg(W \cap B)} \phi(W),$$

see Figure 9 for an example.

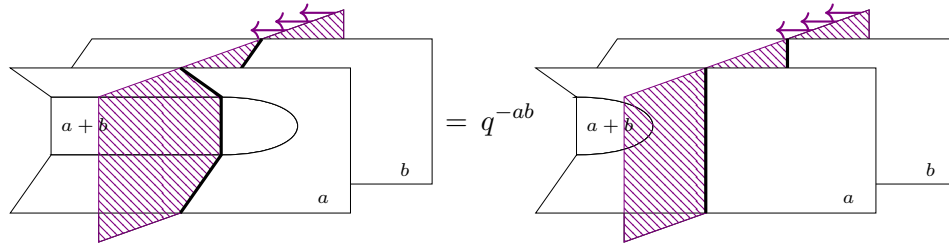


FIGURE 9. The effect of moving a foam through the membrane. The membrane is depicted in hashed purple with its coorientation indicated by purple arrows.

Definition 2.31. The category \mathcal{AFoam}_q is a deformation of \mathcal{AFoam} , where we consider only annular directed webs that intersect μ generically, whereas on foams we impose the quantum horizontal trace relations and only local relations away from the membrane M . We write $\mathcal{AFoam}_q^{\leq 2}$ for its subcategory generated by elementary webs and foams.

Remark 2.32. The quantum trace relation simply identifies a foam W with $\phi(W)$ when $q = 1$. Hence, in this case \mathcal{AFoam}_q coincides with \mathcal{AFoam} .

Propositions 2.20 and 2.21 are proven locally, so that they still hold in the deformed setting. Likewise, the quantum trace relation is enough for Propositions 2.23 and 2.25.

$$\overline{B}_q(\widehat{\omega}) = qHH_0(B(\omega))/(x_\star),$$

where x_\star is the variable associated with the output edge of ω chosen by the marking \star . However, because of the restricted trace relation in \mathcal{AFoam}_q^\star , the cyclicity property (19) does not hold for \overline{B}_q unless in one of the webs, ω_1 or ω_2 , the top most endpoints are connected by an interval disjoint from the rest of the web.

We end this section with a result about singular Soergel bimodules, which explains why we take only the quantum trace to define B_q instead of the full quantum Hochschild homology.

Theorem 2.36. *Assume that $1 - q^d$ is invertible for all $d \neq 0$. Then for any sequence \underline{k} and a bimodule $B \in \mathbf{sSBim}(R^{\underline{k}}, R^{\underline{k}})$ one has*

$$qHH_i(R^{\underline{k}}, B) = 0 \quad \text{for } i > 0.$$

Proof. Because singular Soergel bimodules are direct summands of singular Bott–Samelson bimodules, it is enough to prove the formula only for the latter. For that notice that every singular Bott–Samelson bimodule is of the form $B(\omega)$ for some directed web ω . The thesis follows from Propositions 2.23 and 2.13. \square

3. COMBINATORIAL LINK HOMOLOGIES

In this section we recall the combinatorial framework for HHH , HHH^{red} , as well as the \mathfrak{gl}_1 and \mathfrak{gl}_0 homologies constructed by the last two authors.

Throughout this section we fix a link L represented by an annular closure $\widehat{\beta}$ of a braid diagram β , drawn horizontally from left to right and closed below the braid, see Figure 11. We write k for the number of strands of $\widehat{\beta}$ or its index and \mathfrak{X} for the set of crossings of β . The latter consists of of and n_+ positive n_- negative crossings, and we write $n = n_+ + n_-$ for the total.

3.1. The general cube construction. A map $I: \mathfrak{X} \rightarrow \{0, 1\}$ determines a directed annular web $\widehat{\beta}_I$, called the I -resolution of $\widehat{\beta}$, constructed by replacing locally each crossing by either its smoothing or singularization as indicated in Figure 10. An example is given in Figure 11. Two

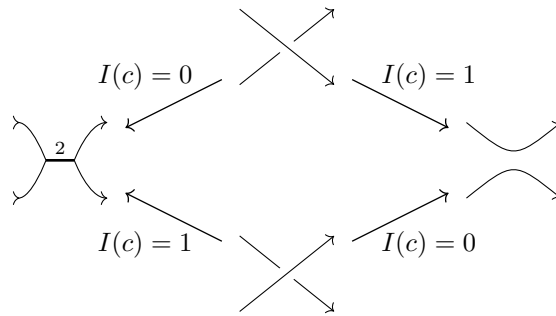


FIGURE 10. The two resolutions of a crossing c : its *singularization* (to the left) and *smoothing* (to the right).

resolutions I and I' are *neighboring* if they agree on all but one crossing c , in which case we write $I \xrightarrow{c} I'$ if $I(c) = 0$ and $I'(c) = 1$. With such two neighboring resolutions we associate a foam $W_{I,c}: \widehat{\beta}_I \rightarrow \widehat{\beta}_{I'}$, which is an unzip in case the crossing c is positive and a zip otherwise. These data can be arranged into a commuting diagram in \mathcal{AFoam} as follows. Given a square of neighboring

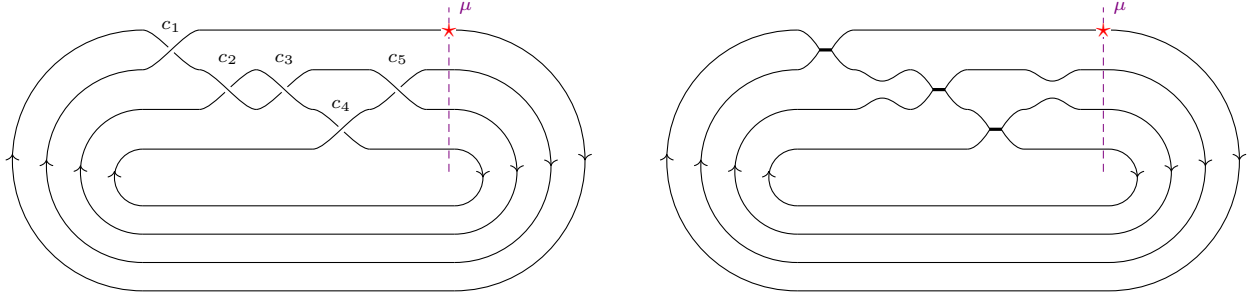


FIGURE 11. A braid diagram of the closure of $\beta = \sigma_1^{-1}\sigma_2^2\sigma_3^{-1}\sigma_2$ and its resolution associated with $(I(c_i))_{1 \leq i \leq 5} = (0, 0, 1, 0, 0)$. The dashed line μ visualizes the trace section and the red star is the position of the marking.

resolutions

$$(20) \quad \begin{array}{ccccc} & & I_{01} & & \\ & c \nearrow & & \searrow c' & \\ I_{00} & & & & I_{11} \\ & c' \searrow & & \nearrow c & \\ & & I_{10} & & \end{array}$$

the foams $W_{I_{00},c} \cup W_{I_{01},c'}$ and $W_{I_{00},c'} \cup W_{I_{10},c}$ coincide upto an ambient isotopy. Choose a sign $\epsilon(I, c) = \pm 1$ whenever $I(c) = 0$, so that

$$\epsilon(I_{00}, c)\epsilon(I_{01}, c') + \epsilon(I_{00}, c')\epsilon(I_{10}, c) = 0$$

for each situation as in (20). For instance, one can take $\epsilon(I, c) := (-1)^{I_{\prec c}}$, where $I_{\prec c} := \sum_{c' \prec c} I(c')$ for a fixed total ordering \prec on \mathfrak{X} . Let $[\hat{\beta}]$ be a formal chain complex in \mathcal{AFoam} supported in homological degrees $[-n_-, n_+]$, given by objects

$$[\hat{\beta}]_i := \bigoplus_{|I|=i+n_-} \mathbf{q}^{-i} \hat{\beta}_I$$

and the differential

$$\partial_i := \sum_{\substack{|I|=i+n_- \\ c: I(c)=0}} \epsilon(I, c) W_{I,c}.$$

A standard argument ensures that the isomorphism type of $[\hat{\beta}]$ does not depend on the choice of signs, see [ORS13, Put14]. Clearly, \mathcal{AFoam} can be replaced with its quantization \mathcal{AFoam}_q .

Theorem 3.1. *The homotopy type of the formal complex $[\hat{\beta}]$, computed either over \mathcal{AFoam} or \mathcal{AFoam}_q , is an invariant of the annular link $L = \hat{\beta}$.*

Remark 3.2. When $\hat{\beta}$ is considered as a link with a marking, placed at the top trace vertex, then $[\hat{\beta}]$ is a complex over \mathcal{AFoam}^\star or \mathcal{AFoam}_q^\star . However, one can only prove its invariance under braid moves and the second Markov move (conjugacy) away from \star . This is not enough for the bracket to be an invariant of links with marked components.

Occasionally it will be worth to consider partial resolutions of a link. These are a special type of diagrams for knotted elementary webs, in which only thin edges cross themselves. Following [OSS09, OS09] we refer to such webs as *singular links* and to the thick edges—*singular crossings*. Although we are not using this in that paper, let us mention that every singular link admits a diagram in a braid position [Bir93].

Following Gilmore [Gil16, Section 2], we shall also extend webs to allow *bivalent vertices*, depicted as short tags, with the obvious local relation that identifies variables associated with incident edges. Notice that a trace vertex is a particular kind of a bivalent vertex where the identification of variables is composed with a multiplication by some power of q (compare Remark 2.34). Subdividing an edge with a bivalent vertex is called an *insertion* [Man14]. Notice that insertion does not change the isomorphism type of the associated Soergel space. We say that a singular link diagram S is *layered* if it is in a braid position and there are vertical lines ℓ_0, \dots, ℓ_n called *levels*, with $\ell_n = \mu$ the trace section, that carry all singular crossings and bivalent vertices of S and which intersect S only at those points, see Figure 12. In order to keep all resolutions of S layered, we require that real crossings are at the lines ℓ_i , which results in a bivalent vertex at the over- and at the underpass. Any diagram in a braid position can be modified to a layered one by a sequence of insertions.

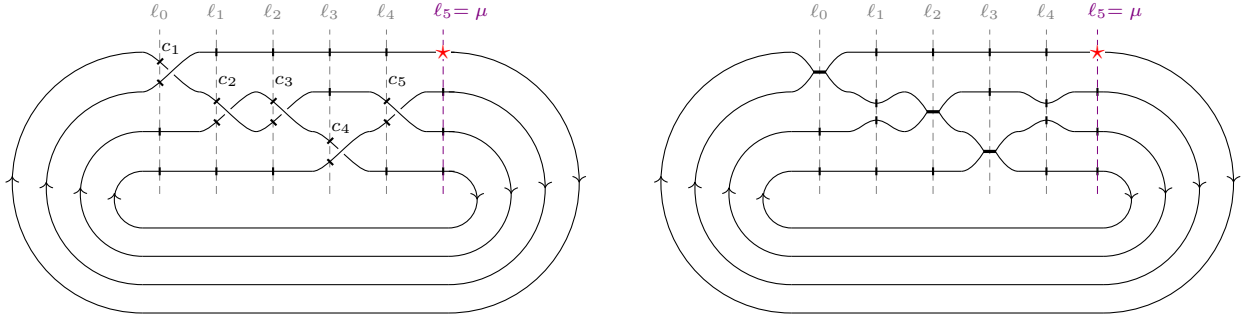


FIGURE 12. Layered diagrams of the braid closure and its resolution from Figure 11. In order to increase the visibility of bivalent vertices, the real crossings in the left picture are moved slightly to the right with respect to the vertical lines ℓ_i .

3.2. Triply graded Khovanov–Rozansky homology. Consider the functor $B: \mathbf{Foam} \rightarrow \mathbf{sSBim}$ from Proposition 2.30. Given a resolution β_I we assign $HH(B(\beta_I))$ to the annular closure $\widehat{\beta}_I$. This results in a functor on \mathcal{AFoam} that, when applied to the formal complex $[\widehat{\beta}]$, produces a complex of bigraded modules that computes the triple graded homology HHH , see [Kho07]. More precisely, writing k for the number of strands of β with $\widehat{\beta} = L$ we define $HHH(L)$ as the homology of the complex of bigraded modules

$$(21) \quad C_i = \bigoplus_j \mathbf{q}^{k-2j} HH_j(B_{i+j}(\beta)), \quad \text{where } B_i(\beta) = \bigoplus_{|I|=i+n_-} \mathbf{q}^{-i}(B(\beta_I))$$

and the extra grading is defined by putting j th Hochschild homology in degree $2j - w - k$, where $w = n_+ - n_-$ is the writhe of β . The differential is induced by the zip and unzip foams, which can be written diagrammatically as follows:

$$(22) \quad \begin{aligned} \text{unzip} \left(\begin{array}{c} 1 \searrow \quad 1 \searrow \\ \quad \quad \quad 2 \\ 1 \nearrow \quad 1 \nearrow \end{array} \right) &= \begin{array}{c} 1 \longrightarrow 1 \\ 1 \longrightarrow 1 \end{array} \\ \text{zip} \left(\begin{array}{c} 1 \longrightarrow 1 \\ 1 \longrightarrow 1 \end{array} \right) &= \begin{array}{c} 1 \nearrow \bullet \quad 1 \searrow \\ \quad \quad \quad 2 \\ 1 \searrow \quad 1 \nearrow \end{array} - \begin{array}{c} 1 \searrow \quad 1 \searrow \\ \quad \quad \quad 2 \\ 1 \nearrow \quad 1 \nearrow \bullet \end{array} \end{aligned}$$

and it preserves both the quantum and (modified) Hochschild grading. The degree shifts are chosen so that the homology is invariant under stabilizations.

Middle homology. It is known that the triple graded homology splits into two copies of *middle homology* HHH^{mid} , shifted in homological and Hochschild degrees. This splitting follows easily when the Hochschild homology of Soergel bimodules $B(\beta_I)$ is computed using the Koszul complex

$$(23) \quad K(\beta_I) := B(\beta_I) \otimes_{R^e} \bigotimes_{i=1}^k (\mathfrak{q}^2 R^e \xrightarrow{x_i \otimes 1 - 1 \otimes x_i} R^e)$$

where $R = \mathbb{k}[x_1, \dots, x_k]$ and $R^e = R \otimes R$ is the enveloping algebra with the left (resp. right) factor acting from the left (resp. right) on $B(\beta_I)$. After changing the basis of the algebra by trading x_1 for e_1 , the first elementary symmetric polynomial, the differential in the factor associated with e_1 vanishes, because the polynomial acts symmetrically. Hence, $K(\beta_I) = K'(\beta_I) \oplus \mathfrak{a}^2 \mathfrak{q}^2 K'(\beta_I)$, where $K'(\beta_I)$ is defined as in (23) except that the big tensor product is taken for $i > 1$. The middle homology HHH^{mid} arises from a complex defined as in (21), except that the homology of K' is taken instead of HH .

Reduced homology. The above constructions can be repeated with the reduced bimodule \overline{B} . Taking the full Hochschild homology as in (21) produces an invariant link homology $HHH'(L)$ that categorifies $(\mathfrak{a} - \mathfrak{a}^{-1})P_L(\mathfrak{a}, \mathfrak{q})$. The complex again splits into two copies of a smaller complex $C^{\text{red}}(L)$ that computes the *reduced homology* $HHH^{\text{red}}(L)$. In order to see this, observe that \overline{B} is isomorphic to the submodule $B' \subset B$ generated by differences of variables; the variable $x_i \in R$ acts on B' by multiplication with $x_i - x_{\star}$. This submodule is isomorphic to the reduced Soergel bimodule as defined in [Rou17] if 2 is invertible.⁶ Furthermore, when k is invertible in \mathbb{k} , then

$$\mathbb{k}[x_1, x_2, \dots, x_k] \cong \mathbb{k}[e_1, x_2 - x_1, x_3 - x_2, \dots, x_k - x_{k-1}].$$

For instance, one has $kx_k = e_1 + \sum_{i=1}^{k-1} i(x_{i+1} - x_i)$. Hence, reducing to K' coincides with taking Hochschild homology with respect to the subalgebra $R' \subset R$ generated by differences of variables. Notice that the identification $\overline{B} \cong B'$ commutes with the natural action of R' on both bimodules. This is how the reduced homology was originally defined [Rou17, Kho07, KR08b]. Its Poincaré polynomial

$$P_L(\mathfrak{t}, \mathfrak{a}, \mathfrak{q}) := \sum_{i,j,n} \mathfrak{t}^i \mathfrak{a}^j \mathfrak{q}^n \dim HHH^{\text{red}, i, j, n}(L)$$

is a new link invariant, where $HHH^{\text{red}, i, j, n}(L)$ is the homology in i th homological, j th (modified) Hochschild and n th quantum degree. This construction categorifies the HOMFLY–PT polynomial $P_L(\mathfrak{a}, \mathfrak{q})$ in the sense that for any link L there is an equality of power series in \mathfrak{q}

$$(24) \quad P_L(\mathfrak{a}, \mathfrak{q}) = P_L(-1, \mathfrak{a}, \mathfrak{q}).$$

Remark 3.3. In order to recover Rasmussen’s grading (i', j', n') , the (modified) Hochschild grading j must be negated and the homological degree replaced with $i' = 2i + j$; the quantum grading n is not changed. This makes the Hochschild differential homogeneous of (i', j', n) -degree $(0, 2, 2)$ and the topological (induced by foams) differential of degree $(2, 0, 0)$. We also have

$$P_L(\mathfrak{t}, \mathfrak{a}, \mathfrak{q}) = P_L^{\text{Ras}}(\mathfrak{t}^{1/2}, \mathfrak{t}^{1/2} \mathfrak{a}^{-1}, \mathfrak{q}),$$

where $P_L^{\text{Ras}}(\mathfrak{t}, \mathfrak{a}, \mathfrak{q})$ is the Poincaré polynomial of HHH^{red} with respect to Rasmussen’s convention.

⁶In the original definition, the reduced Soergel bimodule is generated by the differences of variables associated with edges at the same level, which is only enough to generate twice the difference of any two variables.

3.3. \mathfrak{gl}_1 homology. The technology developed here was first introduced in [RW20b] using *foams* in a more general framework. It was recasted in [RW22] in a foam-free framework. Here we use this latter point of view to recall the construction. Unless stated otherwise, in this section we work with integral coefficients.

With a web ω we have associated in Section 2.5 the *space of decorations* $D(\omega) = \bigotimes_{u \in E(\omega)} R_u$, where the *edge ring* R_u consists of symmetric polynomials in as many variables as the thickness of the edge u . A pure tensor from $D(\omega)$ is visualized by dots on ω , see Figure 8. In what follows we will consider quotients and subquotients of $D(\omega)$.

Definition 3.4. Let ω be an annular web of index k . Denote by $\mathcal{P}(\{X_1, \dots, X_k\})$ the power set of $\{X_1, \dots, X_k\}$. An *omnichrome coloring* of ω is a map $c: E(\omega) \rightarrow \mathcal{P}(\{X_1, \dots, X_k\})$, such that

- for each edge $u \in E(\omega)$ the cardinality of $c(u)$ equals the thickness of u ,
- given a generic section r of the annulus, the union of the sets $c(u)$ for all edges u intersecting r is equal to $\{X_1, \dots, X_k\}$, and
- the *flow condition* holds: if u_1, u_2 and u_3 are three adjacent edges with u_1 the thickest of them, then $c(u_1) = c(u_2) \sqcup c(u_3)$.

The set $c(u)$ is called the *color* of u .

The definition of omnichrome colorings has several direct implications.

- (1) At each vertex of ω , the color of the thickest edge is the disjoint union of the colors of the two thin edges.
- (2) For a generic section r of the annulus, the union of sets $c(u)$ associated with the edges u that intersect r is actually a disjoint union.
- (3) Each coloring c induces an algebra homomorphism $\varphi_c: D(\omega) \rightarrow \mathbb{Z}[X_1, \dots, X_k]$ that for each $u \in E(\omega)$ identifies the ring R_u with the subring $\mathbb{Z}[c(u)]^{\mathfrak{S}_{\ell(u)}}$.

Let ω be an annular web and c be an omnichrome coloring of ω . For each split vertex v , denote by $u_l(v)$ and $u_r(v)$ the left and right edges going out of v . Set

$$Q(\omega, c) := \prod_{\substack{v \text{ split} \\ \text{vertex}}} \prod_{\substack{X_i \in c(u_l(v)) \\ X_j \in c(u_r(v))}} (X_i - X_j).$$

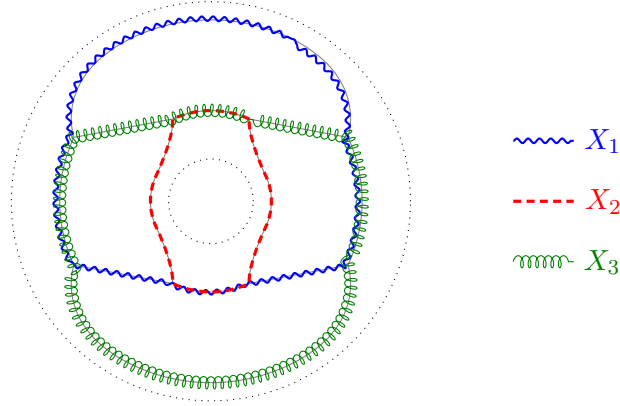
Given a pure tensor $T \in D(\omega)$ write T_u for the factor associated with an edge u . Using the ring morphism φ_c defined in point (3) just above, we set:

$$P(\omega, T, c) = \varphi_c(T) = \prod_{u \in E(\omega)} T_u(c(u))$$

and extend it linearly to all elements of $D(\omega)$. Finally, define a rational function

$$\langle \omega, T, c \rangle_\infty = \frac{P(\omega, T, c)}{Q(\omega, c)} \in \mathbb{Q}(X_1, \dots, X_k).$$

Example 3.5. Consider the omnichrome coloring c



of the decorated annular web (ω, T) from Figure 8. We compute

$$P(\omega, T, c) = X_2^2 X_1 X_3,$$

$$Q(\omega, T, c) = (X_3 - X_1)(X_2 - X_3)(X_1 - X_3)(X_2 - X_1)$$

so that

$$\langle \omega, T, c \rangle_\infty = \frac{X_2^2 X_1 X_3}{(X_3 - X_2)(X_2 - X_1)(X_3 - X_1)^2}.$$

Definition 3.6. For an annular web ω and a decoration $T \in D(\omega)$ define the ∞ -evaluation $\langle \omega, T \rangle_\infty$ of T by

$$\sum_{c: \text{omnichrome coloring}} \langle \omega, T, c \rangle_\infty \in \mathbb{Q}(X_1, \dots, X_k)$$

and the ∞ -pairing is the bilinear form $\langle -; \omega; - \rangle_\infty$ on $D(\omega)$, defined on decorations S and T as $\langle S; \omega; T \rangle_\infty := \langle \omega, ST \rangle_\infty$. The \mathfrak{gl}_∞ state space of ω is the quotient

$$\mathcal{S}_\infty(\omega) := D(\omega) / \text{rad} \langle -; \omega; - \rangle_\infty.$$

For another ring of coefficients \mathbb{k} we set $\mathcal{S}_\infty(\omega, \mathbb{k}) := \mathcal{S}_\infty(\omega) \otimes_{\mathbb{Z}} \mathbb{k}$.

Proposition 3.7. Choose an annular web ω of index k .

- (1) For any $T \in D(\omega)$, the ∞ -evaluation $\langle \omega, T \rangle_\infty$ is a symmetric polynomial in X_1, \dots, X_k with coefficients in \mathbb{Z} .
- (2) The defining ideals for \mathbb{k} -modules $\mathcal{S}_\infty(\omega, \mathbb{k})$ and $B(\omega)$ as quotients of $D(\omega)$ agree. In particular, the Soergel relations (17) hold in $\mathcal{S}_\infty(\omega, \mathbb{k})$.

Proof. The first statement is the content of [RW22, Lemma 3.13] and the second one follows directly from [RW20b, Proposition 4.18], because $B(\omega)$ coincides with $HH_0(B(\tilde{\omega}))$ when ω is a closure of a directed web $\tilde{\omega}$. \square

Definition 3.8. Choose an annular web ω of index k . Define the \mathfrak{gl}_1 evaluation of $T \in D(\omega)$ by

$$\langle \omega, T \rangle_1 := (\langle \omega, T \rangle_\infty)_{|X_1, \dots, X_k \rightarrow 0}.$$

In other words, $\langle \omega, T \rangle_1$ is the constant coefficient of $\langle \omega, T \rangle_\infty$. The \mathfrak{gl}_1 pairing on ω is the bilinear form $\langle -; \omega; - \rangle_1$ on $D(\omega)$ defined on decorations S and T by $\langle S; \omega; T \rangle_1 := \langle \omega, ST \rangle_1$. The \mathfrak{gl}_1 state space of ω is the quotient

$$\mathcal{S}_1(\omega) := D(\omega) / \text{rad} \langle -; \omega; - \rangle_1.$$

For another ring of coefficients \mathbb{k} we set $\mathcal{S}_1(\omega, \mathbb{k}) = \mathcal{S}_1(\omega) \otimes_{\mathbb{Z}} \mathbb{k}$.

Following its very definition $\mathcal{S}_1(\omega)$ is a quotient of $B(\omega)$.

Proposition 3.9.

- (1) The assignment $\omega \mapsto \mathcal{S}_1(\omega)$ extends to a functor $\mathcal{S}_1: \mathcal{AFoam} \rightarrow \text{grMod}$ that is a quotient of the functor from Section 2.5. In particular, the isomorphisms from Proposition 2.20 induce isomorphisms between \mathfrak{gl}_1 state spaces.
- (2) $\mathcal{S}_1(\omega)$ is a free graded \mathbb{k} -module for any web ω . It has rank 1 and is concentrated in quantum degree 0 in case ω is a collection of circular webs.
- (3) Suppose that a generic section of the annulus intersects edges u_1, \dots, u_s of a annular web ω and let $P \in D(\omega)$ represent a homogeneous symmetric polynomial in variables $X_{u_1} \sqcup \dots \sqcup X_{u_s}$ of positive degree. Then P annihilates $\mathcal{S}_1(\omega)$.

Proof. When $\mathbb{k} = \mathbb{Z}$, (1) was first proven in [RW20b, Section 5.1.2] and then reformulated in a foam free language in [RW22, Section 3.4]; (2) is the content of [RW20b, Example 3.25]. Both statements are obtained from the results over \mathbb{Z} after tensoring with \mathbb{k} . Statement (3) follows directly from the definition of $\langle \cdot, \cdot \rangle_1$. \square

Applying the functor $\mathcal{S}_1(-)$ to the formal complex $[\widehat{\beta}]$ results in a chain complex of \mathbb{k} -modules $C^{\mathfrak{gl}_1}(\widehat{\beta}; \mathbb{k})$ with homology denoted by $H^{\mathfrak{gl}_1}(\widehat{\beta}; \mathbb{k})$; we call it the \mathfrak{gl}_1 homology of $\widehat{\beta}$. The differential is induced by the zip and unzip maps listed in (22).

Theorem 3.10 ([RW20b]). *If \mathbb{k} is a field of characteristic 0, then $H^{\mathfrak{gl}_1}(\widehat{\beta}; \mathbb{k})$ is a link invariant. Its graded Euler characteristic is 1 for every link.*

The construction in [RW20b] is done in an equivariant setting and over \mathbb{Q} . Here we consider a simpler non-equivariant setting, in which case the construction can be performed with integral coefficients. The proof of invariance, however, requires inverses of nonzero integers, see [RW20b, Lemma 5.21] and [RW20b, Lemma 5.25].

This invariant can easily be extended to links colored by arbitrary positive integers. The setup described here corresponds to the case where all components are colored by 1, known as the uncolored case.

3.4. \mathfrak{gl}_0 homology. In this section we assume that the braid β of index k is chosen in such a way that its closure is a knot K . Consider the chain complex $C^{\mathfrak{gl}_1}(\widehat{\beta}; \mathbb{k})$. Having picked a basepoint \star on $\widehat{\beta}$, one defines an endomorphism φ_\star of $C^{\mathfrak{gl}_1}(\widehat{\beta}; \mathbb{k})$ that multiplies the decoration of the marked edge by x^{k-1} . Diagrammatically, this reads:

$$k \left\{ \begin{array}{c} \xrightarrow{\star} 1 \\ \vdots \end{array} \right\} \mapsto \left\{ \begin{array}{c} \xrightarrow{k-1} 1 \\ \vdots \end{array} \right\} k.$$

The fact that this is indeed a chain map follows from the locality of the differential and φ_\star . The image of φ_\star is a subcomplex of $C^{\mathfrak{gl}_1}(\widehat{\beta}; \mathbb{k})$.

Let us place a basepoint on the top left endpoint of the braid diagram, and denote by $C^{\mathfrak{gl}_0}(\widehat{\beta}; \mathbb{k})$ and $H^{\mathfrak{gl}_0}(\widehat{\beta}; \mathbb{k})$ the chain complex $\mathbf{q}^{1-k} \text{im}(\varphi_\star)$ and its homology. It is called the \mathfrak{gl}_0 homology of $K = \widehat{\beta}$. Of course, one can act with φ_\star on $\mathcal{S}_1(\omega; \mathbb{k})$ for any pointed annular web ω . The image defines a space $\mathcal{S}_0(\omega; \mathbb{k})$ called the \mathfrak{gl}_0 state space of ω .⁷

Theorem 3.11 ([RW22]). *Assume that \mathbb{k} is a field.*

- (1) The bigraded \mathbb{k} -vector space $H^{\mathfrak{gl}_0}(\widehat{\beta}; \mathbb{k})$ is an invariant of the knot $\widehat{\beta}$.
- (2) Its graded Euler characteristic is the Alexander polynomial $\Delta_{\widehat{\beta}}(\mathbf{q})$ normalized to satisfy the skein relation (1).

⁷In [RW22] this space was denoted by \mathcal{S}'_0 .

- (3) If \mathbb{k} has characteristic 0, then there is a bigraded spectral sequence from the reduced triply graded homology to the \mathfrak{gl}_0 homology.
- (4) Let D_k be the chain of dumbbells of index $k > 0$ (see Definition 2.24 and Figure 7). Then $\mathcal{S}_0(D_k; \mathbb{k})$ has dimension 1.

Let us make a few remarks about these results. In [RW22], everything is defined and stated over \mathbb{Q} . There is no difficulty for extending definition over \mathbb{Z} or any ring \mathbb{k} . The fact that \mathbb{k} is a field is needed for proving that the construction is independent from the basepoint: in the proof of [RW22, Proposition 5.6], one needs to know that the homology of a chain complex has no torsion.

It is important to notice that, contrary to $H^{\mathfrak{gl}_1}$, there is no condition on the invertibility of any integers. This comes from the fact that proofs of invariance under the first Markov move (stabilization) are very different in the two contexts.

The same definition works for links with a basepoint. However the resulting homology may depend on the component of the link where the basepoint is placed. We do not have an example, though, for which different choices of components yield different invariants.

Remark 3.12. The endomorphism φ_\star used to define $C^{\mathfrak{gl}_0}$ admits an alternative description. Instead of adding $k-1$ dots on the edge with basepoint, one can add a dot on each edge below the basepoint. Indeed, in $\mathcal{S}_1(\omega)$, the following relation holds

$$k \left\{ \begin{array}{c} \xrightarrow{k-1} 1 \\ \longrightarrow 1 \\ \longrightarrow 1 \\ \vdots \\ \longrightarrow 1 \end{array} \right\} = (-1)^{k-1} \left\{ \begin{array}{c} \longrightarrow 1 \\ \xrightarrow{\bullet} 1 \\ \xrightarrow{\bullet} 1 \\ \vdots \\ \xrightarrow{\bullet} 1 \end{array} \right\} k$$

because of the equality

$$x_2 \cdots x_k = \sum_{i=1}^k (-1)^{i-1} x_1^{i-1} e_{k-i}(x_1, \dots, x_k)$$

and Proposition 3.9 (3). The signs in this formula has absolutely no consequence on the definition of $C^{\mathfrak{gl}_0}$ since we are only interested in the image of φ_\star .

The complex $C^{\mathfrak{gl}_0}(\widehat{\beta})$ is defined above as a subcomplex of $\mathbf{q}^{1-k} C^{\mathfrak{gl}_1}(\widehat{\beta})$, but one can change the point of view and construct it also as a quotient of $\mathbf{q}^{k-1} C^{\mathfrak{gl}_1}(\widehat{\beta})$, which leads to a definition via a universal construction. Indeed, given a pointed annular web ω , the map φ_\star is the multiplication by a decoration, hence, an endomorphism of $D(\omega)$. This allows us to define a new pairing $\langle -; \omega; - \rangle_0$ on $D(\omega)$ as $\langle S; \omega; T \rangle_0 := \langle \varphi_\star(S), \omega, T \rangle_1$ for all $S, T \in D(\omega)$. Then we have an isomorphism

$$(25) \quad \mathcal{S}_0(\omega; \mathbb{k}) \cong \mathbf{q}^{k-1} D(\omega) / \text{rad} \langle -; \omega; - \rangle_0$$

Clearly,

$$\text{rad} \langle -; \omega; - \rangle_1 \subseteq \text{rad} \langle -; \omega; - \rangle_0$$

and the isomorphism (25) commutes with the differentials, so that $C^{\mathfrak{gl}_0}(\widehat{\beta})$ is a quotient of $\mathbf{q}^{k-1} C^{\mathfrak{gl}_1}(\widehat{\beta})$. In particular, for any pointed annular web ω , the space $\mathcal{S}_0(\omega; \mathbb{k})$ is a quotient of $B(\omega)$.

3.5. The spectral sequence from the reduced triply graded homology to \mathfrak{gl}_0 homology. We shall discuss here the construction of the spectral sequence from HHH^{red} to $H^{\mathfrak{gl}_0}$ sketched in [RW22]. Hereafter it is assumed that \mathbb{k} is a field of characteristic 0.

Given an elementary web ω of index k write $K^{\text{red}}(\omega)$ for the (reduced) Koszul complex associated with ω that is used to compute the reduced triply graded homology. It is defined as in (23), except that the reduced bimodule $\overline{B}(\omega)$ is taken and the tensor product is for $i \geq 2$. Besides the Koszul

differential d_{HH} this complex admits an additional differential d_0 that is induced by identity maps parallel to the components of d_{HH} . Hence, the total complex can be written as

$$(26) \quad K^{d_0}(\omega) := \overline{B}(\omega) \otimes_{R^e} \bigotimes_{i=2}^k (\mathbf{q}^2 R^e \xrightarrow{x_i \otimes 1 - 1 \otimes x_i + 1 \otimes 1} R^e)$$

A quick check shows that d_0 anticommutes with d_{HH} , so that (26) is indeed a chain complex of graded \mathbb{k} -modules. Let us write $H^{d_0}(\omega)$ for the homology of (26).

Proposition 3.13 (cp. [RW22]). *The functor H^{d_0} from \mathcal{AFoam}^* to \mathbb{k} -modules is isomorphic to \mathcal{S}_0 .*

Proof. We first show that $H^{d_0}(\omega)$ vanishes when ω is disconnected. Indeed, suppose that $\omega = \omega' \sqcup \omega''$ with ω' and ω'' of index k' and k'' respectively. Then $e_1(x_{k'+1}, \dots, x_k) \in R$ acts symmetrically on $\overline{B}(\omega)$. After changing the basis of R by trading x_k for the above polynomial, the factor in (26) for $i = k$ is the identity map. Therefore, the complex is acyclic.

Let now $\omega = D_k$ be the chain of $k - 1$ dumbbells as shown in Figure 13. The associated reduced

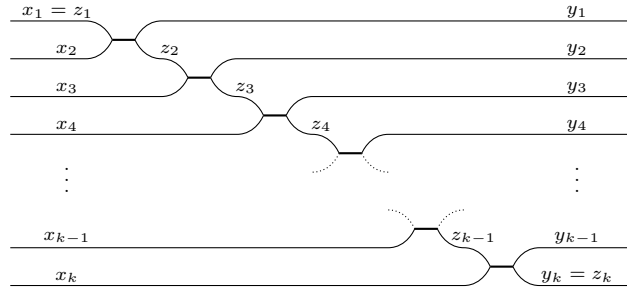


FIGURE 13. A open chain of dumbbells

Soergel bimodule $\overline{B}(\omega)$ is generated by the variables x_i, y_i, z_i modulo local relations and $y_1 = 0$. Notice that the set Λ of these relations is *regular*, that is none of its elements is a zero divisor modulo the others. Hence, the tensor product

$$(27) \quad \bigotimes_{r \in \Lambda} (D(\omega) \xrightarrow{r} D(\omega)),$$

where $D(\omega)$ is the algebra of all decorations of ω , is a projective resolution of $\overline{B}(\omega)$. Enlarging Λ by adding relations

$$(28) \quad x_i = y_i - 1$$

for $1 < i \leq k$ produces a complex that computes $H^{d_0}(\omega)$. We claim that this enlarged set of relations is still regular. For that it is enough to notice that (28) allows to rewrite local linear relations as

$$(29) \quad z_i = y_i + (k - i) \quad \text{for } 1 \leq i \leq k.$$

The local quadratic relations can be then rewritten as

$$\begin{aligned} x_{i+1}z_i - y_iz_{i+1} &= (y_{i+1} - 1)(y_i + (k - i)) - y_i(y_{i+1} + (k - i - 1)) \quad \text{for } 1 \leq i < k \\ &= (y_{i+1} - y_i - 1)(k - i) \end{aligned}$$

and reduced to $y_{i+1} = y_i + 1$, and further to $y_{i+1} = i$. Hence, the complex computing $H^{d_0}(D_k)$ is isomorphic via a base change to the Koszul complex associated with the sequence of relations

$$y_i = i - 1, \quad z_i = (k - 1), \quad x_{i+1} = i - 1,$$

which is clearly a regular set. Thence, higher homology vanishes and $H^{d_0}(\omega) = \mathbb{k}$ is generated by the empty decoration.

It follows now from Proposition 2.25 that $H^{d_0}(\omega)$ is concentrated in degree 0 for any elementary web ω . Hence, it is a quotient of $\overline{B}(\widehat{\omega})$, the Soergel space associated with the annular closure of ω . The same holds for S_0 and the desired isomorphism is induced by the identity on $\overline{B}(\widehat{\omega})$. \square

Proposition 3.13 is the main ingredient in the construction of the desired spectral sequence. Instead of computing H^{d_0} at once, one can first compute the homology with respect to d_{HH} and consider the spectral sequence induced by d_0 . When applied to the cube of resolutions of a braid closure β , this produces the desired spectral sequence from $HHH^{\text{red}}(\widehat{\beta})$ to $H^{\mathfrak{gl}_0}(\widehat{\beta})$. Notice that the differential on the second page is induced by d_0 and of $(\mathfrak{a}, \mathfrak{q}, \mathfrak{t})$ -degree $(-2, 0, 1)$.

Remark 3.14. A priori $H^{d_0}(\omega)$ does not admit the quantum grading, because it is not preserved by the total differential. However, it can be recovered by Proposition 3.13. Another way to introduce the quantum grading on $H^{d_0}(\omega)$ is to consider the spectral sequence on $HH(\overline{B}(\omega))$ induced by d_0 and notice that it collapses immediately [RW22]. Hence, $H^{d_0}(\omega)$ is the homology of the complex $(HH(\overline{B}(\omega)), d_0)$, in which the Hochschild and quantum gradings are collapsed to a single grading.

4. HEEGAARD FLOER HOMOLOGY

We shall now review the (twisted) Heegaard Floer homology for a marked singular link S following [OSS09, OS09]. We write S_0, \dots, S_r for the components of S , ordered top to bottom with respect to their topmost trace vertices. In particular $\star \in S_0$.

4.1. Heegaard diagrams and holomorphic disks. We begin with describing Heegaard diagrams for a pointed singular link S , where the marking is located on the component S_0 . Let $(H_\alpha, H_\beta, \Sigma)$ be a Heegaard splitting of \mathbb{S}^3 , for which there is a thickening $V \approx \Sigma \times [0, 1]$ of Σ satisfying what follows:

- $S \cap V$ is a collection of fibers of V that includes all thick edges of S and an arc with the marking $\star \in S_0$,
- thick edges of S and the arc carrying the marking are oriented from H_α to H_β , and
- $S \setminus V$ consists of untangled arcs in H_α and H_β , so that it can be isotoped onto ∂V .

Partition $S \cap \Sigma$ into $\mathbb{X} \sqcup \mathbb{O}$, where $\mathbb{X} = \{X_0, \dots, X_k\}$ consists of the intersection points, at which the link is oriented from H_α to H_β , and $\mathbb{O} = \{O_0, \dots, O_{k+s}\}$ of the other ones (s is the number of thick edges in S). The intersection points of thick edges with Σ form a subset $\mathbb{XX} \subset \mathbb{X}$. The elements of \mathbb{X} (resp. \mathbb{O}) are called \mathbb{X} -basepoints (resp. \mathbb{O} -basepoints); the points from \mathbb{XX} are *double basepoints*. It is understood that X_0 coincides with the marking $\star \in S$ and O_0 is located on S just before X_0 , i.e. both basepoints are connected with an arc in H_α .

The last condition on the Heegaard splitting guarantees the existence of a collection of $k + g$ disks in H_α with boundary on Σ (here g stands for the genus of Σ) that cut the handlebody into balls, each with one untangled piece of S : either an arc or a Y-shape (a web with a single vertex). The boundary of this collection $\alpha = \{\alpha_1, \dots, \alpha_{g+k}\}$ consists of α -curves that decompose Σ into regions A_0, \dots, A_k , each containing a unique \mathbb{X} -basepoint. By convention we enumerate the regions so that $X_i \in A_i$. We choose a collection $\beta = \{\beta_1, \dots, \beta_{g+k}\}$ of β -curves likewise by decomposing H_β and we write B_0, \dots, B_k for the closures of the connected components of $\Sigma \setminus \beta$, where $X_i \in B_i$. It is assumed that the two families of curves intersect transversely.

The data $(\Sigma, \alpha, \beta, \mathbb{X}, \mathbb{O})$ determines the link S completely. We call it a *multipointed Heegaard diagram for S* . It is not determined by S , but any two Heegaard diagrams for S are related by a finite number of certain moves [OS08, Proposition 3.3].

Example 4.1. Given a diagram of a singular link S , possibly with thin edges subdivided by bivalent vertices, we construct a multipointed Heegaard diagram, called the *initial Heegaard diagram for S* ,

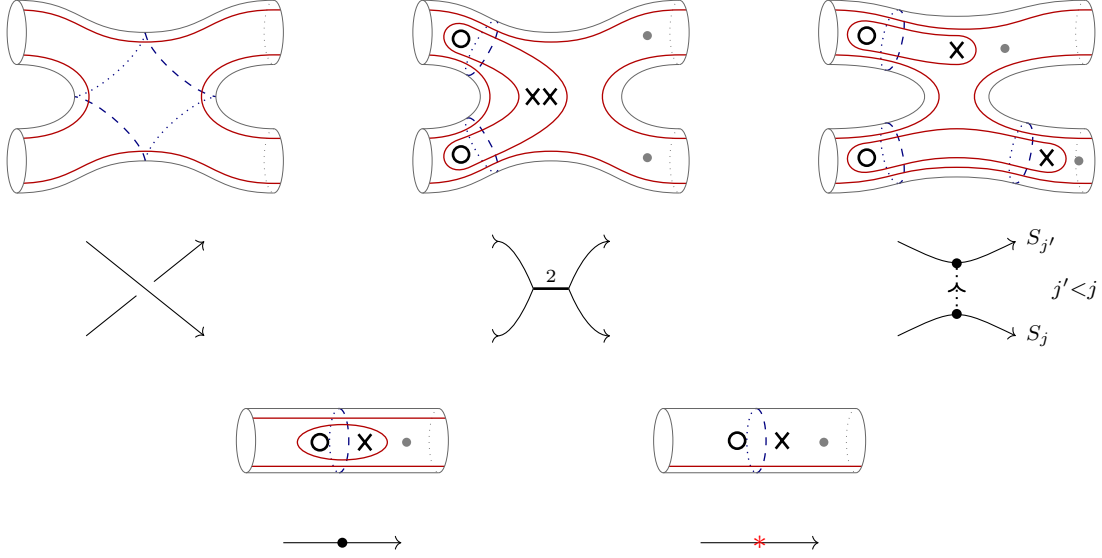


FIGURE 14. Local pictures of the initial Heegaard diagram for a singular link S . The top row shows the pieces of the diagram around a positive crossing (flip the picture for the negative one), a singular crossing, and at a chosen line connecting different components of the link. The bottom row shows configurations around bivalent vertices: a general situation to the left and the case of the distinguished vertex (the marking of S) to the right. Dashed blue and solid red arcs represent α and β curves respectively.

as follows. First, we choose the α - and β -curves in a way, that near crossings and vertices they look as in the left and middle pictures of Figure 14. The blue α -curves are meridians around thin edges of S and curves around real crossings. The red β -curves are either parallel to the contours of the surface or they bound disks containing the X and O basepoints; the latter are called *internal curves*. We then perform two modifications. Let S_0 be the component of S that carries the marking of S . We enumerate other components S_1, \dots, S_r , so that each S_j for $j > 0$ can be connected with an arrow to some $S_{j'}$ with $j' < j$. Attach a handle to the surface along each such arrow, merge two β -curves along this handle and add a new meridional α -curve around S_j as shown in the top right corner of Figure 14.⁸ This guarantees that the surface is connected, but it has two more β -curves than α -curves. We fix it by removing two β -curves near the marking: the internal one and one parallel to the contour of the surface, see the bottom right corner of Figure 14 (this is the piece of the diagram with basepoints X_0 and O_0). The reader is encouraged to check that the resulting diagram satisfies the conditions for a Heegaard diagram. In particular, the number of β -curves matches the number of α -curves.

Consider the symmetric product of the underlying surface $Sym^{g+k}(\Sigma)$. It is a symplectic manifold with Lagrangian tori $\mathbb{T}_\alpha = \alpha_1 \times \dots \times \alpha_{g+k}$ and $\mathbb{T}_\beta = \beta_1 \times \dots \times \beta_{g+k}$ that are totally real with respect to any compatible almost complex structure. Let $\mathfrak{G} = \mathbb{T}_\alpha \cap \mathbb{T}_\beta$ be the set of intersection points between the two tori. Given $\mathbf{x}, \mathbf{y} \in \mathfrak{G}$ denote by $\pi_2(\mathbf{x}, \mathbf{y})$ the set of homotopy classes of *Whitney disks* from \mathbf{x} to \mathbf{y} , i.e. continuous maps of the standard complex disk into $Sym^{g+k}(\Sigma)$ that carry $-i$ (resp. i) to \mathbf{x} (resp. \mathbf{y}) and points on the boundary circle with positive (resp. negative) real part to \mathbb{T}_α (resp. \mathbb{T}_β). This set is never empty when $H_1(Y) = 0$ [OS04b, Section 2]. Under generic conditions, the moduli space $\mathcal{M}(\phi)$ of pseudo-holomorphic representatives of ϕ is an orientable

⁸This configuration differs by a handle slide from the one associated with a smooth resolution in [OS09].

smooth manifold of dimension equal to the *Maslov index* $\mu(\phi)$. It admits a free action of the group of conformal automorphisms of a unit disk that fix the points i and $-i$, which is isomorphic to \mathbb{R} . We write $\widehat{\mathcal{M}}(\phi)$ for the quotient of $\mathcal{M}(\phi)$ by the action of this group and refer to its elements as *unparametrized* disks. In case $\mathbf{x} = \mathbf{y}$ we consider also *degenerate* Whitney disks that carry i to \mathbf{x} and the entire boundary circle either to \mathbb{T}_α (α -degeneracy) or \mathbb{T}_β (β -degeneracy), but there is no additional condition on the image of $-i$. The space $\mathcal{N}(\psi)$ of pseudo-holomorphic representatives of such a degenerate disk ψ is generically an orientable smooth manifold of dimension $\mu(\psi)$ that admits a free action of a two-dimensional subgroup \mathbb{G} of $PSL(2, \mathbb{R})$. In particular, $\mu(\psi)$ is even when $\mathcal{N}(\psi) \neq \emptyset$. We write $\widehat{\mathcal{N}}(\psi)$ for the quotient space.

We shall now recall a combinatorial formula for the Maslov index [Lip06]. Given a Whitney disk ϕ and a point $p \in \Sigma$ we write $n_p(\phi)$ for the algebraic intersection number of ϕ with the subvariety $\{p\} \times \text{Sym}^{g+k-1}(\Sigma)$. Let $\{\Omega_i\}$ be the set of (closures of) connected components of $\Sigma \setminus (\alpha \cup \beta)$, and choose $p_i \in \Omega_i$ for each i . The 2-chain

$$\mathcal{D}(\phi) := \sum_i n_{p_i}(\phi) [\Omega_i] \in C_2(\Sigma, \alpha \cup \beta)$$

is called the *domain associated with ϕ* . It determines ϕ uniquely when $g + k > 2$ and it is *positive*, i.e. with no negative coefficients, when ϕ has a holomorphic representative. The Maslov index $\mu(\phi)$ can be computed as follows. Let $(V, \partial V) \subset (\Sigma, \alpha \cup \beta)$ be a 2-chain bounded by arcs in α and β curves and denote by $\text{ac}(V)$ and $\text{obt}(V)$ the number of acute and obtuse corners of V . The *Euler norm* of V

$$e(V) = \chi(V) + \frac{1}{4}(\text{obt}(V) - \text{ac}(V))$$

is additive under gluing domains together, so that it can be extended linearly to relative 2-chains. The Maslov index of $\phi \in \pi_2(\mathbf{x}, \mathbf{y})$ represented by a domain $\mathcal{D} = \mathcal{D}(\phi)$ is then given as

$$\mu(\phi) = e(\mathcal{D}) + a_{\mathbf{x}} + a_{\mathbf{y}},$$

where $a_{\mathbf{x}}$ (resp. $a_{\mathbf{y}}$) is the sum of average multiplicities of \mathcal{D} over the four regions around each x_i (resp. y_i). In particular, if \mathcal{D} has only multiplicities 0 and 1, then $a_p = \frac{1}{4}$ or $\frac{3}{4}$ when p is an acute or an obtuse corner respectively. Note that both \mathcal{D} and μ are additive with respect to the juxtaposition of Whitney disks $\star: \pi_2(\mathbf{x}, \mathbf{y}) \times \pi_2(\mathbf{y}, \mathbf{z}) \rightarrow \pi_2(\mathbf{x}, \mathbf{z})$.

Example 4.2. Suppose that $\mathcal{D} = \mathcal{D}(\phi)$ is a bigon with acute corners and no intersection point inside. Then $e(\mathcal{D}) = 1 - \frac{2}{4} = \frac{1}{2}$ and $a_{\mathbf{x}} = a_{\mathbf{y}} = \frac{1}{4}$, leading to $\mu(\phi) = 1$. This is consistent with the fact, that ϕ has a unique holomorphic representative up to reparametrization by the Riemann Mapping Theorem. More generally, if \mathcal{D} is a $2n$ -gon with acute corners and intersection points $x_i = y_i$ for $i = 1, \dots, r$ in its interior, then $e(\mathcal{D}) = 1 - \frac{n}{2}$ and $a_{\mathbf{x}} = a_{\mathbf{y}} = \frac{n}{4} + r$, resulting in $\mu(\phi) = 1 + 2r$.

Example 4.3. Let $\psi \in \pi_2(\mathbf{x}, \mathbf{x})$ be a degenerated disk with its associated domain \mathcal{D} equal to A_i or B_j . Because $\mathcal{N}(\psi)$ can be identified with the group \mathbb{G} under certain conditions on the almost complex structure [OS04b, Section 5], we have $\mu(\psi) = \dim \mathbb{G} = 2$. The Maslov index of ψ can be also computed combinatorially as follows. First notice that the α -curves as well as the β -curves decompose Σ into pieces of genus 0. Hence, if $\mathcal{D} = A_i$ (resp. B_j), then it must contain exactly $g = g(\mathcal{D})$ α -curves (resp. β -curves) in its interior and each such curve carries a unique intersection point x_i from \mathbf{x} ; this point contributes 1 towards $a_{\mathbf{x}} = a_{\mathbf{y}}$. Likewise, each boundary component of \mathcal{D} carries an intersection point contributing $\frac{1}{2}$. Therefore $\mu(\psi) = \chi(\mathcal{D}) + 2g + r = 2$ as desired, where we write r for the number of boundary components of \mathcal{D} .

A domain π is *periodic* if its boundary is a linear combination of α - and β -curves. It represents a difference of two Whitney disks connecting the same intersection points. Of particular interest are

periodic domains that vanish at both \mathbb{X} - and \mathbb{O} -basepoints. For instance, there is such a periodic domain

$$(30) \quad \pi_j = \sum_{i: X_i \in S_j} (A_i - B_i)$$

associated with any component S_j of the singular link S . We call them *fundamental periodic domains*. Clearly $\sum_j \pi_j = 0$ and one can show that every periodic domain vanishing at both \mathbb{X} - and \mathbb{O} -basepoints is a linear combination of π_j 's.

We say that a Heegaard diagram is *admissible* if there are no nontrivial positive periodic domains that avoid the set \mathbb{X} .⁹

Lemma 4.4. *Initial Heegaard diagrams are admissible.*

Proof. The argument is motivated by the one in [Man14, Lemma 2.1]. A periodic domain that avoids \mathbb{X} is given by a 2-chain $\pi = \sum_{i=0}^k a_i (A_i - B_i)$. Assume that π is positive, in which case $a_i \geq a_j$ whenever $A_i \cap B_j \neq \emptyset$. In particular, the coefficients a_i cannot decrease when we follow any path in S . Because S can be expressed as an infinite union of oriented circles (see Figure 3), this implies that the coefficients are in fact locally constant, i.e. $a_i = a_{i'}$ if both X_i and $X_{i'}$ lie on the same component of S . This forces $\pi = \sum_j c_j \pi_j$ for some $c_j \in \mathbb{Z}$.

Let S_0, \dots, S_r be the connected components of S , where $\star \in S_0$. Suppose that S_j and $S_{j'}$ are next to each other as in the top right picture of shown on Figure 14 with X_j and $X_{j'}$ the lower and upper X basepoints respectively. Recall that in case $j' = 0$ the red curve around $X_{j'}$ is removed. The disk B_j , bounded by the red curve around X_j , intersects $A_{j'}$ that carries $X_{j'}$. Hence, $c_j \leq c_{j'}$ by the positivity of π . In other words, the values of c_j 's do not decrease when we go along the trace section towards the marking $\star \in S_0$, so that $c_j \leq c_0$ for each j . On the other hand, the region B_0 , obtained from the surface by removing all disks bounded by internal β curves, intersects all A regions. Thus all the coefficients c_j coincide with c_0 , forcing $\pi = c_0 \sum_j \pi_j = 0$. \square

Remark 4.5. The initial diagram from [OS09, Fig. 3] fails to be admissible in case of links, because in this diagram periodic domains associated with different components of the link are disjoint.

The moduli space of unparametrized curves $\widehat{\mathcal{M}}(\phi)$ admits a Gromov compactification that adds as boundary points *nodal disks* or *broken flow lines*, which are juxtapositions of Whitney disks ϕ_1, \dots, ϕ_r , degenerated disks ψ_1, \dots, ψ_s and holomorphic spheres S_1, \dots, S_t with the property that

$$\mathcal{D}(\phi) = \sum_{i=1}^r \mathcal{D}(\phi_i) + \sum_{j=1}^s \mathcal{D}(\psi_j) + \sum_{k=1}^t \mathcal{D}(S_k),$$

where $r > 1$, $s > 0$, or $t > 0$. In particular, $\widehat{\mathcal{M}}(\phi)$ is already compact and 0-dimensional when $\mu(\phi) = 1$ and the same holds for $\widehat{\mathcal{N}}(\psi)$ with $\mu(\psi) = 2$. Note that holomorphic spheres do not appear unless $\mathcal{D}(\phi)$ covers the entire surface, because $\mathcal{D}(S) = \Sigma$ for any holomorphic sphere S , see [OS04b].

Having chosen an orientation of moduli spaces, we can write $\#\widehat{\mathcal{M}}(\phi)$ (resp. $\#\widehat{\mathcal{N}}(\psi)$) for the signed count of points, where the sign of a point depends on whether the action of the parametrization group on the moduli space $\mathcal{M}(\phi)$ (resp. $\mathcal{N}(\psi)$) preserves or reverses the orientation. According to [AE15] one can always choose a system of orientations with the following properties:

- (1) the orientation of $\widehat{\mathcal{M}}(\phi_1) \times \widehat{\mathcal{M}}(\phi_2)$ is induced from $\widehat{\mathcal{M}}(\phi_1 \star \phi_2)$ for any Whitney disks $\phi_1 \in \pi_2(\mathbf{x}, \mathbf{y})$ and $\phi_2 \in \pi_2(\mathbf{y}, \mathbf{z})$,
- (2) $\widehat{\mathcal{N}}(\psi)$ carries the orientation induced from $\widehat{\mathcal{M}}(\psi)$ in case of α -degeneracies and the opposite one in case of β -degeneracies,

⁹This condition is equivalent to the absence of nontrivial positive periodic domains of Maslov index 0.

(3) $\#\widehat{N}(\psi) = 1$ when $\psi = A_i$ or B_j .

As an easy application of the above definition we show the following fact, which is an important tool to analyze the Heegaard Floer differential recalled in Section 4.2.

Lemma 4.6. *Suppose that $A_i \cap B_i$ is a bigon for some i and let ϕ_1 and ϕ_2 be Whitney disks represented by the domains $A_i \setminus B_i$ and $B_i \setminus A_i$. Then $\#\widehat{\mathcal{M}}(\phi_1) + \#\widehat{\mathcal{M}}(\phi_2) = 0$.*

Proof. Choose \mathbf{x} and \mathbf{y} , such that $\phi_1, \phi_2 \in \pi_2(\mathbf{y}, \mathbf{x})$. Let $\phi_0 \in \pi_2(\mathbf{x}, \mathbf{y})$ and $\psi_A, \psi_B \in \pi_2(\mathbf{x}, \mathbf{x})$ be Whitney disks represented by the domains $A_i \cap B_i$, A_i , and B_i respectively. Notice that ϕ_0, ϕ_1 , and ϕ_2 are the only Whitney disks between \mathbf{x} and \mathbf{y} that have Maslov index 1 and are associated with domains contained in $A_i \cup B_i$. Because $\widehat{\mathcal{M}}(\psi_A)$ and $\widehat{\mathcal{M}}(\psi_B)$ are 1-dimensional, counting endpoints of each with signs gives zero. Hence,

$$\begin{aligned} 0 &= \#\partial\widehat{\mathcal{M}}(\psi_A) = \#(\widehat{\mathcal{M}}(\phi_0) \times \widehat{\mathcal{M}}(\phi_1)) + \#\widehat{N}(\psi_A) = \#\widehat{\mathcal{M}}(\phi_0) \cdot \#\widehat{\mathcal{M}}(\phi_1) + 1, \\ 0 &= \#\partial\widehat{\mathcal{M}}(\psi_B) = \#(\widehat{\mathcal{M}}(\phi_0) \times \widehat{\mathcal{M}}(\phi_2)) - \#\widehat{N}(\psi_B) = \#\widehat{\mathcal{M}}(\phi_0) \cdot \#\widehat{\mathcal{M}}(\phi_2) - 1. \end{aligned}$$

Summing up the two equations proves the thesis. \square

Computing the numbers $\#\widehat{\mathcal{M}}(\phi)$ in general is very challenging, but in some cases the answer is known. For instance, $\#\widehat{\mathcal{M}}(\phi) = \pm 1$ if $\mathcal{D}(\phi)$ is a bigon. The following is a generalization of that.

Lemma 4.7 ([OS09, Lemma 3.11]). *Suppose that the 2-chain $\mathcal{D}(\phi)$ associated with a Whitney disk $\phi \in \pi_2(\mathbf{x}, \mathbf{y})$ is a planar region with the following properties:*

- *all its boundary components are α -curves (resp. β -curves) except one that is a $2n$ -gon with acute corners and edges alternating between arcs in α - and β -curves (thus, the corners alternate between components of \mathbf{x} and \mathbf{y}),*
- *there is a collection of arcs in β -curves (resp. α -curves) between boundary components of $\mathcal{D}(\phi)$ that cut the domain into a disk, and*
- *no component x_i or y_i is in the interior of $\mathcal{D}(\phi)$.*

Then $\mu(\phi) = 1$ and $\#\widehat{\mathcal{M}}(\phi) = \pm 1$.

4.2. The Heegaard Floer complex. We are ready to state the definition of the twisted Heegaard Floer homology from [OS09]. As usual \mathbb{k} is a commutative ring and we fix an invertible $t \in \mathbb{k}$.

Definition 4.8. Let $(\Sigma, \alpha, \beta, \mathbb{X}, \mathbb{O})$ be an admissible Heegaard diagram associated with a marked singular link $S \subset Y$. Given a finite set of markings $P \subset \Sigma - (\alpha \cup \beta \cup \mathbb{X} \cup \mathbb{O})$ we define the *twisted Heegaard Floer complex* $\underline{CFK}^-(S, P)$ as the free module over the polynomial algebra $R = \mathbb{k}[U_0, \dots, U_{k+s}]$ with a basis consisting of the intersection points $\mathbf{x} \in \mathfrak{G}$ and the differential given by

$$(31) \quad \partial\mathbf{x} = \sum_{\mathbf{y} \in \mathfrak{G}} \sum_{\substack{\phi \in \pi_2(\mathbf{x}, \mathbf{y}) \\ \mu(\phi)=1 \\ \forall i: X_i(\phi)=0}} \#\widehat{\mathcal{M}}(\phi) t^{P(\phi)} U_0^{O_0(\phi)} \dots U_{k+s}^{O_{k+s}(\phi)} \mathbf{y},$$

where $P(\phi)$ counts multiplicities of $\mathcal{D}(\phi)$ at elements of P , $X_i(\phi)$ is the multiplicity of ϕ at X_i and likewise for $O_i(\phi)$. The complex $\widehat{CFK}(S, P)$ is defined as the quotient $\underline{CFK}^-(S, P)/(U_0 = 0)$ by the variable U_0 associated with the basepoint O_0 that is located on the arc of S that terminates at the marking $\star \in S$. The homology of the complexes are denoted respectively by $\underline{HFK}^-(S, P)$ and $\widehat{HFK}(S, P)$.

Remark 4.9. The admissibility implies that any two points $\mathbf{x}, \mathbf{y} \in \mathfrak{G}$ are connected by only finitely many positive domains that avoid the set \mathbb{X} , making the right hand side of (31) a finite sum.

Remark 4.10. The above definition recovers the usual Heegaard Floer complexes $CFK^-(S)$ and $\widehat{CFK}(S)$ when $t = 1$ or P is empty.

Example 4.11. The Ozsváth–Szabó twisting is given by the set of markings P^{OS} visualized in Figure 14 with gray dots. When S is in a braid position, then we can pick a subset $P^{tr} \subset P^{\text{OS}}$ that consists only of the dots near trace vertices. These two sets lead to essentially the same twisted complex, see Corollary 4.14.

The Heegaard Floer complex is bigraded, with the *Alexander grading* $A(\mathbf{x}) \in \mathbb{Z}$ and the *Maslov grading* $M(\mathbf{x}) \in \mathbb{Z}$. In this paper, however, we consider slightly different gradings: the *quantum grading* $\text{qdeg}(\mathbf{x}) := -2A(\mathbf{x})$ and the *homological grading* $\text{hdeg}(\mathbf{x}) := 2A(\mathbf{x}) - M(\mathbf{x})$ that satisfy

$$(32) \quad \text{qdeg}(\mathbf{y}) - \text{qdeg}(\mathbf{x}) = 2\mathbb{X}(\phi) + 2\mathbb{XX}(\phi) - 2\mathbb{O}(\phi)$$

$$(33) \quad \text{hdeg}(\mathbf{y}) - \text{hdeg}(\mathbf{x}) = \mu(\phi) - 2\mathbb{X}(\phi)$$

for any $\phi \in \pi_2(\mathbf{x}, \mathbf{y})$, where given a finite set $Q \subset \Sigma$ we write $Q(\phi)$ for the sum of multiplicities of ϕ at points from Q . Note that points from \mathbb{XX} are counted four times in (32), because $\mathbb{XX} \subset \mathbb{X}$.

Remark 4.12. At the first sight it might seem that the formulas (32) and (33) do not match those from [OS09, after Definition 2.1, p. 871]. The reason is that double \mathbb{X} -basepoints are considered in [OS09] as pairs of basepoints, so that $\mathbb{X}(\phi)$ from [OS09] matches our $\mathbb{X}(\phi) + \mathbb{XX}(\phi)$.

The homological grading is normalized using the quotient complex $\widehat{CF} = CFK^-(S)/(U_i = 1)$, in which all variables U_i are specialized to 1. It is known that this complex computes the cohomology of the k -torus and we require that the top degree generator of the homology is in degree 0. The quantum grading is then normalized to match the formula

$$\Delta(S) = (\mathfrak{q} - \mathfrak{q}^{-1})^\sigma \sum_{d,s} (-1)^d \mathfrak{q}^s \text{rk} \widehat{HFK}_d(S, P; s),$$

where σ is the number of singular crossings in S and $\widehat{HFK}_d(S, P; s)$ is the degree s component of the d -th homology group.

We finish this section with a short discussion on how the complex depends on the twisting set. It is known that the homology of the twisted complex over the ring of Laurent polynomials is isomorphic to that of the untwisted complex over the base field tensored with the ring of Laurent polynomials [OS09, Lemma 2.2]. The proof can actually be extended to singular knots. In case of a singular link we can only identify complexes when the twisting sets are “proportional” on the fundamental periodic domains π_1, \dots, π_r defined in (30), which are associated with the components of the link that do not carry the marking \star .

Proposition 4.13. *Let S be a singular link and suppose that P and P' are two sets of markings on a Heegaard diagram for S , such that $P(\pi_i) = \lambda P'(\pi_i)$ for some fixed $\lambda \in \mathbb{Z}$ and every fundamental periodic domain π_i . Then there is a \mathbb{k} -linear isomorphism of complexes*

$$\Phi: \underline{CFK}^-(S, P, t) \xrightarrow{\cong} \underline{CFK}^-(S, P', t^\lambda),$$

where the left (resp. right) complex is twisted by t (resp. t^λ). In particular,

$$\Phi: \underline{CFK}^-(S, P) \xrightarrow{\cong} CFK^-(S) \otimes_{\mathbb{Z}} \mathbb{k}$$

for any singular knot S and a twisting set P .

As a direct consequence, there is no essential difference between Ozsváth–Szabó twisting and its restriction to trace vertices in case of layered diagrams as defined in Section 3.1.

Corollary 4.14. *Let S be a layered diagram of a singular link with vertices at n levels. Then there is an isomorphism of twisted complexes*

$$\underline{CFK}^-(S, P^{\text{OS}}, t) \cong \underline{CFK}^-(S, P^{tr}, t^n).$$

Proof. We have $P^{\text{OS}}(\pi_i) = b_i n$ and $P^{\text{tr}}(\pi_i) = b_i$, where b_i is the index of the component S_i . \square

In order to proof Proposition 4.13 we need a suitable decomposition of the twisted complex.

Definition 4.15. Generators $\mathbf{a} = (U_0^{r_0} \cdots U_{k+s}^{r_{k+s}})\mathbf{x}$ and $\mathbf{b} = (U_0^{r'_0} \cdots U_{k+s}^{r'_{k+s}})\mathbf{y}$ are W_0 -equivalent, written $\mathbf{a} \sim \mathbf{b}$, if there is a Whitney disk $\phi \in \pi_2(\mathbf{x}, \mathbf{y})$ such that

$$(34) \quad O_i(\phi) = r'_i - r_i \quad \text{and} \quad X_j(\phi) = 0$$

for each $X_j \in \mathbb{X}$ and $O_i \in \mathbb{O}$.

The W_0 -equivalence is an equivalence relation on the set

$$\mathcal{B} = \left\{ (U_0^{r_0} \cdots U_{k+s}^{r_{k+s}})\mathbf{x} \mid \mathbf{x} \in \mathfrak{G}, r_i \geq 0 \right\}$$

of \mathbb{k} -linear generators of the Heegaard Floer complex and it is compatible with the differential. Hence, it induces a decomposition

$$\underline{\text{CFK}}^-(S, P) = \bigoplus_{r \in \mathcal{B}/\sim} \underline{\text{CFK}}^-(S, P; r)$$

parametrized by the set of equivalence classes. When S is a knot, then for any two generators of the same Alexander degree there is a disk connecting them,¹⁰ so that $\mathcal{B}/\sim \approx \mathbb{Z}$.

Proof of Proposition 4.13. Pick a set $\mathcal{R} \subset \mathcal{B}$ of representants of W_0 -equivalence classes. Given a generator $\mathbf{a} = (U_0^{r_0} \cdots U_{k+s}^{r_{k+s}})\mathbf{x}$ that is W_0 -equivalent to a chosen representant $(U_0^{r'_0} \cdots U_{k+s}^{r'_{k+s}})\mathbf{y} \in \mathcal{R}$ pick a Whitney disk $\phi \in \pi_2(\mathbf{x}, \mathbf{y})$ satisfying (34). A difference between any two such disks is a linear combination of the periodic domains π_1, \dots, π_r , so that the value $P(\phi) - \lambda P'(\phi)$ is independent of the choice of ϕ . Hence,

$$\Phi(\mathbf{a}) := t^{P(\phi) - \lambda P'(\phi)} \mathbf{a}$$

is a well-defined isomorphism of complexes. The case of a singular knot follows, because there are no periodic domains π_i . In particular, the disk ϕ is unique. \square

The assumption on connectivity of the diagram is important for untwisting: the two complexes have drastically different homology when S is a split link. For instance, the twisted homology may vanish for fully singular links with more than one component, see Proposition 4.22 or the proof of [OS09, Proposition 3.4].

4.3. Skein exact triangles. Let us now recall the skein exact triangle for Heegaard Floer homology. In this section we use *planar* Heegaard diagrams that look locally as depicted in Figure 15. For simplicity, we start with the untwisted complex and discuss the differences afterwards.

Lemma 4.16. *The planar Heegaard diagram associated with a singular link is admissible.*

Proof. Suppose that $\pi = \sum_i a_i(A_i - B_i)$ is a positive periodic domain, where A_0 and B_0 are the unbounded regions. Then A_0 intersects each B_i forcing $a_0 \geq a_i$. Likewise, B_0 intersects each A_i forcing $a_0 \leq a_i$. Hence, all a_i coincide and $\pi = 0$. \square

¹⁰Indeed, such a disk can be constructed by correcting any Whitney disk $\phi \in \pi_2(\mathbf{x}, \mathbf{y})$ as follows. First, impose multiplicity zero at each X_i by adding to $\mathcal{D}(\phi)$ domains A_i sufficiently many times. The total multiplicity at \mathbb{O} -basepoints is now equal to $\text{qdeg}(\mathbf{y}) - \text{qdeg}(\mathbf{x}) = \sum_i (r'_i - r_i)$, but local multiplicities at each O_i may not match (34). This is fixed by travelling along the knot and adding differences $A_i - B_i$ to correct the multiplicity at each O_i , which affects the multiplicity only at the next basepoint. Once the last basepoint is reached, the local multiplicity is already as expected.

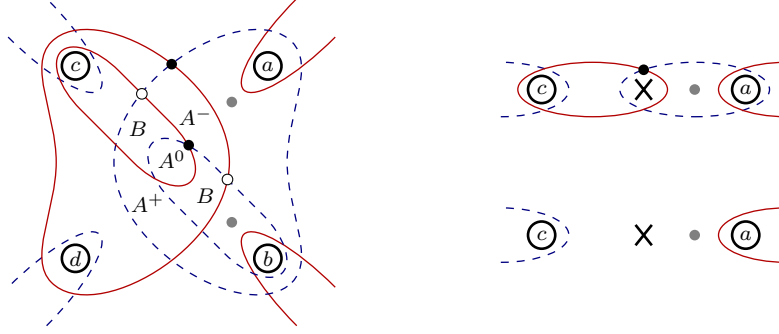


FIGURE 15. Local pictures of the planar Heegaard diagram for a resolution of a singular link. Near a smoothed resolution the left diagram is used with one \mathbb{X} -mark at each region decorated with B , whereas for a positive (resp. negative) crossing we place \mathbb{X} -marks at A^0 and A^+ (resp. A^-); the local diagram for a singular crossing is obtained by placing a double \mathbb{X} -mark at A^0 and removing the pair of ellipses around it. For the convenience of the reader, these diagrams are repeated explicitly on Figure 16. The top right configuration is used near a bivalent vertex other than the basepoint \star , in which case the bottom variant is used instead. The marked intersection points are components of the canonical generator \mathbf{x}_0 : the white points at smooth resolutions and the black points elsewhere. Gray dots represent the twisting markings due to Ozsváth and Szabó.

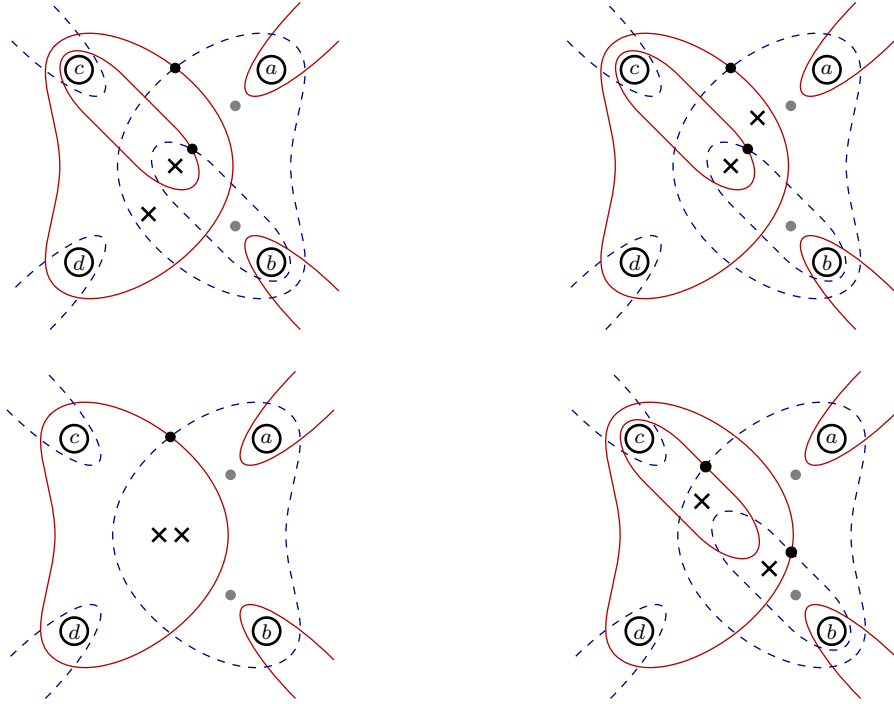


FIGURE 16. From left to right and from top to bottom, local pictures of the planar Heegaard diagram for a positive crossing, a negative crossing, a singular crossing and a smoothing.

We distinguish a generator $\mathbf{x}_0 = \mathbf{x}_0(S) \in CFK^-(S)$ that is given by the intersection points marked on Figure 15 with black dots except neighborhoods of smoothed resolutions, where white

points are taken instead. The gradings can be normalized by specifying

$$(35) \quad \text{hdeg}(\mathbf{x}_0) = 0 \quad \text{and} \quad \text{qdeg}(\mathbf{x}_0) = s - n - 1,$$

where n is the number of real crossings in S and s is the number of Seifert circles, obtained by smoothing in S all crossings (both real and singular). The first choice follows from the observation below, whereas the normalization of the quantum grading is justified at the end of this section.

Lemma 4.17. *The generator \mathbf{x}_0 , when considered as an element of $\widehat{CF} = CFK^-(S)/(U_i = 1)$, is a cycle that generates the top degree homology.*

Proof. Setting $U_i = 1$ for all i allows us to forget the \mathbb{O} -basepoints. The Heegaard diagram can be then reduced, so that each α -curve intersects only one β -curve, exactly in two points, one of which is a component of \mathbf{x}_0 . In fact, \mathbf{x}_0 is the top degree generator of the associated Heegaard Floer complex, hence, a cycle. \square

We call \mathbf{x}_0 the *canonical generator*¹¹ of $CFK^-(S)$. Because \widehat{HF} is the homology of the k -torus [OS04b, Lemma 9.1] and hence free, we obtain a following generalization of Lemma 4.6 that will play an important role in the next section. The case $k = 2$ has been proven in an unpublished version of [OS09].

Corollary 4.18. *Choose an intersection point $\mathbf{y} \in \underline{CFK}^-(S)$ with $\text{hdeg}(\mathbf{y}) = \text{hdeg}(\mathbf{x}_0) - 1$. Then*

$$(36) \quad \#\widehat{\mathcal{M}}(\phi_1) + \dots + \#\widehat{\mathcal{M}}(\phi_k) = 0,$$

where ϕ_1, \dots, ϕ_k are all classes of Whitney disks from \mathbf{y} to \mathbf{x}_0 that have Maslov index one and are disjoint from \mathbb{X} .

Proof. The homology class of \mathbf{x}_0 cannot be free in \widehat{HF} when the sum in (36) does not vanish. \square

Let S_+ , S_- , S_\times , S_0 be diagrams of singular links that differ only in a small neighborhood of a point p , where the first three have respectively a positive, a negative and a singular crossing, whereas in S_0 the crossing is smoothed. Write k (resp. s) for the number of \mathbb{X} -basepoints (resp. double \mathbb{X} -basepoints) in the associated planar Heegaard diagrams and let $R = \mathbb{k}[U_0, \dots, U_{k+s}]$. We write A_a and A_b (resp. B_c and B_d) for the regions bounded by α -curves (resp. β -curves) that contain the \mathbb{O} -basepoints labeled a and b (resp. c and d). Let $U_a^{(p)}$ and $U_b^{(p)}$ (resp. $U_c^{(p)}$ and $U_d^{(p)}$) be the associated variables and consider a two term complex

$$\mathcal{L}_p = \left(\mathbf{q}R \xrightarrow{U_a^{(p)} + U_b^{(p)} - U_c^{(p)} - U_d^{(p)}} \mathbf{q}^{-1}R \right)$$

generated by \mathbf{u} and $\mathbf{1}$ in homological degrees -1 and 0 respectively.

Theorem 4.19 (cf. [OS09]). *There are homotopy equivalences of complexes*

$$\begin{aligned} CFK^-(S_+) &\simeq \mathbf{t}^{-1} \left(CFK^-(S_\times) \otimes_R \mathcal{L}_p \xrightarrow{\text{unzip}_p} \mathbf{q}^{-1} CFK^-(S_0) \right) \\ CFK^-(S_-) &\simeq \left(\mathbf{q} CFK^-(S_0) \xrightarrow{\text{zip}_p} CFK^-(S_\times) \otimes_R \mathcal{L}_p \right) \end{aligned}$$

where $\text{unzip}_p(\mathbf{x}_0(S_\times) \otimes \mathbf{1}) = \mathbf{x}_0(S_0)$ and $\text{zip}_p(\mathbf{x}_0(S_0)) = (U_b^{(p)} - U_c^{(p)})(\mathbf{x}_0(S_\times) \otimes \mathbf{1})$.

Proof. Consider first the case of S_- , so that the Heegaard diagram for $CFK^-(S_-)$ near p has \mathbb{X} basepoints at regions marked A^0 and A^- . Generators containing the intersection point between the regions marked A^0 and A^- span a subcomplex X_- that contains $\mathbf{x}_0(S_-)$ and the differential

¹¹Generally, \mathbf{x}_0 is not a cycle in $CFK^-(S)$ —for instance, the rectangle decorated A^- in a neighborhood of a positive crossing represents a nontrivial holomorphic disk from \mathbf{x}_0 .

of which counts holomorphic disks with multiplicity 0 at the five marked regions. Let Y_- be the quotient complex, spanned by the remaining generators, and consider the diagram

$$\begin{array}{ccc}
 \mathbf{q}^2 \mathbf{t}^2 X_- & \xrightarrow{id} & \mathbf{q}^2 \mathbf{t} X_- \\
 \Phi_{A^-} \downarrow & \searrow \Phi_{A^- B} & \downarrow U_a^{(p)} + U_b^{(p)} - U_c^{(p)} - U_d^{(p)} \\
 Y_- & \xrightarrow{\Phi_B} & X_-
 \end{array}$$

where the maps Φ_B , Φ_{A^-} and $\Phi_{A^- B}$ count Maslov index one holomorphic disks ϕ , such that

- $B(\phi) = 1$ and $A^-(\phi) = A^0(\phi) = 0$ in case of Φ_B ,
- $B(\phi) = 0$ and $A^-(\phi) + A^0(\phi) = 1$ in case of Φ_{A^-} ,
- $B(\phi) = 1$ and $A^-(\phi) + A^0(\phi) = 1$ in case of $\Phi_{A^- B}$,

and $B(\phi)$ is the total multiplicity of ϕ at both regions labeled B . Considering ends of moduli spaces of holomorphic disks of Maslov index two, we get that the total of the diagram is a chain complex, where the terms $U_a^{(p)}$, $U_b^{(p)}$, $U_c^{(p)}$, and $U_d^{(p)}$ come from degenerated disks represented by the domains A_a , A_b , B_c and B_d respectively, which explains the signs. The total chain complex is clearly homotopy equivalent to the mapping cone of Φ_B , which is $CFK^-(S_-)$. The right column is identified with $CFK^-(S_\times) \otimes_R \mathcal{L}_p$ by forgetting the fixed intersection point. This takes $\mathbf{x}_0(S_-) \in X_-$, which is in degree $s - n - 1$, to $\mathbf{x}_0(S_\times) \in CFK^-(S_\times)$, which lives in degree $s - n$. The left column is identified with $\mathbf{q} \mathbf{t} CFK^-(S_0)$, in which $\mathbf{x}_0(S_0)$ is identified with a generator $\mathbf{y}_0^- \in Y_-$ that is given by the same collection of intersection points, but living in homological degree -1 and quantum degree $s - n + 1$ (apply (32) and (33) to the rectangle marked A^-). There are two Whitney disks from \mathbf{y}_0^- to $\mathbf{x}_0(S_-)$ with multiplicity one at B , represented by domains $A_b \setminus B_c$ and $B_c \setminus A_b$. Hence, $\Phi_B(\mathbf{y}_0^-) = \pm(U_b^{(p)} - U_c^{(p)})\mathbf{x}_0(S_-)$, which is compatible with the formula for zip_p .

The case of S_+ is similar. This time the diagram has basepoints at regions A^0 and A^+ . Generators containing the intersection point between the two regions span a quotient complex X_+ of $CFK^-(S_+)$, which is identified with $\mathbf{q} \mathbf{t} CFK^-(S_\times)$: the canonical generator $\mathbf{x}_0(S_\times)$ corresponds to $\mathbf{x}_0^+ \in X_+$ that differ from $\mathbf{x}_0(S_+)$ by picking the other corner of the bigon labelled A^0 . In particular, $\text{hdeg}(\mathbf{x}_0^+) = -1$ and $\text{qdeg}(\mathbf{x}_0^+) = s - n + 1$. Writing Y_+ for the subcomplex spanned by other generators, we consider the diagram

$$\begin{array}{ccc}
 X_+ & \xrightarrow{\Phi_B} & Y_+ \\
 U_a^{(p)} + U_b^{(p)} - U_c^{(p)} - U_d^{(p)} \downarrow & \searrow \Phi_{A^+ B} & \downarrow \Phi_{A^+} \\
 \mathbf{q}^{-2} \mathbf{t}^{-1} X_+ & \xrightarrow{id} & \mathbf{q}^{-2} \mathbf{t}^{-2} X_+
 \end{array}$$

where the maps Φ_B , Φ_{A^+} and $\Phi_{A^+ B}$ are analogues of the maps from the case of a negative crossing, but using the region marked A^+ instead of A^- . Again, the total object is a chain complex that is homotopy equivalent to the mapping cone of Φ_B , which is $CFK^-(S_+)$. The left column is identified with $CFK^-(S_\times) \otimes_R \mathcal{L}_p$ and the right one with $\mathbf{q}^{-1} \mathbf{t}^{-1} CFK^-(S_0)$. The applied degree shifts follow from the observation that \mathbf{x}_0^+ , when considered as a generator of $CFK^-(S_0)$, lives in the same homological and quantum degree as $\mathbf{x}_0(S_0)$, because both are connected by the domain $A^- - A^0$. The property of the unzip map follows easily. \square

Remark 4.20. Theorem 4.19 remains true for twisted complexes once powers of t are properly distributed in the formulas for the differential in \mathcal{L}_p as well as for the zip map. Namely, each $U_x^{(p)}$ must be scaled by t^{m_x} , where m_x counts twisting markings in the region A_x or B_x (depending on

x). In particular, the formulas are unchanged when twisted by P^{tr} , whereas each $U_a^{(p)}$ and $U_b^{(p)}$ is scaled by t in case of the Ozsváth–Szabó marking P^{OS} .

Theorem 4.19 implies immediately that the degree normalization (35) matches the standard one: the polynomial

$$(\mathfrak{q} - \mathfrak{q}^{-1})^\sigma \sum_{d,s} (-1)^d \mathfrak{q}^s \widehat{\text{rk}} \widehat{HFK}_d(S; s)$$

assigned to a diagram S , where σ counts singular crossings, satisfies the skein relation of the Alexander polynomial.

4.4. Computation for planar singular links. Let S be a planar singular knot considered as a diagram with no real crossings. Recall that a Kauffman state of such diagram is a collection of markings at singular crossing as shown in Figure 17, such that each region not adjacent to $\star \in S$ contains exactly one marking. Because switching D^- with D^+ has the effect of replacing \mathfrak{q} with $1/\mathfrak{q}$, the Alexander polynomial $\Delta_S(\mathfrak{q})$ is symmetric. It can be shown that the minimal power of \mathfrak{q} is equal to $s - n - 1$, where s is the number of Seifert circles in S and n is the number of singular crossings.

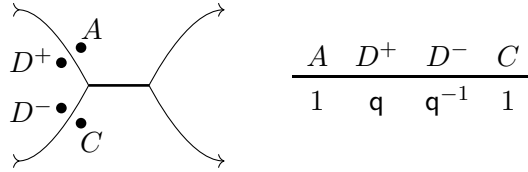


FIGURE 17. Kauffman markings at a singular crossing and their (multiplicative) contributions towards the evaluation of the Kauffman state.

In terms of intersection points on the initial Heegaard diagram, picking a Kauffman state is equivalent to fixing points on the β -curves parallel to the contours of the underlying surface, leaving a choice between two intersection points on each internal β -curve, see Figure 18. Thus, there are 2^n generators associated with a fixed Kauffman state, where n is the total of singular crossings and bivalent vertices in S other than \star . It is shown in [OSS09] that with each Kauffman state

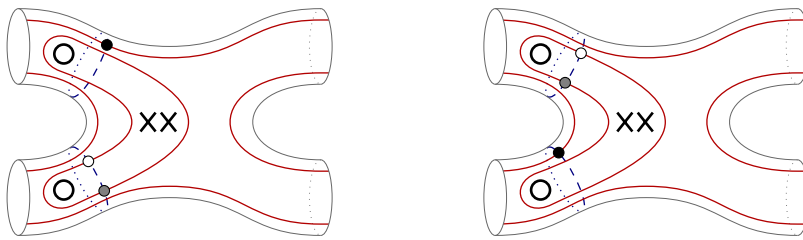


FIGURE 18. Local pictures for generators associated with the A state (to the left) and the D^- state (to the right). The black dot on one of the meridians is fixed by the state, which leaves a choice between the white and gray point on the other meridian. Choosing always the white point produces the generator of the highest homological degree.

there is associated a unique generator of highest (in the conventions of this paper) homological degree, represented in Figure 18 by black and white dots. This generator is actually in homological degree 0 and its quantum grading matches the contribution of the associated Kauffman state to the Alexander polynomial. Our main goal is to provide an argument that no other generators contribute towards the twisted homology.

Consider now the initial diagram for S together with the Ozsváth–Szabó twisting P^{OS} . As in the previous section, given a singular crossing p we denote the \mathbb{O} -basepoints on outgoing (resp. incoming) arcs by $O_a^{(p)}$ and $O_b^{(p)}$ (resp. $O_c^{(p)}$ and $O_d^{(p)}$). Likewise, when p is a bivalent vertex, then $O_a^{(p)}$ and $O_c^{(p)}$ are located at the outgoing and incoming arc respectively. Define

$$\underline{\mathcal{L}}_S := \bigotimes_{p \in \mathfrak{X}} \left(R \xrightarrow{tU_a^{(p)} + tU_b^{(p)} - U_c^{(p)} - U_d^{(p)}} R \right)$$

as the tensor product over R of linear complexes taken over all singular crossings p (where, again, we write R for the \mathbb{k} -algebra of polynomials in all variables U_i).

For a \mathbb{k} -module M , its \mathbb{k} -torsion is the \mathbb{k} -submodule $\{m \in M \mid \exists \lambda \in \mathbb{k} \text{ with } \lambda m = 0\}$.

Proposition 4.21. *Let S be a planar singular knot. Then the quotient of $H_*(\underline{\text{CFK}}^-(S, P^{\text{OS}}) \otimes_R \underline{\mathcal{L}}_S)$ by its \mathbb{k} -torsion is a free $\mathbb{k}[U_0]$ -module concentrated in homological degree zero and generated by Kauffman states of S . The same holds for $H_*(\widehat{\text{CFK}}(S, P^{\text{OS}}) \otimes_R \underline{\mathcal{L}}_S)$ with \mathbb{k} in place of $\mathbb{k}[U_0]$.*

Proof. Without loss of generality we can assume that $\mathbb{k} = \mathbb{Z}[t, t^{-1}]$. We further extend the ring by a square root of t and extend the set of markings as shown in Figure 19. Write Q for this new

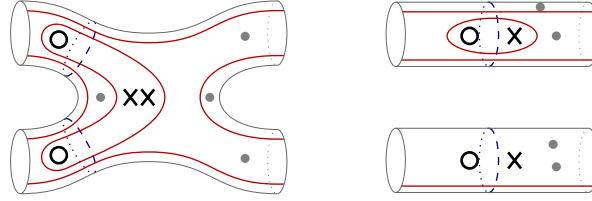


FIGURE 19. The extra twisting markings on an initial Heegaard diagram.

set. Because S is connected, the complex $\underline{\text{CFK}}^-(S, Q; t^{1/2})$ is isomorphic to $\underline{\text{CFK}}^-(S, P^{\text{OS}}; t)$ by Proposition 4.13. Hence, it suffices to prove the thesis for the twisting set Q .

The complex $\widehat{\text{CFK}}(S, Q)$ is filtered with respect to the power of t and the t -degree zero part of the differential relates only generators associated with the same Kauffman state. In fact, the component of the graded associate complex spanned by generators corresponding to a fixed Kauffman state \mathfrak{s} has the form of the tensor product over R

$$\mathcal{N}_{\mathfrak{s}} = \bigotimes_{p \neq \star} \left(R \xrightarrow{U_x^{(p)}} R \right)$$

taken over all singular crossings and bivalent vertices of S other than the basepoint \star , and where $x = c$ or d depending on p and \mathfrak{s} . We claim that the homology of

$$(37) \quad \mathcal{N}_{\mathfrak{s}} \otimes_R \text{gr} \underline{\mathcal{L}}_S \cong \bigotimes_{p \neq \star} \left(R \xrightarrow{U_x^{(p)}} R \right) \otimes_R \bigotimes_{p \in \mathfrak{X}} \left(R \xrightarrow{U_c^{(p)} + U_d^{(p)}} R \right)$$

is freely generated by the highest homological degree generator associated with \mathfrak{s} . This follows from the observation that the set of relations

$$(38) \quad \{U_x^{(p)} \mid p \neq \star\} \cup \{U_c^{(p)} + U_d^{(p)} \mid p \in \mathfrak{X}\}$$

is regular, i.e. each element is a non-zero divisor in the quotient of R by other elements. In particular, the relations eliminate all variables except U_0 . Following the proof of [OS09, Proposition 3.4] we show that the generator of (37) is in homological degree 0, i.e. its Maslov degree is twice the Alexander degree, so that the spectral sequence associated with the filtration collapses immediately. This shows that each component $\mathcal{N}_{\mathfrak{s}} \otimes \text{gr} \underline{\mathcal{L}}_S$ contributes exactly one free generator towards the E^∞ page.

The uniqueness of a limit of a spectral sequence (compare Appendix A.1) implies that

$$H_*(\widehat{\underline{CFK}}^-(S, Q) \otimes_R \underline{\mathcal{L}}_S),$$

when computed over the completed ring $\mathbb{Z}[t^{-1/2}, t^{1/2}][[U_0]]$, is freely generated by Kauffman states and concentrated in homological degree 0. This proves the statement for the twisting set Q and the case of P^{OS} follows from Proposition 4.13. Finally, the computation for $\widehat{\underline{CFK}}$ follows, because adding U_0 to (38) does not affect the regularity of the set. \square

Let us now discuss briefly the case of disconnected diagrams. In [OS09] it is shown that the twisted homology vanishes, because the set of generators is empty (the initial diagram used in the paper is not admissible for disconnected diagrams). This argument is no longer true for our initial diagram, but the vanishing result (up to \mathbb{k} -torsion) still holds.

Proposition 4.22. *Suppose that S is a planar singular link with at least two components. Then both $H_*(\widehat{\underline{CFK}}^-(S, P^{\text{OS}}) \otimes_R \underline{\mathcal{L}}_S)$ and $H_*(\widehat{\underline{CFK}}(S, P^{\text{OS}}) \otimes_R \underline{\mathcal{L}}_S)$ are \mathbb{k} -torsion.*

Proof. We may assume as before that $\mathbb{k} = \mathbb{Z}[t^{1/2}, t^{-1/2}]$ and consider the twisting set Q . For any component S_i of S and the associated periodic domain π_i the equality $Q(\pi_i) = 2P^{\text{OS}}(\pi_i)$ holds, so that Proposition 4.13 provides again an isomorphism between $\widehat{\underline{CFK}}^-(S, Q; t^{1/2})$ and $\widehat{\underline{CFK}}^-(S, P^{\text{OS}}; t)$. Because S has at least two components, the initial diagram contains a neck connecting surfaces built for different components of S . Figure 20 shows four possibly choices of intersection points near such a neck (a black point paired with either a white or a gray point from the same picture). Notice that the top intersection points on the two meridians cannot be picked, because the intersecting β curve must carry an intersection point with some meridian around the upper component of S .

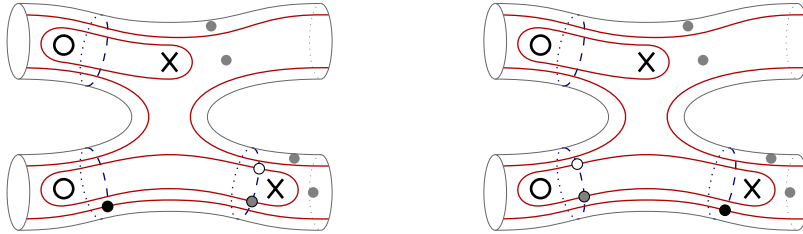


FIGURE 20. Local pictures for generators near a neck connecting different components of a singular link S .

Consider now the graded associate $\text{gr}\widehat{\underline{CFK}}^-(S, Q)$. The differential counts not only bigons carrying the \mathbb{O} -basepoints, but also two rectangles near each connecting neck. In particular, the complex admits a tensor factor of the form

$$R \xrightarrow{\begin{pmatrix} 1 \\ U \end{pmatrix}} R \oplus R \xrightarrow{(U \ -1)} R,$$

where U is the variable associated with the lower \mathbb{O} -basepoint in the picture. This complex is acyclic, and so is the entire graded associate complex. Thus, $\widehat{\underline{CFK}}^-(S, Q)$ is \mathbb{k} -torsion. The statement for $\widehat{\underline{CFK}}^-(S; P^{\text{OS}})$ follows from Proposition 4.13. The argument carries over to $\widehat{\underline{CFK}}$ with no change. \square

5. MAIN RESULTS

In this section we prove the main results of this paper. We start by defining *Gilmore space* as a quotient of the reduced Soergel space $\overline{B}_q(\omega)$ associated with a pointed annular web ω by non-local relations. By inserting this space at vertices in the cube construction we produce the *Gilmore*

complex $C^{AG}(\hat{\beta})$. In Theorem 5.11 we prove that the complex is quasi-isomorphic to the twisted Heegaard Floer complex $\widehat{CFK}(\hat{\beta})$ if $\mathbb{k} = \mathbb{Z}[q^{-1}, q]$. In Section 5.4 we define our algebro-geometric quotient $qAG(\omega)$ of the Gilmore space. By applying the Bockstein spectral sequence to $qAG(\hat{\beta})$ we prove Theorems B and C.

5.1. The normalized Gilmore complex. Choose a pointed annular web ω and recall that the marking \star is on an edge of thickness 1 that is at the same time an outer edge. We say that a simple closed curve γ is *adapted to ω* if it avoids vertices of the web, intersects its edges transversally, and the region R_γ bounded by the curve does not contain the marking \star , see Figure 21. The intersection points between ω and γ fall into two categories: *incoming* and *outgoing* points, at which the web is oriented inwards and outwards the region R_γ respectively.

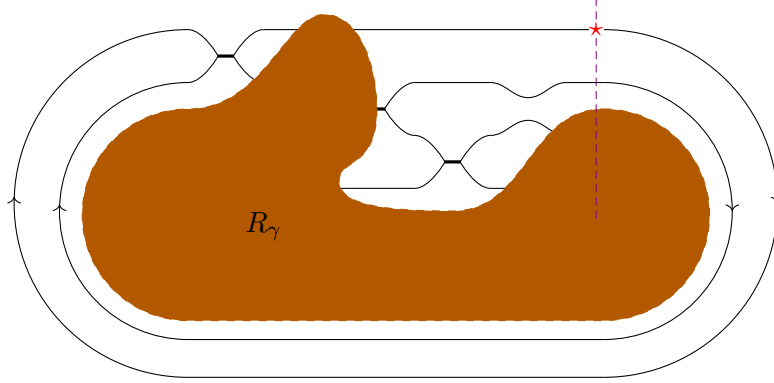


FIGURE 21. A curve γ adapted to the web from Figure 11 and the bounded region R_γ . There are four incoming edges and three outgoing edges, one of which is thick. A curve adapted to ω can have turn-backs and it can cross an edge more than once.

In Section 2.6 we have associated with a pointed annular web ω the polynomial algebra

$$\overline{B}_q(\omega) = qHH_0(R^k; B(\tilde{\omega}))/(\mathbf{x}_\star),$$

where \mathbf{x}_\star is the variable associated with the edge terminating at the basepoint and $\tilde{\omega}$ is the directed web obtained by cutting ω along the trace section. Consider the ideal $\mathcal{N}_\omega \subset \overline{B}_q(\omega)$ of non-local relations defined as follows. Pick a curve γ adapted to ω and write $e_{\text{top}}(X_p)$ for the product of variables associated with the edge containing the intersection point $p \in \omega \cap \gamma$. Define

$$x_{\text{in}(\gamma)} := \prod_{p \in (\omega \cap \gamma)^+} e_{\text{top}}(X_p) \quad \text{and} \quad x_{\text{out}(\gamma)} := \prod_{p \in (\omega \cap \gamma)^-} e_{\text{top}}(X_p),$$

where $(\omega \cap \gamma)^+$ and $(\omega \cap \gamma)^-$ are respectively the sets of incoming and outgoing intersection points, and put

$$(39) \quad NL_\gamma := x_{\text{out}(\gamma)} - q^{2i} x_{\text{in}(\gamma)},$$

where i is the number of trace vertices in R_γ . Note that γ may intersect an edge several times, in which case the variables associated with such an edge appear in both products, possibly with exponents bigger than 1. The ideal \mathcal{N}_ω is generated by NL_γ for all such curves γ .

Definition 5.1. The quotient space

$$\mathcal{A}(\omega) = \overline{B}_q(\omega) / \mathcal{N}_\omega$$

assigned to a pointed annular web ω is called the *Gilmore space* of ω .

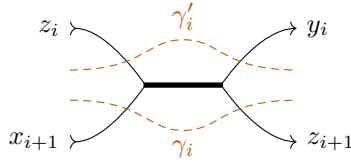
Following the common practice we write $\mathcal{A}(\omega; \mathbb{k})$ to emphasize the choice of coefficients.

Example 5.2. When ω is an elementary web, then $\mathcal{A}(\omega)$ is generated by variables x_i associated to its thin edges modulo the following local relations

$x_c \rightarrow x_a$	$x_c \rightarrow x_a$	$x_c \rightarrow x_a$	$x_c \rightarrow x_a$ $x_d \rightarrow x_b$
$x_a = x_c$	$x_a = q^2 x_c$	$x_a = 0$	$x_a + x_b = x_c + x_d$ $x_a x_b = x_c x_d$

and non-local relations NL_γ for curves γ adapted to ω that do not intersect thick edges. Note the special role of the marking \star : we do not enforce $x_c = 0$, which holds in $\overline{B}_q(\omega)$. This follows from the non-local relation associated with a small loop around the marking, because it forces x_a and x_c to be proportional.

Example 5.3. If ω is a chain of dumbbells (see Figure 22), then $\mathcal{A}(\omega) \cong \mathbb{k}$ is generated by the constant polynomial if $1 - q^d$ is invertible for each $d > 1$. To see this, assign to thin edges of ω variables x_i, y_i , and z_i for $i = 1, \dots, k$, so that at the i -th thick edge we have the following situation:



where the curves γ_i and γ'_i have no more intersections with ω and the edges with variables x_i and y_i meet at a trace vertex, so that $x_i = q^2 y_i$. It is understood that $z_1 = x_1$ and $z_k = y_k$. The non-local relations associated with curves γ_i and γ'_i forces $z_i = q^{2i-2k} y_i$ for each i . Substituting that in the linear local relation

$$z_i + x_{i+1} = y_i + z_{i+1}$$

forces $(q^{2i-2k} - 1)(y_i - q^2 y_{i+1}) = 0$, so that all variables are proportional to each other. In particular, to y_1 , which is killed by the basepoint relation. Finally, since there is no non-trivial relation involving polynomials of degree 0, one has $\mathcal{A}(\omega) \cong \mathbb{k}$ as claimed.

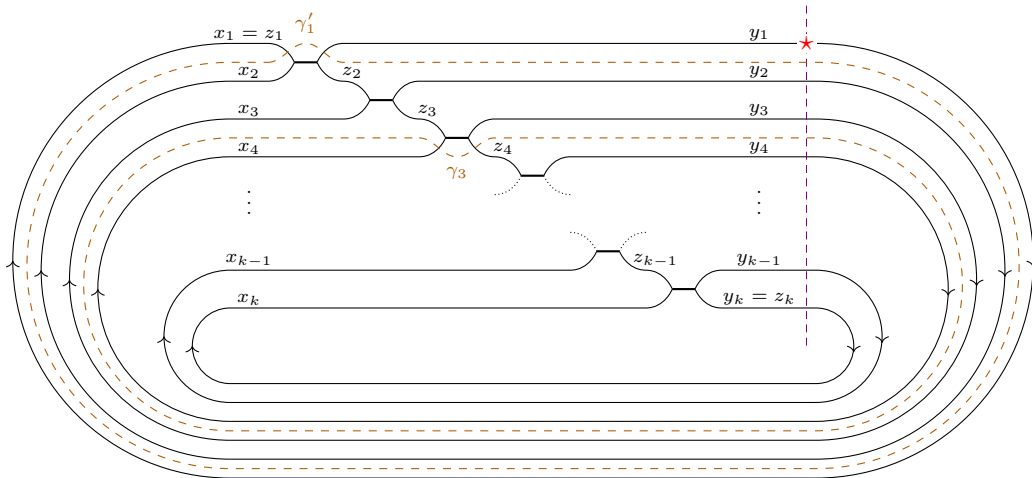


FIGURE 22. A pointed chain of dumbbells with a trace section.

Example 5.4. Suppose that ω is a disjoint union of webs $\omega_0, \dots, \omega_r$, positioned so that ω_i is surrounded by ω_{i-1} for $i = 1, \dots, r$, and write w_i for the index of the component ω_i . Consider a loop γ_i separating ω_{i-1} from ω_i ; the associated non-local relations forces $1 = q^{w_i + \dots + w_r}$. Hence, $\mathcal{A}(\omega)$ is annihilated by $1 - q^{\gcd(w_1, \dots, w_r)}$. In particular, the space vanishes when $1 - q^d$ is invertible for all $d > 0$.

Proposition 5.5. *The assignment $\omega \mapsto \mathcal{A}(\omega)$ extends to a functor*

$$\mathcal{A}: \mathcal{AFoam}_q^\star \rightarrow \text{grMod}$$

that is a quotient of the functor \overline{B}_q from Section 2.6.

In order to prove the proposition, we need the following property of non-local relations.

Lemma 5.6. *Let γ and γ' be curves adapted to a pointed annular web ω that coincide everywhere except a small neighborhood of a vertex v , in which γ intersects only the incoming edges, whereas γ' intersects the outgoing edges. Then $NL_\gamma = NL_{\gamma'}$ in $\overline{B}_q(\omega)$.*

Proof. The only difference between NL_γ and $NL_{\gamma'}$ is that in one of the two terms of NL_γ a product of variables associated with the edges terminating at v is replaced by a product of variables associated with the edges originating at v . The equality of both products is imposed by Soergel relations. \square

Proof of Proposition 5.5. We have to check that linear maps induced by foams preserve the ideal of non-local relations. In all diagrams, the region R_γ enclosed by a simple closed curve γ is located below γ .

There are six maps (cup, cap, zip, unzip, as and coas) to be inspected, but in the view of Lemma 5.6 only zip required a non-trivial check. Indeed, let us demonstrate how the lemma is used in case of the map cap, which eliminates a bigon.

Denote by ω and ω' marked annular webs with a membrane that are identical except in a small disk D disjoint from the membrane and the marking \star , in which

$$\omega = \begin{array}{c} a \\ \nearrow \quad \searrow \\ a+b \quad \quad a+b \\ \nwarrow \quad \nearrow \\ b \end{array} \quad \text{and} \quad \omega' = \begin{array}{c} a+b \\ \longrightarrow \end{array}.$$

If a curve γ does not pass through the bigon in ω , then the relation NL_γ is clearly preserved. Otherwise, we apply Lemma 5.6 to isotope γ away from the bigon:

$$\begin{array}{c} a+b \quad \quad a+b \\ \nearrow \quad \searrow \quad \nearrow \quad \searrow \\ a \quad \quad b \end{array} \quad \rightsquigarrow \quad \begin{array}{c} a+b \quad \quad a+b \\ \nearrow \quad \searrow \quad \nearrow \quad \searrow \\ a \quad \quad b \end{array}$$

Analogue arguments ensure that as, coas, cup and unzip induce morphisms on quotient spaces.

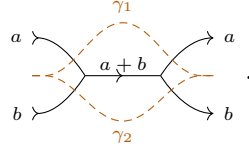
Let us now deal with zip. Denote by ω and ω' pointed annular webs with a membrane that are identical except in a small disk D disjoint from the membrane and the marking \star , in which

$$\omega = \begin{array}{c} a \longrightarrow \\ b \longrightarrow \end{array} \quad \text{and} \quad \omega' = \begin{array}{c} a \nearrow \quad \searrow a \\ a+b \\ b \nearrow \quad \searrow b \end{array}.$$

The only problematic curves are the ones that, inside D , go between the two edges of ω :

$$\begin{array}{c} a \longrightarrow \\ \text{---} \text{---} \text{---} \gamma \text{---} \text{---} \text{---} \\ b \longrightarrow \end{array}.$$

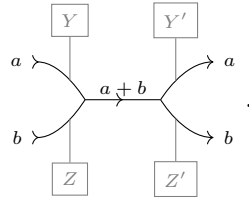
Let us denote by γ_1 and γ_2 curves adapted to ω' that are identical to γ outside of D , whereas inside they look like in the following diagram:



In order to prove that the zip map is well-defined, we shall show that NL_γ is mapped onto an element of the form

$$(40) \quad NL_{\gamma_1} \sum_{\alpha \in T(a-1, b)} (-1)^{|\hat{\alpha}|} s_\alpha(Y') s_{\hat{\alpha}}(Z) + NL_{\gamma_2} \sum_{\alpha \in T(a, b-1)} (-1)^{b+|\hat{\alpha}|} s_\alpha(Y') s_{\hat{\alpha}}(Z),$$

where the set of variables Y , Z , Y' , and Z' are associated with edges of the web as indicated in the figure below:



This implies that $\text{zip}(NL_\gamma)$ belongs to $\mathcal{N}_{\omega'}$, hence, non-local relations are preserved by the map. Using the equality

$$(41) \quad \sum_{\alpha \in T(a, b)} (-1)^{|\hat{\alpha}|} s_\alpha(Y') s_{\hat{\alpha}}(Z) = \sum_{\alpha \in T(a, b)} (-1)^{|\hat{\alpha}|} s_\alpha(Y) s_{\hat{\alpha}}(Z')$$

that holds in $B(\omega')$, we can rewrite the image of $NL_\gamma = x_{\text{out}(\gamma)} - q^{2i} x_{\text{in}(\gamma)}$ as

$$(42) \quad x_{\text{out}(\gamma)} \sum_{\alpha \in T(a, b)} (-1)^{|\hat{\alpha}|} s_\alpha(Y') s_{\hat{\alpha}}(Z) - q^{2i} x_{\text{in}(\gamma)} \sum_{\alpha \in T(a, b)} (-1)^{|\hat{\alpha}|} s_\alpha(Y) s_{\hat{\alpha}}(Z').$$

We shall analyze each term separately. Notice first that

$$(43) \quad x_{\text{in}(\gamma_1)} = x_{\text{in}(\gamma)} e_a(Y), \quad x_{\text{in}(\gamma_2)} = x_{\text{in}(\gamma)} e_b(Z'),$$

$$(44) \quad x_{\text{out}(\gamma_1)} = x_{\text{out}(\gamma)} e_a(Y'), \quad x_{\text{out}(\gamma_2)} = x_{\text{out}(\gamma)} e_b(Z).$$

Denote by $T_1(a, b)$ the subset of Young diagrams with exactly a boxes in the first column and set $T_2(a, b) = T(a, b) \setminus T_1(a, b)$. Note that $\hat{\beta}$ has exactly b boxes the first column when $\beta \in T_2(a, b)$. Hence, for such α and β one has

$$\begin{aligned} s_\alpha(Y) &= e_a(Y) s_{\alpha'}(Y), & s_{\hat{\beta}}(Z) &= e_b(Z) s_{\hat{\beta}'}(Z), \\ s_\alpha(Y') &= e_a(Y') s_{\alpha'}(Y'), & s_{\hat{\beta}}(Z') &= e_b(Z') s_{\hat{\beta}'}(Z'), \end{aligned}$$

where α' (resp. $\hat{\beta}'$) is the Young diagram α (resp. $\hat{\beta}$) with its first column removed. On the one hand, using (44) one obtains:

$$\begin{aligned} (45) \quad x_{\text{out}(\gamma)} \sum_{\alpha \in T(a, b)} (-1)^{|\hat{\alpha}|} s_\alpha(Y') s_{\hat{\alpha}}(Z) \\ &= x_{\text{out}(\gamma_1)} \sum_{\alpha \in T_1(a, b)} (-1)^{|\hat{\alpha}|} s_{\alpha'}(Y') s_{\hat{\alpha}}(Z) + x_{\text{out}(\gamma_2)} \sum_{\alpha \in T_2(a, b)} (-1)^{|\hat{\alpha}|} s_\alpha(Y') s_{\hat{\alpha}}(Z) \\ &= x_{\text{out}(\gamma_1)} \sum_{\alpha \in T(a-1, b)} (-1)^{|\hat{\alpha}|} s_\alpha(Y') s_{\hat{\alpha}}(Z) + x_{\text{out}(\gamma_2)} \sum_{\alpha \in T(a, b-1)} (-1)^{b+|\hat{\alpha}|} s_\alpha(Y') s_{\hat{\alpha}}(Z). \end{aligned}$$

On the other hand, using (43) and Corollary 2.3 one computes

$$\begin{aligned}
(46) \quad x_{\text{in}(\gamma)} & \sum_{\alpha \in T(a,b)} (-1)^{|\hat{\alpha}|} s_{\alpha}(Y) s_{\hat{\alpha}}(Z') \\
&= x_{\text{in}(\gamma_1)} \sum_{\alpha \in T(a-1,b)} (-1)^{|\hat{\alpha}|} s_{\alpha}(Y) s_{\hat{\alpha}}(Z') + x_{\text{in}(\gamma_2)} \sum_{\alpha \in T(a,b-1)} (-1)^{b+|\hat{\alpha}|} s_{\alpha}(Y) s_{\hat{\alpha}}(Z') \\
&= x_{\text{in}(\gamma_1)} \sum_{\alpha \in T(a-1,b)} (-1)^{|\hat{\alpha}|} s_{\alpha}(Y \sqcup Z) s_{\hat{\alpha}}(Z' \sqcup Z) + x_{\text{in}(\gamma_2)} \sum_{\alpha \in T(a,b-1)} (-1)^{b+|\hat{\alpha}|} s_{\alpha}(Y \sqcup Z) s_{\hat{\alpha}}(Z' \sqcup Z) \\
&= x_{\text{in}(\gamma_1)} \sum_{\alpha \in T(a-1,b)} (-1)^{|\hat{\alpha}|} s_{\alpha}(Y' \sqcup Z') s_{\hat{\alpha}}(Z' \sqcup Z) + x_{\text{in}(\gamma_2)} \sum_{\alpha \in T(a,b-1)} (-1)^{b+|\hat{\alpha}|} s_{\alpha}(Y' \sqcup Z') s_{\hat{\alpha}}(Z' \sqcup Z) \\
&= x_{\text{in}(\gamma_1)} \sum_{\alpha \in T(a-1,b)} (-1)^{|\hat{\alpha}|} s_{\alpha}(Y') s_{\hat{\alpha}}(Z) + x_{\text{in}(\gamma_2)} \sum_{\alpha \in T(a,b-1)} (-1)^{b+|\hat{\alpha}|} s_{\alpha}(Y') s_{\hat{\alpha}}(Z).
\end{aligned}$$

Putting (45) and (46) together, we get that formulas (40) and (42) coincide as desired. \square

Proposition 5.5 allows us to use the framework from Section 3.1 to associate with a braid diagram $\hat{\beta}$ of a link a chain complex $C^{AG}(\hat{\beta})$, by applying the functor \mathcal{A} to the formal complex $[\hat{\beta}]$. We refer to it as the *(normalized) Gilmore complex of $\hat{\beta}$* . It follows immediately that the homotopy type of $C^{AG}(\hat{\beta})$ is invariant under braid moves and conjugation away from the marking \star . It can be also shown that the homology is invariant under stabilization if $1 - q^d$ is invertible for all $d > 0$. The question whether the complex is truly a knot invariant remains open.

5.2. The identification with \widehat{HFK} . Hereafter we show that $C^{AG}(\hat{\beta})$ computes the twisted Heegaard Floer homology of $\hat{\beta}$. The first step is to compare the two constructions for diagrams with no real crossings; the general case follows by applying the exact skein triangle. We begin by reducing the set of generators of the ideal \mathcal{N}_{ω} . Consider a *coherent cycle* Z in S , i.e. a directed closed path in ω with no self-intersections that does not pass through the distinguished vertex \star . Write NL_Z for the nonlocal relation associated with the curve γ_Z obtained from Z by pushing the cycle slightly away from the region R_Z enclosed by Z . This is illustrated in Figure 23.

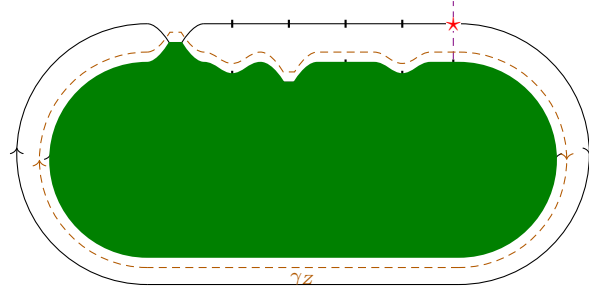


FIGURE 23. A coherent cycle Z in a web and the corresponding curve γ_Z .

Lemma 5.7. *The polynomials NL_Z parametrized by coherent cycles in S generate the ideal \mathcal{N}_{ω} .*

Proof. Pick a curve γ adapted to ω . When γ does not surround any vertex of S , then $\text{in}(\gamma) = \text{out}(\gamma)$ and $NL_{\gamma} = 0$. Suppose the converse and that there is an arc $\alpha \subset R_{\gamma}$ disjoint from S that connects two points of γ . Performing a surgery on γ along this arc produces two curves γ' and γ'' adapted to ω ; NL_{γ} is clearly a consequence of $NL_{\gamma'}$ and $NL_{\gamma''}$. Likewise, we can perform surgery along such an arc if it is inside the interior of an edge u . In this case

$$\text{in}(\gamma) = \text{in}(\gamma')\text{in}(\gamma'')x_u \quad \text{and} \quad \text{out}(\gamma) = \text{out}(\gamma')\text{out}(\gamma'')x_u,$$

so that NL_γ is again a consequence of $NL_{\gamma'}$ and $NL_{\gamma''}$.

The above together with Lemma 5.6 allows us to restrict generators of \mathcal{N}_ω to relations NL_γ parametrized by curves γ surrounding at least one vertex of S and for which none of the above surgeries can be performed. Such a curve γ must intersect every edge of S at most once and if it surrounds a vertex p , then it must also surround at least one edge going out of p and one edge coming to p . Such curves are exactly those of the form γ_Z , where Z consists of the edges of S that are contained in R_γ and that can be connected to γ by an arc with its interior disjoint from S . \square

Define $\tilde{\mathcal{A}}(\omega)$ as $\mathcal{A}(\omega)$ but ignoring the marking \star : the usual trace relation is applied at this vertex and non-local relations are also imposed for curves than engulfs it. Alternatively, we can think of \star as placed at infinity, outside of ω , or that ω is put inside a marked loop. The following is a direct consequence of Lemma 5.7.

Lemma 5.8. *Let S be a planar singular link in a braid position with components S_0, \dots, S_r , where S_i is nested inside S_{i-1} for $i = 1, \dots, r$ and S_0 carries the marking \star . Then*

$$\mathcal{A}(S) \cong \mathcal{A}(S_0) \otimes \tilde{\mathcal{A}}(S_1) \otimes \cdots \otimes \tilde{\mathcal{A}}(S_r)$$

Notice that $\tilde{\mathcal{A}}(\omega)$ is annihilated by $1 - q^{2w}$, where w is the index of ω . Hence, $\mathcal{A}(\omega)$ is torsion when ω is disconnected, as already shown in Example 5.4.

A similar result holds for the twisted Heegaard Floer complex. The following is inspired by [Man14, Lemma 2.2].

Lemma 5.9. *Let S be a singular link in a braid position with split components S_0, \dots, S_r , where $\star \in S_0$. Then there is an isomorphism of complexes*

$$(47) \quad \underline{CFK}^-(S) \cong \underline{CFK}^-(S_0) \otimes \underline{CFK}^-(U \sqcup S_1) \otimes \cdots \otimes \underline{CFK}^-(U \sqcup S_r),$$

where in each $U \sqcup S_i$ the marking lies on the unknotted component.

Proof. The planar Heegaard diagram for S can be seen as a sequence of nested annular diagrams $\mathcal{H}_0, \dots, \mathcal{H}_r$ with X_0 outside of them as shown at the left side of Figure 24. Here \mathcal{H}_0 together with X_0 represents the component S_0 , whereas each \mathcal{H}_i for $i > 0$, with an extra pair of basepoints outside, represents $U \sqcup S_i$ with $\star \in U$. Thence the isomorphism (47) is clear at the level of chain groups. In order to compare the differentials we first modify the Heegaard diagram, so that the components \mathcal{H}_i are no longer nested, but instead they are contained in disjoint disks on the sphere and the complement of those disks is decorated with X_0 , see the right side of Figure 24. We argue then that the differential of the chain complex associated with this modified diagram matches with that of the right hand side of (47).

For the first step, we use the following generalization of a handle slide. Suppose that $\mathcal{H} = \mathcal{H}' \sqcup \mathcal{H}''$, where \mathcal{H}'' is contained in a disk D disjoint from \mathcal{H}' and all basepoints and markings of \mathcal{H}'' are surrounded by α -curves of this diagram. Then any α -curve of \mathcal{H}' can be slid over \mathcal{H}'' . This claim is easy to check by using handle slides and isotopies.

Observe now that each \mathcal{H}_i for $i > 0$ has all its basepoints and twisting markings inside α -curves (compare Figure 15) and the union $\mathcal{H}_+ = \mathcal{H}_1 \amalg \cdots \amalg \mathcal{H}_r$ is contained in a disk. Furthermore, \mathcal{H}_0 intersects the trace section only in α -curves. Hence, we can apply the generalized handle slide to these α -curves, pushing \mathcal{H}_+ outside of \mathcal{H}_0 as the result. Applying the same procedure inductively to \mathcal{H}_+ we complete the first step.

For the second step, we observe first that the resulting Heegaard diagram \mathcal{H}' represents the connected sum $(\mathbb{S}^2, \mathcal{H}_0) \# \cdots \# (\mathbb{S}^2, \mathcal{H}_r)$ of $r+1$ copies of a sphere decorated with Heegaard diagrams \mathcal{H}_i .¹² It follows now from [OS08, Theorem 5.1] that any holomorphic disk ϕ in the symmetric power of $(\mathbb{S}^2, \mathcal{H}')$ and with multiplicity 0 at X_0 corresponds to a collection of holomorphic disks ϕ_i , each supported in the symmetric power of $(\mathbb{S}^2, \mathcal{H}_i)$, such that $\mathcal{D}(\phi) = \sum_i \mathcal{D}(\phi_i)$ and $\mu(\phi) = \sum_i \mu(\phi_i)$.

¹²Strictly speaking we equip \mathcal{H}_i for $i > 0$ with an extra pair of basepoints.

Hence, $\mu(\phi) = 1$ forces all ϕ_i except one to be constant, so that $\text{supp } \phi$ is contained in exactly one of the diagrams \mathcal{H}_i . This shows that the differentials of the two sides of (47) coincide modulo 2. Finally, in order to match the signs in the differentials, we can equip moduli spaces of holomorphic curves in the symmetric power of $(\mathbb{S}^2, \mathcal{H})$ with orientations induced from the moduli spaces of holomorphic curves in the symmetric powers of $(\mathbb{S}^2, \mathcal{H}_i)$. \square

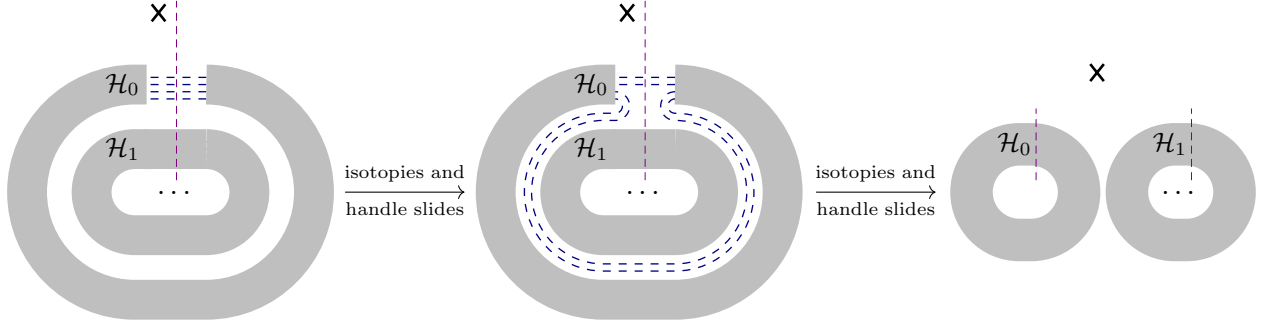


FIGURE 24. Sketches of the planar Heegaard diagram for a split link and the diagram desired for the proof of Lemma 5.9. Each thick circle represent a collection of α - and β -curves that intersect each other and represent one of the components of the link.

Consider now the complex $\underline{CFK}^-(S)$ computed from the planar Heegaard diagram for S , where the link diagram is considered to consists only of singular crossings and bivalent vertices. This simplifies the diagram a lot: each basepoint, except the one related to the marking \star , lies in a bigon. The generators of the complex are associated in [OS09, Section 3] with *coherent multicycles* in S , i.e. (possibly empty) collections of disjoint coherent cycles; the multicycle Z associated with a generator \mathbf{x} consists of the edges of S that corresponds to those bigons with \bigcirc -basepoints that have a component of \mathbf{x} at one of the corners. Other components of \mathbf{x} are corners of bigons containing \mathbb{X} -basepoints.

Theorem 5.10 (cp. [OS09, Theorem 3.1]). *Let S be a diagram of a planar singular link in a braid position. Then there is an isomorphism*

$$H_0(\widehat{\underline{CFK}}(S) \otimes \mathcal{L}_S) \cong \mathcal{A}(S)$$

that sends the homology class of \mathbf{x}_0 to the unit of $\mathcal{A}(S)$ and for every thin edge e identifies the action of U_e with the multiplication by x_e .

Proof. Assume first that S has only one component. Following [OS09] we show first that \mathbf{x}_0 is a cycle that generates the homology. For that define the *deviation* of a generator $\mathbf{x} \in \underline{CFK}^-(S)$ as the number of components of \mathbf{x} that are right corners of bigons. As in [OS09, Section 3] we can show that $\text{hdeg}(\mathbf{x}) = -|Z| - d$, where $|Z|$ is the number of components of the multicycle Z associated with \mathbf{x} and d is the deviation of the generator. Hence, each multicycle Z admits a unique generator \mathbf{x}_Z of maximal homological degree $-|Z|$. In particular, this implies that $\mathbf{x}_0 = \mathbf{x}_\emptyset$ is a cycle that generates the 0th homology. The relations come from counting pseudo-holomorphic disks from generators of degree -1 to \mathbf{x}_0 . There are two types of such generators: the deviation 1 generators associated to $Z = \emptyset$ and the generators \mathbf{x}_Z associated with (connected) coherent cycles Z .

The first kind of generators impose local relations on \mathbf{x}_0 . Let \mathbf{x} be deviated from \mathbf{x}_0 at one bigon. Because $Z = \emptyset$, the bigon contains a basepoint X_p that corresponds to a vertex $p \in S$. Write A_p and B_p for the regions containing X_p and bounded respectively by α - and β -curves. The differential $\partial \mathbf{x}$ has only two terms that correspond to $A_p \setminus B_p$ and $B_p \setminus A_p$, and which appear with opposite

signs due to Lemma 4.6. Thence,

$$\partial \mathbf{y} = \pm \left(U_a^{(p)} U_b^{(p)} - U_c^{(p)} U_d^{(d)} \right) \mathbf{x}_0$$

when p is a singular crossing and

$$\partial \mathbf{y} = \pm \left(\tau U_a^{(p)} - U_c^{(p)} \right) \mathbf{x}_0$$

in case of a bivalent vertex, where $\tau = t$ appears only in case of trace vertices and $\tau = 1$ otherwise. Hence, all local relations hold in the homology.

The second kind of generators impose non-local relations on \mathbf{x}_0 . For any connected coherent cycle Z there are exactly two positive Maslov index one Whitney disks from \mathbf{x}_Z to \mathbf{x}_0 that avoid \mathbb{X} :

$$(48) \quad \phi_1 = (R_Z \cup \bigcup_{X_i \in Z} B_i) \setminus \bigcup_{i>0} A_i \quad \text{and} \quad \phi_2 = (R_Z \cup \bigcup_{X_i \in Z} A_i) \setminus \bigcup_{i>0} B_i,$$

see [OS09, Figure 10]. Note that the connectivity of S is important for this to hold. By Lemma 4.7, $\widehat{\mathcal{M}}(\phi_i) = \pm 1$, and $\widehat{\mathcal{M}}(\phi_1) + \widehat{\mathcal{M}}(\phi_2) = 0$ by Corollary 4.18. In our framework, the disks ϕ_1 and ϕ_2 contribute (up to sign) towards $\partial \mathbf{x}_Z$ respectively $t^{w(Z)} U_{\text{out}(Z)}$ and $U_{\text{in}(Z)}$, where $U_{\text{out}(Z)}$ (resp. $U_{\text{in}(Z)}$) is the product of variables associated with edges going out of (resp. coming into) the (closed) region R_Z bounded by Z and $w(Z)$ is the number of trace vertices in R_Z . Hence,

$$\partial \mathbf{x}_Z = \pm \left(t^{w(Z)} U_{\text{out}(Z)} - U_{\text{in}(Z)} \right) \mathbf{x}_0,$$

where the difference in parentheses matches NL_{γ_Z} for $t = q^{-2}$. Together with Lemma 5.7 this implies that non-local relations hold in the homology.

Suppose now that $S = U \sqcup S'$, where S' is connected and surrounded by the unknot U that carries the basepoint \star . The same argument as above shows that the 0th homology coincides with $\mathcal{A}(S) = \widetilde{\mathcal{A}}(S')$. Together with Lemmata 5.8 and 5.9 this proves the general case. \square

Choose now a braid diagram $\widehat{\beta}$ of a link. By applying Theorem 4.19 we can replace $\widehat{\text{CFK}}(\widehat{\beta})$ with a homotopy equivalent complex $\widetilde{C}(\widehat{\beta})$ modelled on the cube of resolutions from Section 3.1:

- a vertex corresponding to a full resolution S is decorated with $\widehat{\text{CFK}}(S) \otimes \mathcal{L}_S$,
- edges are decorated with zip and unzip maps,
- higher components of the differential are possible.

The column filtration on this cube leads to a spectral sequence converging to $\widehat{\text{HFK}}(\widehat{\beta})$. When \mathbb{k} is q -complete, e.g. $\mathbb{k} = \mathbb{Z}[q^{-1}, q]$, then $H(\widehat{\text{CFK}}(S) \otimes \mathcal{L}_S)$ is concentrated in homological degree 0 by Proposition 4.21 and the first page of the spectral sequence coincides with $C^{\text{AG}}(\widehat{\beta})$. In particular, the spectral sequence collapses on the second page.

Theorem 5.11. *Suppose that $\widehat{\beta}$ is a braid diagram of a knot and let $\mathbb{k} = \mathbb{Z}[q^{-1}, q]$ with $t = q^{-2}$. Then there is a quasi-isomorphism*

$$\widehat{\text{CFK}}(\widehat{\beta}) \xrightarrow{\sim} C^{\text{AG}}(\widehat{\beta}).$$

In particular, $H(C^{\text{AG}}(\widehat{\beta})) \cong \widehat{\text{HFK}}(\widehat{\beta}) \otimes \mathbb{k}$ is a knot invariant.

Proof. The desired quasi-isomorphism is a composition of a sequence of homotopy equivalences from Theorem 4.19, which replaces $\widehat{\text{CFK}}(\widehat{\beta})$ with a cube of complexes computed from full resolutions of $\widehat{\beta}$, followed by an epimorphism onto $C^{\text{AG}}(\widehat{\beta})$ given by

$$\widehat{\text{CFK}}(\widehat{\beta}_I) \otimes \mathcal{L}_{\widehat{\beta}_I} \longrightarrow H_0(\widehat{\text{CFK}}(\widehat{\beta}_I) \otimes \mathcal{L}_{\widehat{\beta}_I}) \cong \mathcal{A}(\widehat{\beta}_I)$$

at each resolution $\widehat{\beta}_I$. The projection on 0th homology is well-defined, because the canonical generator $\mathbf{x}_0 \in \widehat{CFK}(\widehat{\beta}_I)$ has the maximal homological degree. It is a quasi-isomorphism, because higher homology groups vanish, see Proposition 4.21. \square

5.3. An identification with the original Gilmore complex. Choose a braid diagram $\widehat{\beta}$ of a knot and its complete resolution $\widehat{\beta}_I$. The original construction of the algebra $\mathcal{A}(\widehat{\beta}_I)$ as described in [OS09, Gil16] computes the Heegaard Floer homology twisted by the set P^{OS} . This algebra, denoted here by $\mathcal{A}'(\widehat{\beta}_I)$, assumes $\widehat{\beta}_I$ is layered in the sense of Section 3.1 with $n+1$ levels, where n is the number of crossings in $\widehat{\beta}$ (the extra level is the trace section) and it is generated like $\mathcal{A}(\widehat{\beta}_I)$ by thin edges of $\widehat{\beta}_I$. The local relations, however, are twisted differently:

$x_c \rightarrow x_a$	$x_c \rightarrow x_a$	$x_c \rightarrow x_a$	$\begin{array}{c} x_c \searrow \\ x_d \swarrow \end{array} \rightarrow \begin{array}{c} x_a \\ x_b \end{array}$
$tx_a = x_c$	$x_a = x_c$	$x_a = 0$	$t(x_a + x_b) = x_c + x_d$ $t^2 x_a x_b = x_c x_d$

and non-local relations, parametrized by coherent cycles Z in S , take the form

$$NL'_Z = t^{|Z|} x_{\text{out}(Z)} - x_{\text{in}(Z)},$$

where $|Z|$ is a weighted counts of (non-trace) vertices in R_Z : each (non-trace) bivalent vertex contributes 1, whereas a singular crossing contributes 2. The form of local relations suggests already an isomorphism between the two algebras.

Proposition 5.12. *Let $\mathbb{k} = \mathbb{Z}[t^{1/2}, t^{-1/2}]$ and set $q = t^{-n/2}$, where n is the number of crossings in $\widehat{\beta}$. Then there is an isomorphism of algebras*

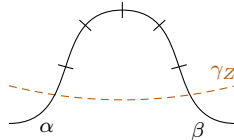
$$\mathcal{A}'(\widehat{\beta}_I) \ni x_\alpha \xrightarrow{\cong} t^{-n(\alpha)} x_{\overline{\alpha}} \in \mathcal{A}(\widehat{\beta}_I),$$

where $\overline{\alpha}$ is the edge of ω that contains the image of the semi-arc α in the resolution and $n(\alpha)$ is the number of crossings in β to the left of α .

Proof of Proposition 5.12. Renormalize the basis of $\mathcal{A}'(\widehat{\beta}_I)$ by setting $\tilde{x}_\alpha := t^{n(\alpha)} x_\alpha$. Clearly, the local relations at non-trace vertices do not involve t anymore, whereas at a trace vertex the linear relation $x_a = x_c$ is replaced with $\tilde{x}_a = t^n \tilde{x}_c$, that coincides with the quantum trace relation $\tilde{x}_a = q^{-2} \tilde{x}_c$. In particular, variables at both sides of a bivalent vertex other than the trace vertex are identified.

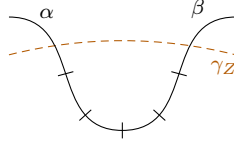
It remains to show that the non-local relation NL'_Z associated with a coherent cycle Z , when rewritten in the new basis, takes the form (39) for $\gamma = \gamma_Z$ a small push of Z . In other words, the power of t must equal in , where i is the number of trace vertices in R_Z . For that resolve $\widehat{\beta}_I$ into a collection of concentric loops ℓ_1, \dots, ℓ_k by replacing every singular crossing with two horizontal lines, each with a bivalent vertex on it. The exponent of t in NL'_Z counts then bivalent vertices inside γ_Z .

Consider first a loop ℓ_r , the trace vertex of which is inside γ_Z . If it is entirely contained by γ_Z , then it contributes exactly n towards the power of t . Otherwise, each arc with s bivalent vertices outside of γ_Z



lowers the contributions of the loop towards $w(\gamma_Z)$ by s . However, the semi-arcs α and β containing the left and right endpoints of the arc satisfy $n(\beta) = n(\alpha) + s$, so that renormalizing the variables increases the contribution back. Hence, in the renormalized basis, each such loop contributes exactly n towards $w(\gamma_Z)$.

Conversely, if the trace vertex of ℓ_r is not contained by γ_Z , then ℓ_r does not contribute towards the power of t . Indeed, for every arc of ℓ_r with s vertices inside γ_Z



and the left and right endpoints on semi-arcs α and β respectively, we have $n(\beta) - n(\alpha) = s$. Hence, renormalizing variables lowers the power of t by s , cancelling the contribution of the vertices from the arc.

Hence, the power of t in NL'_Z , when rewritten in the new basis, is equal to in as desired. \square

5.4. A pseudo completion. In this section, we introduce a functor qAG that interpolates \mathfrak{gl}_0 homology and knot Floer homology. It comes from the observation that Theorem 5.11 relates Gilmore’s construction to knot Floer homology when coefficients are $\mathbb{Z}[q^{-1}, q]$. On the other hand, the definition of \mathfrak{gl}_0 homology can be “morally” thought of as the Gilmore one specialized at $q = 1$. The functor qAG aims to take the best of these two incompatible worlds.

Coefficients over which chain complexes are considered will play an important role in this section. We emphasize this importance by writing them systematically. Moreover, despite the construction of qAG makes sense for any pointed annular web, we focus on the case of elementary webs.

Given an annular web ω , consider the map:

$$Q_\omega: \mathcal{A}(\omega; \mathbb{Z}[q, q^{-1}]) \longrightarrow \mathcal{A}(\omega; \mathbb{Z}[q^{-1}, q])$$

given by extending the scalars. It may not be injective. Define

$$qAG(\omega) := \mathcal{A}(\omega; \mathbb{Z}[q, q^{-1}]) / \ker Q_\omega$$

and more generally $qAG(\omega; \mathbb{k}) := qAG(\omega) \otimes_{\mathbb{Z}[q, q^{-1}]} \mathbb{k}$ for any $\mathbb{Z}[q, q^{-1}]$ -module \mathbb{k} . Notice that in $qAG(\omega)$ we kill every decoration $x \in D(\omega)$ that is annihilated in $\mathcal{A}(\omega; \mathbb{Z}[q, q^{-1}])$ by some nontrivial polynomial $p(q) \in \mathbb{Z}[q, q^{-1}]$. Because the homomorphism Q_ω is natural with respect to actions of foams, $qAG(-; \mathbb{k})$ extends to a functor on \mathcal{AFoam}_q^* .

Lemma 5.13. *If \mathbb{k} is a PID and ω is an elementary pointed annular web, then $qAG(\omega; \mathbb{k})$ is a free \mathbb{k} -module of finite rank.*

Proof. Notice first that $qAG(\omega; \mathbb{k})$ vanishes when ω is disconnected and is free of rank one when ω is a chain of dumbbells, see Example 5.3. The thesis follows now from the functoriality of $qAG(-; \mathbb{k})$ and Proposition 2.25, because a submodule of a finitely generated free module over a PID is finitely generated and torsion-free, hence free. \square

Using the cube of resolutions approach one extends qAG to braid diagrams and we write $qAGH(\hat{\beta}; \mathbb{k})$ for the homology of the corresponding complex. This complex plays a central in our subsequent constructions. We simplify the notation to AG and AGH respectively when $q = 1$.

While it can be shown that $qAGH(\hat{\beta}; \mathbb{k})$ is a braid invariant that is preserved under stabilization, checking the first Markov move (conjugacy) is challenging.

Conjecture 1. *If \mathbb{k} is a field of characteristic 0, then $qAGH$ is a knot invariant for any q .*

As a direct consequence of the construction, $qAG(\omega)$ can be identified with a $\mathbb{Z}[q, q^{-1}]$ -subspace of $\mathcal{A}(\omega; \mathbb{Z}[q^{-1}, q])$ of maximal rank. This observation leads immediately to the following result.

Proposition 5.14. *For any braid closure $\widehat{\beta}$, $qAG(\widehat{\beta}; \mathbb{Z}[q^{-1}, q])$ and $C^{AG}(\widehat{\beta}; \mathbb{Z}[q^{-1}, q])$ are isomorphic complexes of graded $\mathbb{Z}[q^{-1}, q]$ -modules. In particular, $qAG(\widehat{\beta}; \mathbb{Z}[q^{-1}, q])$ is quasi-isomorphic to $\widehat{CFK}(\widehat{\beta}) \otimes \mathbb{Z}[q^{-1}, q]$ when $\widehat{\beta}$ is a knot.*

Proof. The map $qAG(\omega, \mathbb{Z}[q, q^{-1}]) \rightarrow \mathcal{A}(\omega, \mathbb{Z}[q^{-1}, q])$ induced by the inclusion of the coefficients is injective, due to the definition of qAG , and it becomes an isomorphism after tensoring with $\mathbb{Z}[q^{-1}, q]$ over $\mathbb{Z}[q, q^{-1}]$. The last statement follows from Theorem 5.11. \square

Specializing the complex $C^{AG}(\widehat{\beta})$ at $q = 1$ does not recover the \mathfrak{gl}_0 complex, e.g. $\mathcal{A}(\omega)$ may not vanish for a disconnected web ω . The situation is different for qAG .

Proposition 5.15. *For any elementary pointed annular web ω there is an isomorphism $AG(\omega; \mathbb{k}) \cong \mathcal{S}_0(\omega; \mathbb{k})$ that intertwines the action of foams. In particular, $AG(\widehat{\beta}; \mathbb{k})$ and $C^{\mathfrak{gl}_0}(\widehat{\beta}; \mathbb{k})$ are naturally isomorphic as complexes of graded \mathbb{k} -modules.*

Proof. Both $AG(\omega; \mathbb{k})$ and $\mathcal{S}_0(\omega; \mathbb{k})$ are quotients of the Soergel space $B(\omega)$ of the web ω . We claim that the identity on $B(\omega)$ induces the desired isomorphism. Due to functoriality of both constructions and Proposition 2.25 it is enough to check the claim for basic elementary webs.

This is clear when ω has more than one component, because in this case both spaces are zero. Otherwise ω is either a single circle or a chain of dumbbells and in each case both spaces are freely generated by the empty decoration, see Theorem 3.11, Examples 5.2 and 5.3. \square

Proposition A from the introduction is an immediate corollary of the above result.

Proposition A. *The homology theories AGH and $H^{\mathfrak{gl}_0}$ coincide. Hence, AGH is a knot invariant if \mathbb{k} is a field.*

Proof. The first statement follows from applying Proposition 5.15 to each vertex in the cube of resolutions. Since the \mathfrak{gl}_0 homology is a knot invariant when \mathbb{k} is a field, then so is AGH . \square

Remark 5.16. Another consequence of Proposition 5.15 is that $AG(\omega)$ is a free \mathbb{k} -module for any elementary pointed web ω and any ring \mathbb{k} , because $\mathcal{S}_0(\omega; \mathbb{k})$ is free. This strengthens Lemma 5.13 when $q = 1$.

5.5. The spectral sequence. In this short section we establish the main result of the paper. The idea is to apply to $qAGH(\widehat{\beta})$ the $(q \mapsto 1)$ Bockstein spectral sequence, discussed in details in Appendix A. For this purpose we fix an arbitrary field \mathbb{K} and work over a PID $\mathbb{K}[q, q^{-1}]$, where we can specialize $q = 1$.

Theorem B. *Assume that \mathbb{K} is a field and K is a knot represented by a braid closure $\widehat{\beta}$. Then the $(q \mapsto 1)$ Bockstein spectral sequence applied to $qAG(\widehat{\beta}; \mathbb{K}[q, q^{-1}])$ has $H^{\mathfrak{gl}_0}(K; \mathbb{K})$ as its first page and converges after finitely many steps. The last page is (non-canonically) isomorphic to $\widehat{HFK}(K; \mathbb{K})$.*

Proof. The thesis follows directly from Proposition A.7, which we can apply thanks to Lemma 5.13. Indeed it states that the $(q \mapsto 1)$ Bockstein spectral sequence has $AGH(\widehat{\beta}; \mathbb{K})$ on the first page and converges to the quotient of $qAGH(\widehat{\beta}; \mathbb{K}[q^{-1}, q])$ by its torsion submodule, tensored with \mathbb{K} . The former is isomorphic to $H^{\mathfrak{gl}_0}(K, \mathbb{K})$ by Proposition A and we identify the latter with $\widehat{HFK}(K, \mathbb{K})$ as follows.

Because $\mathbb{K}[q^{-1}, q]$ contains the field of fractions of $\mathbb{K}[q, q^{-1}]$, the universal coefficient theorem and Proposition 5.14 imply that the homology groups of $qAG(\widehat{\beta}; \mathbb{K}[q, q^{-1}])$ and $C^{AG}(\widehat{\beta}; \mathbb{K}[q^{-1}, q])$ have the same rank. On the other hand, we know from Theorem 5.11 that $H(C^{AG}(\widehat{\beta}; \mathbb{K}[q^{-1}, q]))$ is isomorphic to $\widehat{HFK}(\widehat{\beta}) \otimes \mathbb{K}[q^{-1}, q]$. Hence, the quotient of $qAGH(\widehat{\beta}; \mathbb{K}[q, q^{-1}])$ by its torsion submodule has the same rank as $\widehat{HFK}(\widehat{\beta}) \otimes \mathbb{K}[q, q^{-1}]$ and we conclude by tensoring both sides with \mathbb{K} . \square

If the characteristic of \mathbb{K} is 0, then we can consider this spectral sequence together with the one from Theorem 3.11, establishing the DGR Conjecture.

Theorem C (DGR Conjecture). *For any knot K and any field of characteristic zero, the bigraded dimension of HHH^{red} (after forgetting the \mathfrak{a} -grading) is greater or equal to the bigraded dimension of \widehat{HFK} .*

APPENDIX A. ON BOCKSTEIN SPECTRAL SEQUENCES

A.1. Limits of spectral sequences. This short section is a survey of [McC01, Chapter 3]. In what follows, we consider decreasing filtrations of modules and chain complexes, not necessary bounded. More explicitly, a *filtration* of a \mathbb{k} -module M is a sequence $(F^n)_{n \in \mathbb{Z}}$ of submodules of M satisfying

$$F^n \supseteq F^{n+1} \quad \text{for all } n \in \mathbb{Z}.$$

Its *associated graded* module $\text{gr}^\bullet(M)$ is defined as the sequence of quotients

$$\text{gr}^n(M) = F^n / F^{n+1} \quad \text{for } n \in \mathbb{Z}.$$

For a chain complex (C, d) it is understood that the submodules F^n are subcomplexes. In such case each chain group C_i is filtered by $F^n C_i := F^n \cap C_i$ and $d(F^n C_i) \subseteq F^n C_{i+1}$ for all $i, n \in \mathbb{Z}$. There is also an associated filtration on the homology with $F^n H(C, d)$, defined as the image of the natural map $H(F^n, d) \rightarrow H(C, d)$.

With every filtered chain complex (C, d, F) there is an associated *spectral sequence* $\{E_r\}_{r \in \mathbb{N}}$ with the first page

$$E_1^{n, p-n} = H^p(\text{gr}^n(C)).$$

We say that the spectral sequence *converges* to the homology of the filtered chain complex (C, d, F) if the ∞ -page is directly related to the filtration of $H(C, d)$ by

$$E_\infty^{n, p-n} = \text{gr}^n H^p(C, d).$$

By [McC01, Theorem 3.2] this is the case if the filtered chain complex (C, d, F) is *exhaustive*, i.e. $\bigcup_n F^n C = C$, and *weakly convergent*. The latter holds for instance when $\bigcap_n F^n C = 0$; for the general definition see [McC01, Definition 3.1].

Example A.1. Consider graded filtered \mathbb{k} -complexes (C, d, F) and $(C \oplus \mathbb{k}, d \oplus 0, \tilde{F})$ with $\tilde{F}^n = F^n \oplus \mathbb{k}$. The associated graded of these complexes coincide, so that they induce the same exact sequence. We deduce that the spectral sequence converges simultaneously to both $H(C, d)$ and $H(C, d) \oplus \mathbb{k}$.

To assure the uniqueness of the limit of a spectral sequence associated with (C, d, F) , the filtration needs to be *Hausdorff*, that is weakly convergent and

$$\bigcap_{n \in \mathbb{Z}} F^n H(C, d) = 0.$$

Note that the second filtration in Example A.1 is not Hausdorff. An important source of exhaustive and Hausdorff filtrations is provided by *completions* of filtered chain complexes.

Recall that the *completion* of a filtered module (M, F) is the inverse limit

$$\widehat{M} := \varprojlim_s M / F^s$$

together with the filtration

$$\widehat{F}^n := \varprojlim_s F^n / F^{n+s}.$$

The filtered module $(\widehat{M}, \widehat{F})$ is exhaustive and Hausdorff by [McC01, Prop. 3.12]. Finally, given a map $f: (M, F_M) \rightarrow (N, F_N)$ of exhaustive filtered modules, the induced map $\hat{f}: \widehat{M} \rightarrow \widehat{N}$ is

an isomorphism if and only if $\text{gr}f: \text{gr}M \rightarrow \text{gr}N$ is an isomorphism [McC01, Prop. 3.14]. This implies the following important statement (compare [McC01, Cor. 3.15]).

Theorem A.2. *Assume that $\{f_r: E_r \rightarrow E'_r\}_{r \geq 0}$ is a morphism of spectral sequences E_r and E'_r that converges to (M, F_M) and (N, F_N) respectively. If f_n is an isomorphism for some n , then f_∞ induces an isomorphism of filtered modules $(\widehat{M}, \widehat{F}_M)$ and $(\widehat{N}, \widehat{F}_N)$.*

Example A.3. Consider the module $\mathbb{Z}[t]$ filtered by powers of t . Its associated graded

$$\text{gr } \mathbb{Z}[t] = \bigoplus_{n \in \mathbb{N}} \frac{t^n \mathbb{Z}[t]}{t^{n+1} \mathbb{Z}[t]} = \bigoplus_{n \in \mathbb{N}} \mathbb{Z}\{t^n\}$$

can be identified with $\mathbb{Z}[t]$ as an abelian group (note that the action of t annihilates $\text{gr } \mathbb{Z}[t]$), whereas the completion is exactly $\mathbb{Z}[[t]]$. Consider $M := \mathbb{Z}[t]/(1 - tp)$ for some $p \in \mathbb{Z}[t]$ with the induced filtration. Then $F^n M = M$ for any n , because t is invertible in M . This forces $\text{gr}^n M = 0$ for all $n \geq 0$ and $\widehat{M} = 0$ as a result. Note that the filtration is not weakly convergent and also $M[[t]] = 0$.

Example A.4. Consider the ring of Laurent polynomials $\mathbb{Z}[t, t^{-1}]$ as a $\mathbb{Z}[t]$ -module and let F^n be generated by t^n for $n \in \mathbb{Z}$. Contrary to the previous case, this filtration is not bounded from below. The associated graded can be identified as an abelian group with $\mathbb{Z}[t, t^{-1}]$ as in the previous example and the completion

$$\widehat{\mathbb{Z}[t, t^{-1}]} = \lim_{\leftarrow s} \frac{\mathbb{Z}[t^{-1}, t]}{t^s \mathbb{Z}[t]} = \mathbb{Z}[t^{-1}, t]$$

is filtered by $\widehat{F}^n = t^n \mathbb{Z}[[t]]$ for $t \in \mathbb{Z}$. Note that the filtration is exhaustive and weakly convergent. As before, consider $M := \mathbb{Z}[t, t^{-1}]/(1 - tp)$ for some polynomial $p \in \mathbb{Z}[t]$ with the induced filtration. Again, t is invertible in M , so that both $\text{gr}M$ and \widehat{M} vanish.

A.2. The mod- p Bockstein spectral sequence. The aim of this section is to recall the classical Bockstein sequence in the context of \mathbb{Z} -modules, following [May09]. This is generalized in section A.3 to the case of modules over Laurent polynomials and specializing the value of the formal variable.

Let C be a chain complex of \mathbb{Z} -modules and p a prime number. The short exact sequence

$$0 \longrightarrow \mathbb{Z} \xrightarrow{\cdot p} \mathbb{Z} \xrightarrow{\pi} \mathbb{Z}/p\mathbb{Z} \longrightarrow 0$$

induces a long exact sequence of homology groups¹³

$$\dots \xrightarrow{\partial} H_\bullet(C; \mathbb{Z}) \xrightarrow{H(\cdot p)} H_\bullet(C; \mathbb{Z}) \xrightarrow{H(\pi)} H_\bullet(C; \mathbb{Z}/p\mathbb{Z}) \xrightarrow{\partial} H_{\bullet+1}(C; \mathbb{Z}) \xrightarrow{H(\cdot p)} \dots$$

which can be thought of as an exact triangle

$$\begin{array}{ccc} H(C; \mathbb{Z}) & \xrightarrow{H(\cdot p)} & H(C; \mathbb{Z}) \\ & \searrow \partial & \swarrow H(\pi) \\ & H(C; \mathbb{Z}/p\mathbb{Z}) & \end{array}$$

and described in terms of exact couples as we explain below.

Recall from [Mas52] that an *exact couple* is a tuple (A, B, f, g, h) consisting of objects A and B from an abelian category and morphisms $f: A \rightarrow A$, $g: A \rightarrow B$ and $h: B \rightarrow A$ satisfying $\text{im } f = \ker g$, $\text{im } g = \ker h$ and $\text{im } h = \ker f$. Defining

- $A' = \text{im } f$,
- $B' = \ker(g \circ h) / \text{im}(g \circ h)$,

¹³Recall that for us a differential in a chain complex has degree $+1$, i.e. it increases the homological degree.

- $f': A' \rightarrow A'$ as the restriction of f to A' ,
- $h': B' \rightarrow A'$ as induced by h , and
- $g': A' \rightarrow B'$ by declaring that $a' = f(a) \in A'$ is mapped on $g(a') = g(a) \in B'$

yields another exact couple (A', B', f', g', h') . Inductively one constructs a sequence of exact couples $(A^{(n)}, B^{(n)}, f^{(n)}, g^{(n)}, h^{(n)})_{n \in \mathbb{N}}$ and checks that $(B^{(n)}, g^{(n)} \circ f^{(n)})$ is a spectral sequence¹⁴. The *Bockstein spectral sequence* arises from the exact couple

$$(H(C; \mathbb{Z}), H(C; \mathbb{Z}/p\mathbb{Z}), H(\cdot p), H(\pi), \partial).$$

Example A.5. Consider the chain complex $C = \mathbb{Z} \xrightarrow{p^k} \mathbb{Z}$ for some $k \geq 1$. The first exact couple at stake is:

$$\begin{array}{ccc} \mathbb{Z}/p^k\mathbb{Z} & \xrightarrow{\cdot p} & \mathbb{Z}/p^k\mathbb{Z} \\ & \swarrow (p^{k-1} \ 0) \quad \searrow \begin{pmatrix} 0 \\ 1 \end{pmatrix} & \\ & \mathbb{Z}/p\mathbb{Z} \oplus \mathbb{Z}/p\mathbb{Z} & \end{array}.$$

In general, for $1 \leq i \leq k$, the i th exact couple is given by:

$$\begin{array}{ccc} \mathbb{Z}/p^{k+1-i}\mathbb{Z} & \xrightarrow{\cdot p} & \mathbb{Z}/p^{k+1-i}\mathbb{Z} \\ & \swarrow (p^{k-i} \ 0) \quad \searrow \begin{pmatrix} 0 \\ 1 \end{pmatrix} & \\ & \mathbb{Z}/p\mathbb{Z} \oplus \mathbb{Z}/p\mathbb{Z} & \end{array}$$

and finally the $(k+1)$ -st exact couple is identically 0.

Proposition A.6. *The first page of the Bockstein spectral sequence of a chain complex C of abelian groups is $H(C; \mathbb{Z}/p\mathbb{Z})$. If the chain complex C is free and finitely generated, then the Bockstein spectral sequence converges in finitely many steps and the infinite page is canonically isomorphic to the quotient of $H(C; \mathbb{Z})$ by its torsion submodule, tensored with $\mathbb{Z}/p\mathbb{Z}$.*

Sketch of the proof. This is a very classical result and the proof is rather elementary. First, using Smith normal form of differentials, one obtains that every free and finitely generated complex of \mathbb{Z} -modules is a direct sum of shifted complexes of the form

- (1) $0 \rightarrow \mathbb{Z} \rightarrow 0$,
- (2) $0 \rightarrow \mathbb{Z} \xrightarrow{\cdot r} \mathbb{Z} \rightarrow 0$ with r an integer coprime with p ,
- (3) $0 \rightarrow \mathbb{Z} \xrightarrow{\cdot p^k r} \mathbb{Z} \rightarrow 0$ with $k \geq 1$ and r an integer coprime with p .

In case (1), the spectral sequence converges immediately and its infinite page is equal to $\mathbb{Z}/p\mathbb{Z}$. In case (2), the spectral sequence converges immediately and its infinite page is equal to 0. Case (3) is dealt with in Example A.5: it converges to 0 at the $(k+1)$ -st page. \square

A.3. The $(q \mapsto 1)$ Bockstein sequence. Let \mathbb{K} be a field and $\mathbb{L} := \mathbb{K}[q, q^{-1}]$ be the ring of Laurent polynomial over \mathbb{K} . Note that \mathbb{L} is a principal ideal domain (PID), so that Smith's normal form result applies. We endow \mathbb{K} with an \mathbb{L} -module structure by letting q act by 1. In other words, we have an exact sequence of \mathbb{L} -modules

$$0 \rightarrow \mathbb{L} \xrightarrow{\cdot(q-1)} \mathbb{L} \xrightarrow{q \mapsto 1} \mathbb{K} \rightarrow 0.$$

Let C be a chain complex of \mathbb{L} -modules. Just like in subsection A.2, one can use the induced long exact sequence of homology to construct an exact couple

$$(H(C; \mathbb{L}), H(C; \mathbb{K}), H(\cdot(q-1)), H(q \mapsto 1), \partial).$$

¹⁴Not necessarily bigraded in general.

This exact couple induces a spectral sequence, which we call the $(q \mapsto 1)$ *Bockstein spectral sequence*.

Proposition A.7. *The first page of the $(q \mapsto 1)$ Bockstein spectral sequence of a chain complex C of \mathbb{L} -modules is $H(C; \mathbb{K})$. If the chain complex C is free and finitely generated, then the $(q \mapsto 1)$ Bockstein spectral sequence converges in finitely many steps the infinite page is canonically isomorphic to the quotient of $H(C; \mathbb{L})$ by its torsion submodule, tensored with \mathbb{K} .*

Sketch of the proof. The proof follows the same line as the one of Proposition A.6. Every free and finitely generated complex of \mathbb{L} -module is a direct sum of shifted complexes of the form

- (1) $0 \longrightarrow \mathbb{L} \longrightarrow 0$,
- (2) $0 \longrightarrow \mathbb{L} \xrightarrow{\cdot p(q)} \mathbb{L} \longrightarrow 0$ with $p(q)$ a polynomial coprime with $q - 1$, or
- (3) $0 \longrightarrow \mathbb{L} \xrightarrow{\cdot (q-1)^k p(q)} \mathbb{L} \longrightarrow 0$ with $k \geq 1$ and $p(q)$ a polynomial coprime with $q - 1$.

In case (1), the spectral sequence converges immediately and its infinite page is equal to \mathbb{K} . In case (2), the spectral sequence converges immediately and its infinite page is equal to 0. Case (3) is similar to Example A.5. The first exact couple at stake is

$$\begin{array}{ccc} \mathbb{L}/\langle (q-1)^k p(q) \rangle & \xrightarrow{\cdot (q-1)} & \mathbb{L}/\langle (q-1)^k p(q) \rangle \\ \nwarrow ((q-1)^{k-1} p(q) \ 0) & & \nearrow \begin{pmatrix} 0 \\ 1 \end{pmatrix} \\ & \mathbb{K} \oplus \mathbb{K} & \end{array} .$$

In general, for $1 \leq i \leq k$, the i th exact couple is given by

$$\begin{array}{ccc} \mathbb{L}/\langle (q-1)^{k+1-i} p(q) \rangle & \xrightarrow{\cdot (q-1)} & \mathbb{L}/\langle (q-1)^{k+1-i} p(q) \rangle \\ \nwarrow ((q-1)^{k-i} p(q) \ 0) & & \nearrow \begin{pmatrix} 0 \\ 1 \end{pmatrix} \\ & \mathbb{K} \oplus \mathbb{K} & \end{array} .$$

Finally, the $(k+1)$ -st exact couple is identically 0. Hence, in all three cases the $(q \mapsto 1)$ Bockstein spectral sequence converges to the quotient of $H(C; \mathbb{L})$ by its torsion submodule, tensored with \mathbb{K} as desired. \square

APPENDIX B. CYCLICITY OF THE QUANTUM HOCHSCHILD HOMOLOGY

For this section we fix a graded algebra A and consider its quantum Hochschild complex $qCH_\bullet(A)$ with the differential denoted by ∂ . The complex arises actually from a *simplicial module*,¹⁵ which means that each chain group $qCH_n(A)$ admits two families of homomorphisms: the family of *face maps* $\{d_i: M_n \rightarrow M_{n-1}\}_{0 \leq i \leq n}$ and of *degeneracy maps* $\{s_j: M_n \rightarrow M_{n+1}\}_{0 \leq j \leq n}$, which satisfy the equalities

$$(49) \quad d_i d_j = d_{j-1} d_i \quad \text{for } i < j,$$

$$(50) \quad s_i s_j = s_j s_{i-1} \quad \text{for } i > j,$$

$$(51) \quad d_i s_j = \begin{cases} s_{j-1} d_i & \text{for } i < j, \\ id & \text{for } i = j, j+1, \\ s_j d_{i-1} & \text{for } i > j+1. \end{cases}$$

¹⁵For more details about simplicial and cyclic module see [Lod98].

Indeed, the face maps are the components of the quantum Hochschild differential,

$$d_i(a_0 \otimes \cdots \otimes a_n) := \begin{cases} a_0 a_1 \otimes a_2 \otimes \cdots \otimes a_n & \text{if } i = 0, \\ a_0 \otimes \cdots \otimes a_i a_{i+1} \otimes \cdots \otimes a_n & \text{if } 0 < i < n, \\ q^{-|a_n|} a_n a_0 \otimes a_1 \otimes \cdots \otimes a_{n-1} & \text{if } i = n, \end{cases}$$

whereas the degeneracy map s_j inserts $1 \in A$ after j -th factor:

$$s_j(a_0 \otimes \cdots \otimes a_n) := a_0 \otimes \cdots \otimes a_j \otimes 1 \otimes a_{j+1} \otimes \cdots \otimes a_n.$$

In addition to that, there is a family of component-wise endomorphisms

$$t_n(a_0 \otimes \cdots \otimes a_n) := q^{-|a_n|} a_n \otimes a_0 \otimes \cdots \otimes a_{n-1},$$

which satisfy the equalities

$$(52) \quad d_i t_n = \begin{cases} d_n & \text{for } i = 0, \\ t_{n-1} d_{i-1} & \text{for } i > 0, \end{cases} \quad s_j t_n = \begin{cases} t_{n+1}^2 s_n & \text{for } j = 0, \\ t_{n+1} s_{j-1} & \text{for } j > 0. \end{cases}$$

Consider the endomorphism T of $qCH_\bullet(A)$ defined by $T_n := t_n^{n+1}$. It is the identity map when $q = 1$, which means that the classical Hochschild homology is a cyclic module, but in general case it scales a homogeneous degree d Hochschild chain by q^d . However, it is not far from the identity map.

Lemma B.1. *The endomorphism T is chain homotopic to the identity map.*

Proof. Define $\sigma_n := t_{n+1} s_n$, so that

$$(53) \quad d_i \sigma_n = \begin{cases} id & \text{for } i = 0, \\ \sigma_{n-1} d_{i-1} & \text{for } 0 < i < n, \\ t_n & \text{for } i = n. \end{cases}$$

We claim that $h_n = \sum_{j=0}^n (-1)^{jn} \sigma_n t_n^j$ is a desired chain homotopy. First, write

$$(54) \quad h_{n-1} \partial_n = \sum_{j=0}^{n-1} \sum_{i=0}^n (-1)^{i+j(n-1)} \sigma_{n-1} t_{n-1}^j d_i$$

$$(55) \quad \partial_{n+1} h_n = \sum_{i=0}^{n+1} \sum_{j=0}^n (-1)^{i+jn} d_i \sigma_n t_n^j$$

and notice the following cancellation in (55):

$$(56) \quad (-1)^{n+1+jn} d_{n+1} \sigma_n t_n^j = -(-1)^{(j+1)n} t_n^{j+1} = -(-1)^{(j+1)n} d_0 \sigma_n t_n^{j+1}.$$

Hence,

$$(57) \quad \sum_{j=0}^n (-1)^{jn} (d_0 - (-1)^n d_{n+1}) \sigma_n t_n^j = d_0 \sigma_n - d_{n+1} \sigma_n t_n^n = id - t_n^{n+1}.$$

Put the remaining terms of ∂h as well as the terms of $h \partial$ in the lexicographic order with respect to i then j , to create $n(n+1)$ pairs:

$$(58) \quad \begin{array}{ccccccccc} d_1 \sigma_n & < & d_2 \sigma_n & < & \cdots & < & d_n \sigma_n & < & d_1 \sigma_n t_n & < & d_2 \sigma_n t_n & < & \cdots \\ \updownarrow & & \updownarrow & & & & \updownarrow & & \updownarrow & & \updownarrow & & \updownarrow & & \\ \sigma_{n-1} d_0 & < & \sigma_{n-1} d_1 & < & \cdots & < & \sigma_{n-1} d_{n-1} & < & \sigma_{n-1} d_n & < & \sigma_{n-1} t_{n-1} d_0 & < & \cdots \end{array}$$

It is enough to show that none of the pair contributes to $\partial h + h \partial$.

The term $d_{i+1}\sigma_n t_n^j$ is at the position $jn + i + 1$ in the upper sequence of (58) and it appears in (55) with sign $(-1)^{jn+i+1}$. We compute

$$(59) \quad d_{i+1}\sigma_n t_n^j = \sigma_{n-1} d_i t_n^j = \begin{cases} \sigma_{n-1} t_{n-1}^{j-1} d_{i-j+n+1} & \text{if } 0 \leq i < j, \\ \sigma_{n-1} t_{n-1}^j d_{i-j} & \text{if } j \leq i < n, \end{cases}$$

obtaining a term at the position $jn + i + 1$ in the lower sequence of (58), which appears in (54) with sign $(-1)^{j(n-1)+i-j} = (-1)^{jn+i}$. Hence, the two terms cancel each other and the thesis follows. \square

We are now ready to prove the statement about quantum Hochschild homology for a polynomial algebra R^k . In fact, Proposition 2.13 is a special case of the following result.

Proposition B.2. *Suppose that A is supported in nonnegative degrees and that $1 - q^d$ is invertible for $d \neq 0$. Then the inclusion of the degree zero subalgebra $A_0 \subset A$ induces a homotopy equivalence of chain complexes $qCH_\bullet(A_0) \rightarrow qCH_\bullet(A)$. In particular, $qHH_\bullet(A) \cong qHH_\bullet(A_0)$.*

Proof. Let T be the endomorphism of $qCH_\bullet(A)$ that maps a homogeneous chain c to $q^{|c|}c$. The map $T - id$ is nullhomotopic by Lemma B.1, so that the subcomplex generated by chains of positive degree is contractible, whereas the degree 0 subcomplex coincides with $qCH_\bullet(A_0)$. \square

APPENDIX C. COMPUTATIONS OF \mathfrak{gl}_0 HOMOLOGY

This section provides details of computation of the \mathfrak{gl}_0 homology of the two trefoil knots, the figure eight knot and the $(5, 2)$ -torus knot. These computation is used in the introduction to prove detection results.

C.1. Trefoils. We see the right-handed (resp. left-handed) trefoil 3_1 (resp. $\bar{3}_1$) as the closure of the braid σ_1^3 (resp. σ_1^{-3}) in the braid group on two strands. We start with 3_1 . Following the definition of $H^{\mathfrak{gl}_0}$, we consider the hypercube given on Figure 25. On this figure bases of some \mathfrak{gl}_0 -state spaces are given. The fact that they are indeed bases follows directly from the digon relation and Theorem 3.11 (4).

In the bases given in Figure 25, the two non-trivial differentials are given by:

$$\begin{pmatrix} 1 & X_1 & X_2 & X_1 X_2 \\ 1 & 0 & 0 & 0 \\ 1 & 0 & 0 & 0 \\ 1 & 0 & 0 & 0 \\ 0 & 0 & 1 & 0 \\ 0 & 1 & 1 & 0 \\ 0 & 1 & 0 & 0 \end{pmatrix} \begin{matrix} 1_a \\ 1_b \\ 1_c \\ X_a \\ X_b \\ X_c \end{matrix} \quad \text{and} \quad \begin{pmatrix} 1_a & 1_b & 1_c & X_a & X_b & X_c \\ -1 & 1 & 0 & 0 & 0 & 0 \\ -1 & 0 & 1 & 0 & 0 & 0 \\ 0 & -1 & 1 & 0 & 0 & 0 \end{pmatrix}$$

Hence, the Poincaré polynomial of $H^{\mathfrak{gl}_0}(3_1)$ with coefficients in either \mathbb{F} or \mathbb{Q} is equal to:

$$t^0 q^2 + t q^0 + t^2 q^{-2}.$$

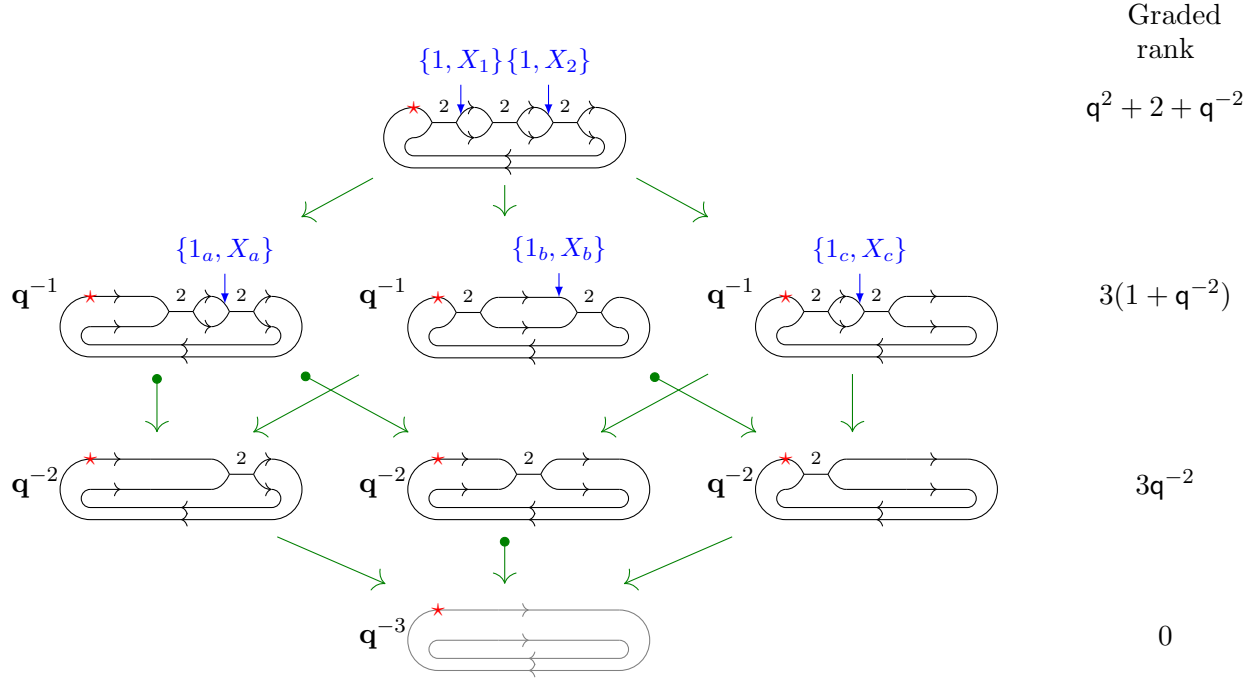


FIGURE 25. The hypercube for computing the \mathfrak{gl}_0 homology of the right-handed trefoil. On the upper four diagrams their homogeneous bases are given schematically in blue. The diagram on top (resp. bottom) is in homological degree 0 (resp. 3) and all maps between diagrams are given by unzips. A dot at the beginning of an arrow indicates the multiplication by (-1) in the differential.

For the left-handed trefoil all arrows in the hypercube are reversed whereas the homological degree and the q -grading shifts are opposite to that of Figure 25. The matrices of the two non-trivial differentials are

$$\begin{pmatrix} 0 & 0 & 0 \\ 0 & 0 & 0 \\ 0 & 0 & 0 \\ -1 & -1 & 0 \\ 1 & 0 & -1 \\ 0 & 1 & 1 \end{pmatrix} \begin{matrix} 1_a \\ 1_b \\ 1_c \\ X_a \\ X_b \\ X_c \end{matrix} \quad \text{and} \quad \begin{pmatrix} 1_a & 1_b & 1_c & X_a & X_b & X_c \\ 0 & 0 & 0 & 0 & 0 & 0 \\ 1 & 1 & 0 & 0 & 0 & 0 \\ 0 & 1 & 1 & 0 & 0 & 0 \\ 0 & 0 & 0 & 1 & 1 & 1 \end{pmatrix} \begin{matrix} 1 \\ X_1 \\ X_2 \\ X_1 X_2 \end{matrix}.$$

Hence, the Poincaré polynomial of $H^{\mathfrak{gl}_0}(\bar{3}_1)$ with coefficients in either \mathbb{F} or \mathbb{Q} is equal to:

$$t^{-2}q^2 + t^{-1}q^0 + t^0q^{-2}.$$

For a comparison we give the Poincaré polynomials of the reduced triply graded homology of the trefoil knots below:

$$\begin{aligned} P_{3_1}(t, a, q) &= t^2 a^{-2} q^{-2} + t^1 a^{-4} q^0 + t^0 a^{-2} q^2, \\ P_{\bar{3}_1}(t, a, q) &= t^{-2} a^2 q^2 + t^{-1} a^4 q^0 + t^0 a^2 q^{-2}. \end{aligned}$$

C.2. Figure-eight knot. We consider the figure-eight knot 4_1 as the closure of the braid $\sigma_1 \sigma_2^{-1} \sigma_1 \sigma_2^{-1}$ on three strands. Following the definition of $H^{\mathfrak{gl}_0}$ we build the hypercube given on Figure 26 (disconnected diagrams are skipped, because the associated spaces vanishes). One could compute

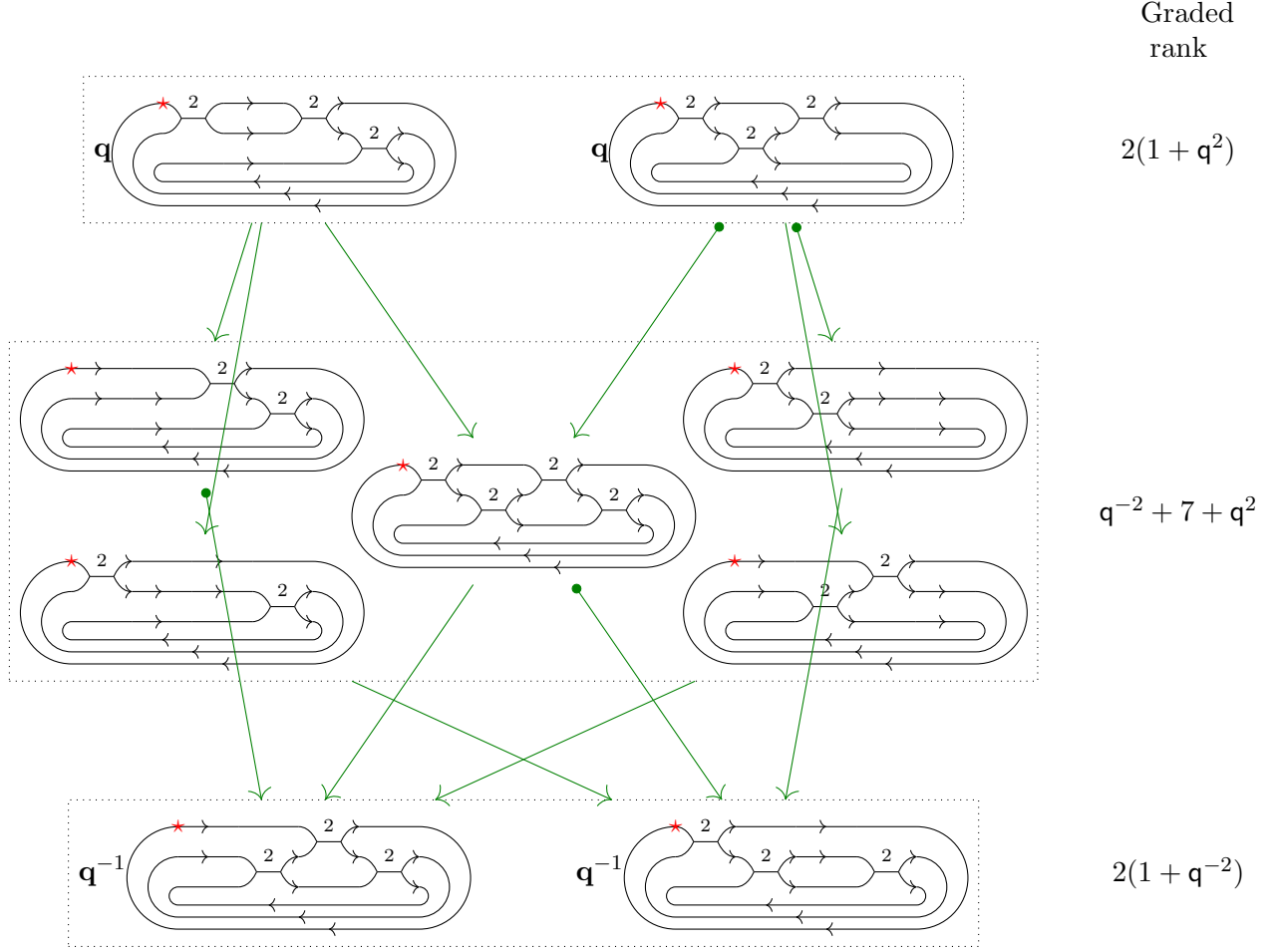


FIGURE 26. The hypercube for computing the \mathfrak{gl}_0 homology of the figure-eight knot. The two diagrams on top (resp. bottom) are in homological degree -1 (resp. 1).

explicit bases for all diagrams. However, this is not necessary. Over \mathbb{F} or \mathbb{Q} one easily obtains that the graded rank of $H^{\mathfrak{gl}_0}(4_1)$ in homological degrees -1 and 1 is respectively q^2 and q^{-2} . Using the Euler characteristic argument, we conclude that the Poincaré polynomial of $H^{\mathfrak{gl}_0}(4_1)$ with coefficients in either \mathbb{F} or \mathbb{Q} is equal to:

$$t^{-1}q^2 + 3t^0q^0 + t^1q^{-2}.$$

For comparison we give the Poincaré polynomials of the reduced triply graded homology of the figure-eight knot:

$$P_{4_1}(t, a, q) = t^0a^2q^0 + t^1a^0q^{-2} + t^0a^0q^0 + t^{-1}a^0q^2 + t^0a^{-2}q^0$$

C.3. (5,2)-torus knot. The $(5,2)$ -torus knot 5_1 can be presented as the closure of the braid σ_1^5 on two strands. Computing its homology directly from the hypercube of resolutions is a bit tedious, since it requires *a priori* to compute 32 state spaces (which are, however, quite simple). Fortunately, the complex of Soergel bimodules associated with σ_5 is homotopic (see [Kho07]) to:

$$\begin{array}{ccccccc} \begin{array}{c} 1 \searrow \\ 2 \\ 1 \nearrow \end{array} & \xrightarrow{x-y'} & \begin{array}{c} 1 \searrow \\ 2 \\ 1 \nearrow \end{array} & \xrightarrow{x-x'} & \begin{array}{c} 1 \searrow \\ 2 \\ 1 \nearrow \end{array} & \xrightarrow{x-y'} & \begin{array}{c} 1 \searrow \\ 2 \\ 1 \nearrow \end{array} & \xrightarrow{x-x'} & \begin{array}{c} 1 \searrow \\ 2 \\ 1 \nearrow \end{array} & \xrightarrow{\text{unzip}} & \begin{array}{c} 1 \longrightarrow \\ 1 \longrightarrow \end{array} \end{array}$$

where x and y act on the left and x' and y' on the right. We ignore homological grading shifts for the moment. In this setting all arrows except the last one have degree 2, the last one has degree 1.

We can use this simplification for computing \mathfrak{gl}_0 homology. In that context, all spaces have dimension 1, the last one has dimension 0 and all maps are zero. Taking care of the (q, t) -grading, we obtain that the Poincaré polynomial for $H^{\mathfrak{gl}_0}(5_1)$ with coefficients in either \mathbb{F} or \mathbb{Q} is equal to:

$$t^0q^4 + t^1q^2 + t^2q^0 + t^3q^{-2} + t^4q^{-4}.$$

For comparison, here is the Poincaré polynomials of the reduced triply graded homology:

$$P_{5_1}(t, a, q) = t^0a^{-4}q^4 + t^1a^{-6}q^2 + t^2a^{-4}q^0 + t^3a^{-6}q^{-2} + t^4a^{-4}q^{-4}.$$

REFERENCES

- [AE15] Akram S. Alishahi and Eaman Eftekhary. A refinement of sutured Floer homology. *J. Sympl. Geom.*, 13(3):609–743, 2015. [doi:10.4310/JSG.2015.v13.n3.a3](#).
- [BDL⁺21] John A. Baldwin, Nathan Dowlin, Adam Simon Levine, Tye Lidman, and Radmila Sazdanovic. Khovanov homology detects the figure-eight knot. *Bull. Lond. Math. Soc.*, 53(3):871–876, 2021. [doi:10.1112/blms.12467](#).
- [BHS21] John A. Baldwin, Ying Hu, and Steven Sivek. Khovanov homology and the cinquefoil, 2021. [arXiv:2105.12102](#).
- [Bir93] Joan S. Birman. New points of view in knot theory. *Bull. Amer. Math. Soc. (N.S.)*, 28(2):253–287, 1993. [doi:10.1090/S0273-0979-1993-00389-6](#).
- [BM20] Fraser Binns and Gage Martin. Knot floer homology, link floer homology and link detection, 2020. [arXiv:2011.02005](#).
- [BPW19] Anna Beliakova, Krzysztof K. Putyra, and Stephan M. Wehrli. Quantum link homology via trace functor I. *Invent. Math.*, 215(2):383–492, 2019. [doi:10.1007/s00222-018-0830-0](#).
- [BS22] John A. Baldwin and Steven Sivek. Khovanov homology detects the trefoils. *Duke Math. J.*, 171(4):885–956, 2022. [doi:10.1215/00127094-2021-0034](#).
- [BVV18] John Baldwin and David Shea Vela-Vick. A note on the knot Floer homology of fibered knots. *Algebr. Geom. Topol.*, 18(6):3669–3690, 2018. [doi:10.2140/agt.2018.18.3669](#).
- [DGR06] Nathan M. Dunfield, Sergei Gukov, and Jacob A. Rasmussen. The superpolynomial for knot homologies. *Experiment. Math.*, 15(2):129–159, 2006. URL: <http://projecteuclid.org/euclid.em/1175789736>.
- [Dow17] Nathan Dowlin. A Categorification of the HOMFLY-PT Polynomial with a Spectral Sequence to Knot Floer Homology, 2017. [arXiv:1703.01401](#).
- [Dow18] Nathan Dowlin. A spectral sequence from Khovanov homology to knot Floer homology, 2018. [arXiv:1811.07848](#).
- [EMTW20] Ben Elias, Shotaro Makisumi, Ulrich Thiel, and Geordie Williamson. *Introduction to Soergel bimodules*, volume 5 of *RSME Springer Series*. Springer, Cham, 2020. [doi:10.1007/978-3-030-48826-0](#).
- [ETW18] Michael Ehrig, Daniel Tubbenhauer, and Paul Wedrich. Functoriality of colored link homologies. *Proc. Lond. Math. Soc. (3)*, 117(5):996–1040, 2018. [doi:10.1112/plms.12154](#).
- [FRW22] Ethan Farber, Braeden Reinoso, and Luya Wang. Fixed point-free pseudo-anosovs and the cinquefoil, 2022. [arXiv:2203.01402](#).
- [Ghi08] Paolo Ghiggini. Knot Floer homology detects genus-one fibred knots. *Amer. J. Math.*, 130(5):1151–1169, 2008. [doi:10.1353/ajm.0.0016](#).
- [Gil16] Allison Gilmore. Invariance and the knot Floer cube of resolutions. *Quantum Topol.*, 7(1):107–183, 2016. [doi:10.4171/QT/74](#).
- [Kho00] Mikhail Khovanov. A categorification of the Jones polynomial. *Duke Math. J.*, 101(3):359–426, 2000. [doi:10.1215/S0012-7094-00-10131-7](#).
- [Kho07] Mikhail Khovanov. Triply-graded link homology and Hochschild homology of Soergel bimodules. *Internat. J. Math.*, 18(8):869–885, 2007. [doi:10.1142/S0129167X07004400](#).
- [KLMS12] Mikhail Khovanov, Aaron D. Lauda, Marco Mackaay, and Marko Stošić. Extended graphical calculus for categorified quantum $\mathfrak{sl}(2)$. *Mem. Amer. Math. Soc.*, 219(1029):vi+87, 2012. [doi:10.1090/S0065-9266-2012-00665-4](#).
- [KM11] Peter B. Kronheimer and Tomasz S. Mrowka. Khovanov homology is an unknot-detector. *Publ. Math. Inst. Hautes Études Sci.*, (113):97–208, 2011. [doi:10.1007/s10240-010-0030-y](#).
- [KR08a] Mikhail Khovanov and Lev Rozansky. Matrix factorizations and link homology. *Fund. Math.*, 199(1):1–91, 2008. [doi:10.4064/fm199-1-1](#).

- [KR08b] Mikhail Khovanov and Lev Rozansky. Matrix factorizations and link homology. II. *Geom. Topol.*, 12(3):1387–1425, 2008. doi:10.2140/gt.2008.12.1387.
- [Lip06] Robert Lipshitz. A cylindrical reformulation of Heegaard Floer homology. *Geom. Topol.*, 10(2):955 – 1096, 2006. doi:10.2140/gt.2006.10.955.
- [Lip20] Robert Lipshitz. A remark on quantum hochschild homology, 2020. arXiv:2008.03155.
- [Lod98] Jean-Louis Loday. *Cyclic homology*, volume 301 of *Grundlehren der mathematischen Wissenschaften*. Springer-Verlag, Berlin, second edition, 1998. Appendix E by María O. Ronco, Chapter 13 by the author in collaboration with Teimuraz Pirashvili. doi:10.1007/978-3-662-11389-9.
- [Mac15] Ian G. Macdonald. *Symmetric functions and Hall polynomials*. Oxford Classic Texts in the Physical Sciences. The Clarendon Press, Oxford University Press, New York, second edition, 2015. With contribution by A. V. Zelevinsky and a foreword by Richard Stanley.
- [Man14] Ciprian Manolescu. An untwisted cube of resolutions for knot Floer homology. *Quantum Topol.*, 5(2):185–223, 2014. doi:10.4171/QT/50.
- [Man15] Ciprian Manolescu. Floer theory and its topological applications. *Jpn. J. Math.*, 10(2):105–133, 2015. doi:10.1007/s11537-015-1487-8.
- [Mar23] Laura Marino. Computing the symmetric \mathfrak{gl}_1 -homology, 2023. arXiv:2309.16371.
- [Mas52] William S. Massey. Exact couples in algebraic topology. I, II. *Ann. of Math. (2)*, 56:363–396, 1952. doi:10.2307/1969805.
- [May09] Jon Peter May. A primer on spectral sequences, 2009. URL: <http://www.math.uchicago.edu/~may/MISC/SpecSeqPrimer.pdf>.
- [McC01] John McCleary. *A user’s guide to spectral sequences*, volume 58 of *Cambridge Studies in Advanced Mathematics*. Cambridge University Press, Cambridge, second edition, 2001.
- [Ni07] Yi Ni. Knot Floer homology detects fibred knots. *Invent. Math.*, 170(3):577–608, 2007. doi:10.1007/s00222-007-0075-9.
- [ORS13] Peter S. Ozsváth, Jacob Rasmussen, and Zoltán Szabó. Odd Khovanov homology. *Algebr. Geom. Topol.*, 13(3):1465–1488, 2013. doi:10.2140/agt.2013.13.1465.
- [OS04a] Peter Ozsváth and Zoltán Szabó. Holomorphic disks and genus bounds. *Geom. Topol.*, 8:311–334, 2004. doi:10.2140/gt.2004.8.311.
- [OS04b] Peter Ozsváth and Zoltán Szabó. Holomorphic disks and topological invariants for closed three-manifolds. *Ann. Math.*, 159(3):1027–1058, 2004. arXiv:math/0101206, doi:10.4007/annals.2004.159.1027.
- [OS08] Peter Ozsváth and Zoltán Szabó. Holomorphic disks, link invariants and the multi-variable Alexander polynomial. *Algebr. Geom. Topol.*, 8(2):615–692, 2008. doi:10.2140/agt.2008.8.615.
- [OS09] Peter Ozsváth and Zoltán Szabó. A cube of resolutions for knot Floer homology. *J. Topol.*, 2(4):865–910, 2009. doi:10.1112/jtopol/jtp032.
- [OSS09] Peter Ozsváth, András Stipsicz, and Zoltán Szabó. Floer homology and singular knots. *J. Topol.*, 2(2):380–404, 2009. doi:10.1112/jtopol/jtp015.
- [Put14] Krzysztof K. Putyra. A 2-category of chronological cobordisms and odd Khovanov homology. In *Knots in Poland III. Part III*, volume 103 of *Banach Center Publ.*, pages 291–355. Polish Acad. Sci. Inst. Math., Warsaw, 2014. doi:10.4064/bc103-0-12.
- [QR16] Hoel Queffelec and David E. V. Rose. The \mathfrak{sl}_n foam 2-category: a combinatorial formulation of Khovanov–Rozansky homology via categorical skew Howe duality. *Adv. Math.*, 302:1251–1339, 2016. doi:10.1016/j.aim.2016.07.027.
- [QRS18] Hoel Queffelec, David E. V. Rose, and Antonio Sartori. Annular evaluation and link homology, 2018. arXiv:1802.04131.
- [QW21] Hoel Queffelec and Paul Wedrich. Khovanov homology and categorification of skein modules. *Quantum Topol.*, 12(1):129–209, 2021. doi:10.4171/qt/148.
- [Ras15] Jacob A. Rasmussen. Some differentials on Khovanov–Rozansky homology. *Geom. Topol.*, 19(6):3031–3104, 2015. doi:10.2140/gt.2015.19.3031.
- [Rou17] Raphaël Rouquier. Khovanov–Rozansky homology and 2-braid groups. In *Categorification in geometry, topology, and physics*, volume 684 of *Contemp. Math.*, pages 147–157. Amer. Math. Soc., Providence, RI, 2017.
- [RW20a] Louis-Hadrien Robert and Emmanuel Wagner. A closed formula for the evaluation of foams. *Quantum Topol.*, 11(3):411–487, 2020. doi:10.4171/qt/139.
- [RW20b] Louis-Hadrien Robert and Emmanuel Wagner. Symmetric Khovanov–Rozansky link homologies. *J. Éc. polytech. Math.*, 7:573–651, 2020. doi:10.5802/jep.124.
- [RW22] Louis-Hadrien Robert and Emmanuel Wagner. A quantum categorification of the Alexander polynomial. *Geom. Topol.*, 26(5):1985–2064, 2022. arXiv:1902.05648, doi:10.2140/gt.2022.26.1985.
- [Wed19] Paul Wedrich. Exponential growth of colored HOMFLY-PT homology. *Adv. Math.*, 353:471–525, 2019. doi:10.1016/j.aim.2019.06.023.

UNIVERSITÄT ZÜRICH, INSTITUTE OF MATHEMATICS, WINTERTHURERSTRASSE 190, CH-8057 ZÜRICH, SWITZERLAND

Email address: anna@math.uzh.ch

UNIVERSITÄT ZÜRICH, INSTITUTE OF MATHEMATICS, WINTERTHURERSTRASSE 190, CH-8057 ZÜRICH, SWITZERLAND

Email address: krzysztof.putyra@math.uzh.ch

UNIVERSITÉ CLERMONT AUVERGNE, LMBP, CAMPUS DES CÉZEAUX, 3 PLACE VASARELY, CS 60026, 63178 AUBIÈRE CEDEX, FRANCE

Email address: louis-hadrien.robert@uca.fr

UNIVERSITÉ DE PARIS, IMJ-PRG, UMR 7586 CNRS, 8 PLACE AURÉLIE NEMOURS, F-75013, PARIS, FRANCE

Email address: emmanuel.wagner@imj-prg.fr